FINAL PROJECT REPORT

Milestone I
Final Report Preparation

IN PARTIAL FULFILLMENT OF THE ERA PROJECT
Proof-of-Concept Testing: Software to Quantify Methane Emission Rates in Real-Time
ERA PROJECT O160052

PREPARED FOR
Emissions Reduction Alberta
Edmonton, Alberta

SUBMITTED TO
Dallas Johnson, Ph.D., Project Advisor
Alberta Innovates
Edmonton, Alberta
dallas.johnson@albertainnovates.ca
(780) 429-7650

April 17, 2019

SUBMITTED BY
Minnich and Scotto, Inc.
Freehold, New Jersey, USA

Timothy R. Minnich
PROJECT RECIPIENT LIAISON
trminnich@msiair.net
(732) 409-9900

DISCLAIMER

ERA and Her Majesty the Queen in right of Alberta and each of them make no warranty, express or implied, nor assume any legal liability or responsibility for the accuracy, completeness, or usefulness of any information contained in this publication, nor that use thereof does not infringe on privately owned rights. The views and opinions of the author expressed herein do not necessarily reflect those of ERA and Her Majesty the Queen in right of Alberta and each of them. The directors, officers, employees, agents and consultants of ERA and the Government of Alberta are exempted, excluded and absolved from all liability for damage or injury, howsoever caused, to any person in connection with or arising out of the use by that person for any of this publication or its contents.

CONTENTS

CONTENTS (Cont'd)

CONTENTS (Cont'd)

_____

* Appended to the end of Attachment C are all experimental test-design configurations and e-Calc 2 results for the controlled-release portion of this project (not previously provided).

TABLES

TABLES (Cont'd)

FIGURES

FIGURES (Cont'd)

SELECTED ACRONYMS AND ABBREVIATIONS

Item	Meaning
A	actual (or controlled) methane emission rate
ACCO	Alberta Climate Change Office
AERMET	AERMOD meteorological preprocessor
AERMOD	***A***merican Meteorological Society / ***E***PA ***R***egulatory ***Mod***el
C	Centigrade
C_M	measured path-integrated concentration (attribution) (mg/m^2);
C_U	predicted unity-based, path-integrated concentration along the measurement path (mg/m^2)
C_{UE}	predicted unity-based, path-integrated concentration along an extended measurement path (mg/m^2)
CAFO	combined animal feeding operations
CALPUFF	***Cal***ifornia ***Puff*** Model
CFR	U.S. Code of Federal Regulations
CH_4	methane
CNRL	Canadian Natural Resources Limited
CO_2	carbon dioxide
CRDS	cavity ring-down spectroscopy
CSV	comma-separated value
DAS	data acquisition system
DQO	Data Quality Objective
e-Calc 1	Minnich and Scotto's ***e***missions ***calc***ulation software (first-generation)
e-Calc 2	Minnich and Scotto's e-Calc software (second-generation)
EPA	U.S. Environmental Protection Agency
ER	emission rate
ERA	Emissions Reduction Alberta
FTIR	Fourier-transform infrared
GB	gigabyte
GHG	greenhouse gas
GHz	gigahertz
GPS	global positioning system
H	sensible heat flux
IB	interpolated background
L	Monin-Obukhov length
m	meter
MD	Major Deliverable
MDT	Mountain Daylight Time
MEP	measurement event pair
mg	milligram
MGP	manufactured gas plant

SELECTED ACRONYMS AND ABBREVIATIONS (Cont'd)

Item	Meaning
mm	millimeter
modified e-Calc 2	Minnich and Scotto's modified e-Calc software (second-generation)
MQO	Measurement Quality Objective
mT	metric ton
NOAA	U.S. National Oceanic and Atmospheric Administration
O&G	oil and gas
ORS	optical remote sensing
P	predicted methane emission rate; atmospheric pressure
PC	plume capture; personal computer
"pfl"	AERMOD profile file
PIC	path-integrated concentration
PICMET	***P***ath-***I***ntegrated ***C***oncentration – ***Met***eorology
ppb	parts per billion
ppbv	parts-per-billion by volume
ppm	parts per million
ppm-m	parts-per-million times meter
ppmv	parts-per-million by volume
PQL	Practical Quantitation Limit
Q_A	actual emission rate
Q_U	unity-based emission rate
QAPP	Quality Control Project Plan
QC	quality control
r^2	correlation coefficient
R&D	research and development
RH	relative humidity
RSD	relative standard deviation
SA	source attribution
SCAQMD	South Coast Air Quality Management District (California)
"sfc"	AERMOD surface file
sigma theta (σ_θ)	standard deviation of the horizontal wind direction
sigma w (σ_W)	standard deviation of the vertical wind speed (also called sigma phi, σ_ϕ)
SOP	Standard Operating System
T (or T_A)	actual temperature
TDL	tunable diode laser
u	east-west wind component
u*	friction velocity
v	north-south wind component
w	up-down wind component
WD	wind direction
WS	wind speed
z_0	surface roughness length

SECTION 1 – INTRODUCTION

This Final Project Report represents the culmination of an 18-month methods-development program, sponsored by the Province of Alberta and administered by Emissions Reduction Alberta (ERA) as part of their "Methane Challenge Initiative." The title of our project was, "Proof-of-Concept Testing: Software to Quantify Methane Emission Rates in Real-Time." The end-product was a fully integrated, methane emission-rate measurement system (i.e., the "System"), which calculates, in real-time, methane emission rates from certain oil-and-gas (O&G) industry sources.

Drawing heavily from a total of five Major Deliverables (MD's) spanning this period, this Final Project Report provides an overview and general chronology of the technical tasks leading to development of a Set of Specifications for eventual System commercialization. The software tested is known as e-Calc 2 (***e***missions ***calc***ulation, second-generation). Nine days of successful field testing, carried out during August 2018, involved the continual, outdoor release of carefully controlled amounts of methane by our project team member, InnoTech Alberta, at their research facility in Vegreville. Other members of the project team were: Boreal Laser, Inc. (Edmonton), responsible for all methane measurements using their tunable diode laser (TDL) system; Met One Instruments, Inc. (Happaugue, New York), responsible for the design and assembly of the specialized meteorological measurement system used in the field; and Loover Partnership (Morristown, New Jersey), responsible for necessary e-Calc software modification and statistical consulting.

1.1 Document Organization

Table 1-1 identifies the project milestones set forth in our Scope of Work. Also shown are those milestones which required preparation of comprehensive MD's. Preparation of an ERA Progress Report was also required upon completion of each project milestone.

TABLE 1-1. PROJECT MILESTONES AND ASSOCIATED MAJOR DELIVERABLES

Project Milestone	MD Required?
A. ACCO Mine-Face and Tailings Pond Data Analysis and Reporting (e-Calc 1)	✔
B. Work Plan Preparation	✔
C. E-Calc Modification	
D. Construction and Mobilization	
E. Controlled-Release Data Collection	
F. Controlled-Release Data Analysis (e-Calc 2)	✔
G. ACCO Mine-Face and Tailings Pond Data Analysis and Reporting (e-Calc 2)	✔
H. Specification Preparation	✔
I. Final Report Preparation	✔

Table 1-2 identifies, for each section of this Final Project Report, the corresponding Major Deliverable which serves as the primary basis of information. All MD's are included in their entirety as attachments to this report. While the report sections listed in Table 1-2 are generally consistent with the project milestone chronology, Sections 2 and 3 represent necessary departures, as the successful creation of e-Calc 2 was prerequisite to the preparation of the corresponding MD's.

TABLE 1-2. FINAL REPORT SECTIONS AND CORRESPONDING MAJOR DELIVERABLES

Report Section	Corresponding MD (Milestone Designation)
1. Introduction	
2. E-Calc 2 Description	H
3. ACCO Mine-Face and Tailings Pond Analyses (both e-Calc versions)	G
4. Field-Work Planning	B
5. Controlled-Release Program	F
6. Initial System Specification	H
7. Supplemental Booster-Station Analysis	(I)
8. Final System Specification	H, (I)

There is another issue concerning Table 1-2 for which some explanation would be helpful. Our original Scope of Work did not envision the need for Section 7, "Supplemental Booster-Station Analysis" (and, accordingly, two iterations of the System specification). The impetus for this extra work occurred during preparation of the Major Deliverable for Milestone F (Section 5 of this report) when, upon further examination of the field data, we believed we had identified a significant issue related to the treatment of the background methane and the meteorological data used as input to e-Calc 2. If this analysis were explored, we knew the results would likely lead to a refinement of the System specification. Therefore, in the Milestone F Report, we committed to perform this additional analysis as part of the Major Deliverable for Milestone H: Set of Specifications (Appendix E).

The additional Milestone H analysis proved successful, providing tangible improvement to the System specification. However, while performing this analysis, another pathway for further exploration presented itself. This time, though, successful results would enable extension of the System specification to the booster station – previously eliminated as a source due to issues with methane background concentrations. This supplemental booster-station analysis was also successful, and is presented as its own section (Section 7) in this Final Project Report. The final System specification is, accordingly, presented as Section 8.

Finally, most sections can be broadly thought of as summaries of the corresponding Major Deliverables. Therefore, the reader is advised to consult the actual MD's (attachments) for those details not discussed in the main body of this Final Project Report.

1.2 Project Overview

The software tested is generically referred to as e-Calc (***e***missions ***calc***ulation). The first-generation version of this software (e-Calc 1) calculates mass-per-time emission rates during daytime hours from ground-level sources. E-Calc 1 employs what is often referred to as "inverse modeling," based on AERMOD (***A***merican Meteorological Society / ***E***PA ***R***egulatory ***Mod***el) – a U.S. Environmental Protection Agency (U.S. EPA) "Guideline" air dispersion model for regulatory application. Instead of predicting a downwind concentration at a point in space from a known source emission rate (as AERMOD typically does), e-Calc 1 predicts that emission rate from a measured downwind (crosswind), path-integrated concentration and contemporaneous onsite meteorology.

E-Calc 1 can derive emission rates of methane (or any other measured compound) from most ground-based sources. Importantly, this software offers the capability of generating such emission rates in real-time. However, a significant up-front effort is required, prior to field deployment, to enable AERMOD (and thus e-Calc 1) to simulate the vertical wind-speed profile and atmospheric turbulence – critical model input parameters. AERMOD employs what is known as the *flux-gradient approach* for simulating these input parameters.

Two distinct goals comprised our ERA project. The primary goal was, first, to modify the software to accommodate a more sophisticated and robust treatment of meteorology (i.e., to create e-Calc 2 based on a new version of AERMOD – modified to employ the *eddy-correlation approach* for simulating the above model input parameters) and, second, to field-test this second-generation version of the e-Calc software, based on carefully controlled methane releases from simulated, leaking upstream sources. The intent was to eliminate the need for the arduous pre-field tasks and make possible the software use during the nighttime.

The four simulated sources were:

- a booster station, comprised of a compressor engine and a condensate tank;
- a gas-gathering pipeline assembly;
- a gas-transmission line; and
- a production pad.

Only one simulated source was tested on any given measurement day. As mentioned, all controlled methane releases were conducted by InnoTech Alberta, with all field work performed at InnoTech Alberta's Vegreville R&D facility. Path-integrated methane measurements were performed by Boreal Laser using one of their GasFinder TDL spectrometers; all TDL measurements were made at a height of 1.0 meters above the ground. All meteorological measurements were made using a sonic anemometry system designed and assembled by Met One Instruments. The methane source was compressed natural gas, with a methane concentration of 76.6 percent (760,000 ppmv).

It should be noted that there has never been a performance evaluation of AERMOD based on this more sophisticated treatment of meteorology, nor has the U.S. EPA yet provided the software coding for this model option. In theory, the AERMOD results should be improved (and, accordingly, the corresponding e-Calc predictions); however, such results could not be guaranteed.

The secondary goal, a benefit to the Alberta Climate Change Office (ACCO), was to apply e-Calc (both versions) to essentially re-create the fugitive methane and carbon dioxide emission rates from the Canadian Natural Resources Limited (CNRL) mine-face and tailings pond operations in Fort McMurray, as reported in CNRL's two latest (at the time) annual submissions on facility greenhouse gas (GHG) emissions. Our analysis used onsite, 15-minute-averaged path-integrated methane and carbon dioxide data, collected across portions of these sources in 2015 and 2016 by CNRL using a Boreal Laser TDL spectrometer, together with onsite, coincident meteorological data and contemporaneous flux-chamber sampling data. The hope was that e-Calc would be demonstrated a viable and attractive alternative to the techniques currently employed for measuring GHG's from the oil-sands sources, and that the time and cost for GHG reporting would be greatly reduced.

1.3 Market Need

We know of no other measurement system which can, in real-time, generate accurate estimates of methane emissions from ground-level sources. It is difficult for the Province of Alberta to enforce existing methane reduction mandates without an accurate baseline against which to compare. The rapid and inexpensive means of measuring methane emission rates afforded by the success of this Project is clearly a disruptive technology.

When used in combination with the TDL system, e-Calc offers a common-sense approach for prioritizing repairs in the O&G industry, which can reduce product loss while adding bottom-line profit. By quantifying methane emissions from principal source types within a given industrial sector, the quality of emissions inventories should be vastly improved, thereby facilitating an accurate methane baseline against which future reductions can be reliably assessed.

In addition to leaking upstream process components, target markets in Alberta for this System include: (a) municipal landfills; (c) combined animal feeding operations (CAFO) facilities; and (c) major oil-sands sources, consisting of tailings ponds and mine faces. In fact, the feasibility of employing e-Calc 2 to assess methane emissions from these oil-sands sources was demonstrated during the work for ACCO (secondary project goal), thereby laying the groundwork for a proposed field demonstration at a tailings pond.

SECTION 2 – E-CALC 2 DESCRIPTION

Section 2.1 presents a brief history of e-Calc 2's development. **Section 2.2** presents relevant technical considerations. **Section 2.3** details the functional logic governing the software. **Section 2.4** identifies the required input data and associated usage.

2.1 Developmental History

Minnich and Scotto is the architect of e-Calc – an emissions-calculation software package developed in order to generate air pollutant emission rates from a wide range of fugitive-type, ground-level sources (as well as elevated area sources). This Windows-based, client-server software calculates contaminant emission rates – precise 15-minute-averaged "snapshots" – from these source types. E-Calc is suitable for use with a TDL spectrometer, or any other optical remote sensing (ORS) instrument which generates a path-integrated concentration (PIC). The software can also be used with a rapid-sampling, mobile point-monitoring device, such as a cavity ring-down spectrometer, from which a PIC output can be approximated.

E-Calc is a logical extension of our 2004 PICMET (***P***ath-***I***ntegrated ***C***oncentration – ***Met***eorology) software, created to rapidly assess compliance with pre-established action levels at off-site receptors (e.g., residences), primarily during hazardous waste site cleanups. The PICMET software displays maximum concentrations at user-specified distances downwind of the emissions source, based on path-integrated measurements and atmospheric stability and transport considerations.

PICMET was employed during active cleanups at former manufactured gas plant (MGP) sites in November 2004, and again during December 2006 and May 2007 as part of a 2½-year applied R&D study for the Gas Technology Institute (Des Plaines, Illinois). Results from this latter study demonstrated superior residential protection when compared to traditional monitoring approaches.

Development work on e-Calc began in 2008. E-Calc was originally created for use with open-path Fourier-transform infrared (FTIR) spectroscopy to help municipal solid waste landfill owners comply with mandated emissions reporting and permitting requirements for methane and other greenhouse gases. Based on AERMOD, the software incorporates the output from the PIC-generating instrument with coincident onsite meteorological data and other information.

In June 2011, we employed e-Calc to support a legal proceeding by measuring emission rates from several process sources at an Alabama pulp-and-paper mill, including a 1-square-kilometer polishing pond. In August 2014, we used it to measure emission rates from the preliminary settling tanks at a large New York City municipal wastewater treatment plant. In September 2015, we participated in an extensive field project for the South Coast Air Quality Management District (SCAQMD), a California governmental agency, in which we used e-Calc to measure emission rates from 16 oil production wells and tanks, 17 gas stations, and two cattle farms, all in the Los Angeles basin.

We have participated in two third-party e-Calc validation studies, results of which were presented at the March 2016 "Air Quality Measurement Methods and Technology Conference," sponsored jointly by the Air & Waste Management Association (A&WMA) and the U.S. EPA.

First, as part of our project for the SCAQMD (described above), our e-Calc software was validated during a 2-day, controlled-release experiment (October 12-13, 2015). Over the study, propane was released at varying emission rates from a scissors-type lift at a pre-designated height of 3 meters (even though e-Calc was designed for ground-level releases only). Thirteen monitoring events (15-minute-averaged) were performed on Day 1, with an additional seven on Day 2.

Next, under contract to Texas A&M University (San Antonio, Texas), we performed a 2-day, e-Calc validation study (November 4-5, 2015), which involved the controlled release of sulfur hexafluoride (SF_6) from ground-level locations simulating a compressor/condensate tank complex (Day 1) and an assembly of gas-gathering pipelines (Day 2).

As mentioned, e-Calc 1 employs the U.S. EPA regulatory version of AERMOD in order to preserve the model's legal Guideline status. For each monitoring event, the generation of input files requires meteorological data together with emissions-characterization and monitoring configuration data. Dispersion coefficients under this approach (i.e., flux-gradient) are assigned based on wind speed, land-use, solar insolation, and statistical data treatments such as the standard deviations of the horizontal wind direction and vertical wind speed. From this information the friction velocity is determined, which is used to develop the vertical wind-speed profile. The vertical wind-speed profile primarily governs the predicted (back-calculated) emission rate in e-Calc 1 (and e-Calc 2).

The flux-gradient approach currently employed in AERMOD has been extensively evaluated in model-validation studies performed by the U.S. EPA over the years. Similarly, the performance of e-Calc 1 was successfully demonstrated during the two validation studies described above.

The upgraded (second-generation) version of e-Calc (e-Calc 2) was created specifically for this ERA project, primarily to eliminate the need for relatively labor-intensive pre-field tasks. As mentioned, e-Calc 2 employs a more sophisticated means of assigning dispersion coefficients – the eddy-correlation (or covariance) approach. This approach typically requires wind measurements (using sonic anemometry) at two heights above the ground. Covariance statistics, calculated from the lower of these two sensors, are then used to determine the friction velocity. The U.S. EPA is planning to update AERMOD to enable application of the eddy-correlation approach, but has yet to release the software coding for this version.

Additional information about how the vertical wind-speed profile is generated in e-Calc 2 can be found in Section 6.1.1 of this report.

2.2 Technical Considerations

Discussed in this section are:

- the difference between a concentration and an emission rate;
- the drawbacks with conventional approaches for deriving emission rates;
- the benefits of open-path monitoring; and
- the area-source technique for measuring emission rates, upon which e-Calc is based (both versions).

2.2.1 Concentration vs. Emission Rate

The difference between a source emission rate (mass per time) and an ambient air concentration (mass per volume) is often poorly understood. Further, few investigators truly appreciate the utility of the path-integrated concentration when coupled with onsite meteorology and air dispersion modeling. When properly applied, open-path spectroscopy eliminates the spatial data-representativeness problem inherent in approaches which rely solely on point-sampling techniques. This "whole-plume" sampling approach offers, perhaps, the only means of complying with the U.S. EPA's Data Quality Objective (DQO) process while measuring emission rates, thereby ensuring that end-user needs are met.

For point-type monitors, gaseous concentrations are typically reported as the mass of contaminant per volume of gas, such as micrograms per cubic meter (ug/m^3), or the volume of contaminant per volume of gas, such as parts per billion (ppbv) or parts per million (ppmv). Path-integrated concentrations, however, are usually reported as parts-per-million times meter (ppm-m). It is often desirable to convert path-integrated concentrations from ppm-m to milligrams-per-cubic-meter times meter (mg/m^3 x m, or mg/m^2) in order to avoid having to consider the compound's molecular weight.

2.2.2 Drawbacks with Conventional Approaches for Deriving Emission Rates

Emission rates derived from point-monitoring data are frequently underestimated, as there is no way of knowing how far away a hand-held monitor (or Summa canister) might be from the plume centerline, especially given the fact that wind direction is never constant; in fact, it is generally not possible to ensure the sample isn't inadvertently collected outside of the downwind plume altogether. This fundamental sampling design flaw explains, at least in part, the extreme variability in emission rates reported for most O&G industry process components.

Figure 2-1 illustrates how concentration at any point downwind of a source drops off rapidly as one moves away from the plume centerline.

FIGURE 2-1. CONCENTRATION DROP-OFF AWAY FROM PLUME CENTERLINE

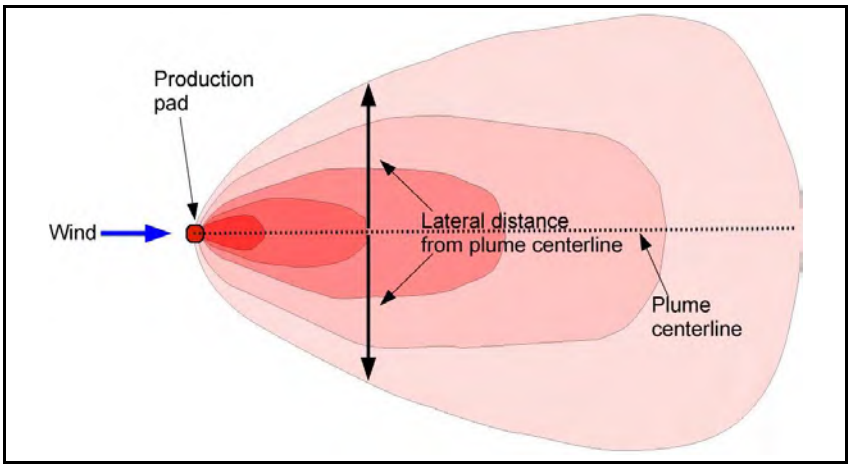

2.2.3 Benefits of Open-Path Monitoring

An open-path spectrometer collects path-integrated data – meaning that contaminants downwind of the source are measured along the entire crosswind dimension of the plume. The spectrometer essentially counts the molecules of the analyte, thus ensuring that concentrations are not "missed" anywhere along the beam-path.

Figure 2-2 illustrates how the entire crosswind plume is sampled with open-path TDL spectroscopy.

FIGURE 2-2. CROSSWIND TDL PLUME SAMPLING

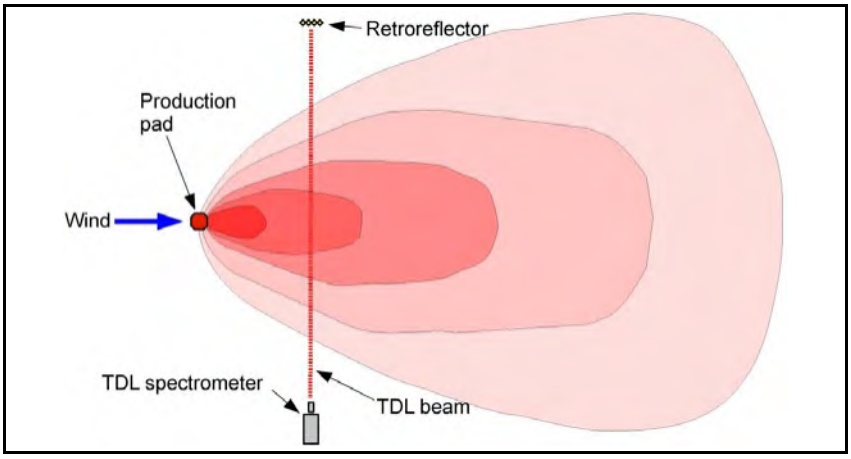

A principal reason that open-path spectroscopy is still not generally recognized as the powerful tool that it is for deriving emission rates is that the resultant path-integrated data is not of a form which can be compared directly to ambient air standards (i.e., point concentrations). But as alluded to earlier, when appropriately coupled with air dispersion modeling, a path-integrated concentration measurement made downwind of an emitting source contains far more information than any point measurement (or collection of point measurements) ever could for purposes of assigning a source emission rate and assessing the resultant downwind impact.

Using dispersion modeling relationships, a source emission rate is "back-calculated," based on the downwind (cross-plume) path-integrated concentration and onsite meteorology. This source emission rate can be viewed as a mass-per-time "snapshot" over the 15-minute interval necessary to yield the measured downwind, path-integrated concentration under the particular atmospheric dispersion and transport conditions during that precise block of time.

The *area-source technique* provides the most accurate means of back-calculating this emission rate (discussed next). E-Calc 2 uses AERMOD in its inverse form, together with the area-source technique, for this back-calculation, in real-time.

2.2.4 Area-Source Technique

The area-source technique for emission-rate generation is appropriate for fugitive ground-level and elevated area sources – both homogeneous (uniformly emitting) and heterogeneous (non-uniformly emitting). Employing the principle of mass balance, it identifies a time-averaged source attribution based on a series of downwind path-integrated measurements (1- to 2-meter height), enabling the subsequent generation of emission rates using AERMOD. AERMOD requires measurement of coincident onsite meteorological data, from which atmospheric dispersion and transport are simulated between the source and the beam-path.

General Approach

The following three-step approach is employed using a TDL spectrometer downwind of a given source.

1. Identify Source Attribution

A series of 15-minute-averaged, path-integrated TDL measurements (i.e., monitoring events) are made immediately downwind of the source, such that the cross-plume mass contained within the beam-path is maximized. When significant, the upwind path-integrated concentration can be subtracted from the downwind measurement, thus reducing the conservatism of the source-attribution calculation.

2. Predict the Unity-Based, Path-Integrated Concentration Along the Measurement Path

AERMOD is used to predict the *unity-based*, path-integrated concentration (as opposed to the actual path-integrated concentration) along the downwind TDL measurement path defined in Step 1. This is accomplished by: (a) predicting the point concentration (mg/m^3) at every meter along this path based on a "unity" emission rate (e.g., 1 mg/s) across the source, and the actual meteorology and source configuration; (b) determining, via summing each predicted point concentration, the *path-averaged*, unity-based concentration along the measurement path; and (c) multiplying this path-averaged concentration (mg/m^3) by the TDL measurement path length (m).

For the primary project goal, the unity-based emission rate assumed that emissions were uniform across the entire source surface (i.e., there were no "hot spots"), and that only a single source existed. However, for the secondary project goal, hot spots were represented in the unity modeling by assigning a relative emission factor to each source subarea.

In cases where the source is unlikely to emit homogeneously, individual rectangular emission "subareas" must generally be defined for maximum accuracy to be achieved. The *relative source strength* of each subarea is expressed in the area-source technique (and, thus, e-Calc) in terms of multiples of unity, in which the lowest-emitting subarea is assigned a unity emission rate (i.e., 1 mg/s over the entire rectangle), with higher-emitting ("hot-spot") subareas expressed as multiples of unity.

In this case, assignment of relative source strengths was based on results of flux-chamber sampling performed by CNRL across the surfaces of the mine face and tailings pond.

3. Scale Unity-Based Modeling Results to Calculate Emission Rate

The actual emission rate, Q_A, is calculated in accordance with the following ratio:

$$\mathbf{C_M / Q_A = C_U / Q_U} \qquad \textbf{(Equation 2-1)}$$

where:

C_M	=	measured path-integrated concentration (attribution) (mg/m^2);
Q_A	=	actual emission rate (mg/s);
C_U	=	predicted unity-based, path-integrated concentration along the measurement path (mg/m^2);* and
Q_U	=	unity-based emission rate (mg/s).

This equation describes the inherent relationship between: (a) the unity-based dispersion modeling; and (b) the actual emission rate and downwind measurements. The cornerstone of the area-source technique, this ratio states that the measured path-integrated concentration (C_M) is to the actual emission rate (Q_A) as the unity-based, path-integrated (modeled) concentration (C_U) is to *its* unity-based emission rate (Q_U); the only unknown term in this equation is the actual emission rate (Q_A).

Plume Capture

An important feature of the area-source technique (included in the e-Calc software) is the capability of generating accurate emission rates without capturing the entire downwind cross-plume mass. Despite measuring only a portion of this mass, employment of the area-source technique allows a

* The predicted unity-based, path-integrated concentration along the measurement path can be thought of as the concentration the TDL would "see" if the source were emitting at its assigned, unity-based emission rate.

"whole-source" emission rate to be determined. The crosswind plume capture, expressed as a percentage of the plume mass, is derived in accordance with the following equation:

$$\mathbf{PC = (C_U / C_{UE}) \times 100} \qquad \textbf{(Equation 2-2)}$$

where, for any given pollutant:

PC = plume capture (crosswind) (%);
C_U = predicted unity-based, path-integrated concentration along the measurement path (mg/m^2); and
C_{UE} = predicted unity-based, path-integrated concentration along an extended measurement path (mg/m^2).

The "extended" measurement path includes the actual TDL beam-path but, for dispersion modeling purposes, this path is extended laterally (each direction from the actual beam-path endpoints) to distances beyond which the predicted impacts are essentially zero.

Meteorological Data

As discussed earlier, coincident onsite meteorological monitoring data is required for simulating atmospheric dispersion and transport, as required in AERMOD. Dispersion and transport parameters are calculated and assigned by e-Calc 2, based on measured and calculated meteorological data (addressed in subsequent sections of this report).

2.3 Functional Logic

Figure 2-3 presents the functional logic for e-Calc 2.

FIGURE 2-3. E-CALC 2 FUNCTIONAL LOGIC

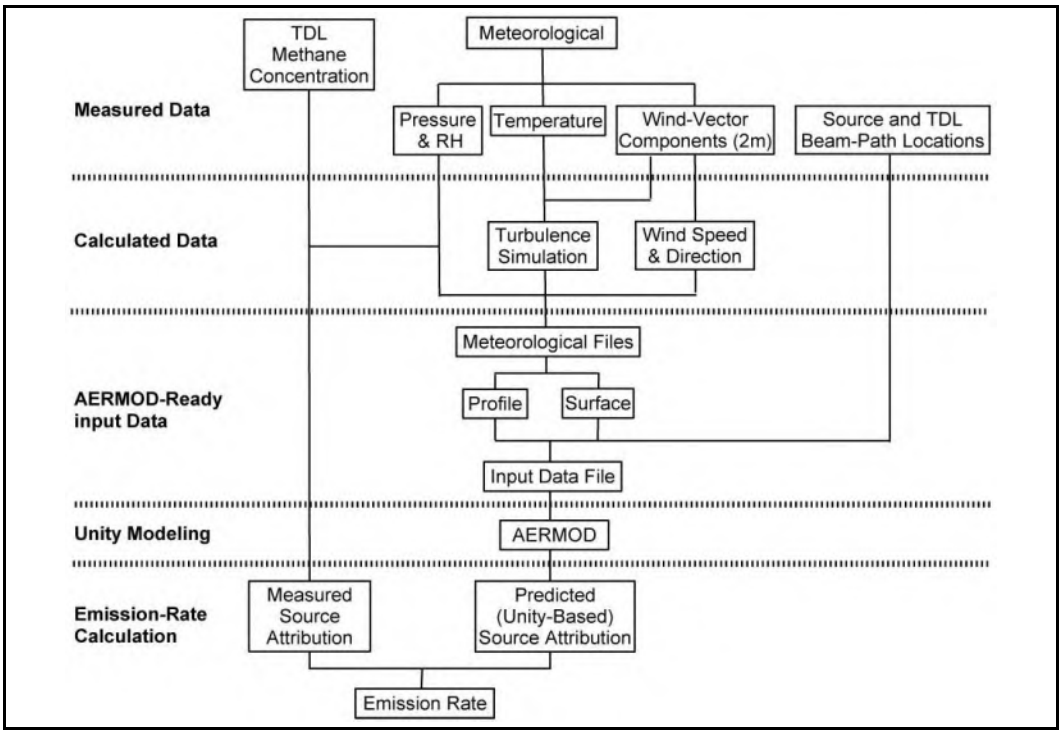

The main elements of this logic are discussed next.

Measured Data

Measured data consists of the TDL methane concentration(s), meteorological parameters, and source and TDL beam-path locations.

TDL Methane Concentration(s)

These are the measurements for determining source attribution. In general, this requires subtracting the downwind, path-integrated concentration from the upwind PIC. However, when it can be shown that the upwind PIC is negligible by comparison, source attribution can be reasonably approximated simply from the downwind PIC.

Meteorological Parameters

Measured meteorological parameters consist of vector component wind speed (u,v,w), ambient temperature, relative humidity, and barometric pressure, all from a height of 2 meters (except pressure, 0 to 1 meter).

Source and TDL Beam-Path Locations

A GPS (global positioning system) is used to determine the precise locations of the source, as well as the downwind TDL beam-path endpoints.

Calculated Data

The calculated data simulates the atmospheric turbulence in order for acceptance by AERMOD (i.e., "AERMOD-ready"). As discussed more thoroughly in Section 6.1.1, e-Calc 2 employs the eddy-correlation (or covariance) approach, which requires the measurement of wind using sonic anemometry. Covariance statistics are used to determine the friction velocity. The power-law equation is then used to generate the vertical wind-speed profile in the lower few meters of the atmosphere, based on the calculated friction velocity and the sonic anemometer wind measurements.

AERMOD-Ready Input Data

All meteorological data must be in precise formats for AERMOD acceptance. Two types of AERMOD-ready files are generated: a "profile" file and a "surface" file.

Profile File

The profile file ("pfl") contains the meteorological data necessary to create a vertical wind-speed profile. This data consists of wind speed and direction, as well as the information to simulate turbulence. This latter information includes temperature and wind-based statistics to estimate the fluctuating components of the wind.

Surface File

The surface file ("sfc") contains standard meteorological surface observations (wind speed, wind direction, and temperature, all from measurements at 2 meters), together with turbulence estimates. This includes other calculated parameters as discussed in Section 2.4.

Unity Modeling

The purpose and procedure for performing the unity modeling in AERMOD is described in Step 2 of the area-source technique approach (see Section 2.2.4).

Emission-Rate Calculation

Figure 2-4 presents an example Monitoring Event Analysis Screen (actual screen from the field-testing). The methane emission rate is calculated in accordance with Equation 2-1, presented in Step 3 of the area-source technique approach (Section 2.2.4). Review, editing, validation, and printing of e-Calc results are performed by pressing the "Edit/Print Event" button at the bottom of this screen.

FIGURE 2-4. EXAMPLE MONITORING EVENT ANALYSIS SCREEN

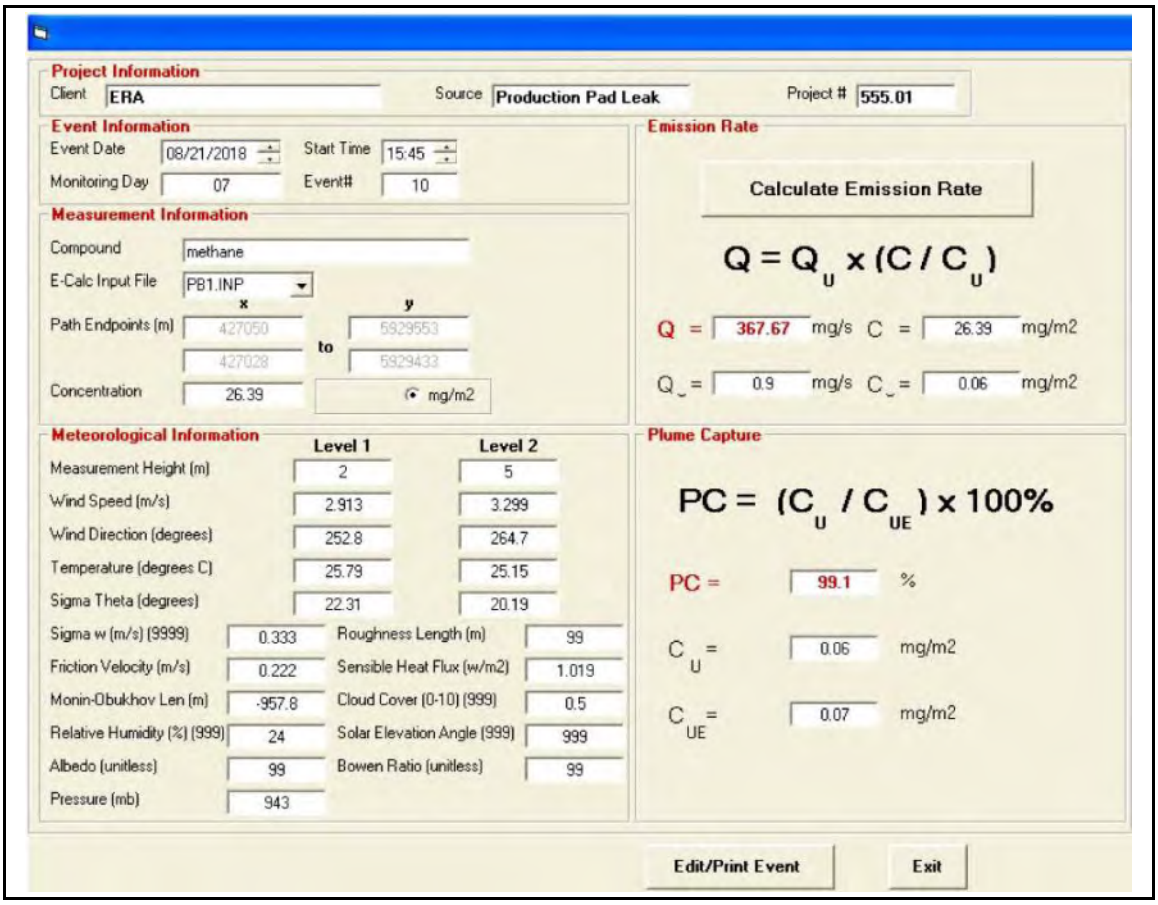

2.4 Required Input Data and Associated Usage

Table 2-1 identifies all input data collected to support e-Calc 2. Also depicted is whether each parameter was measured or calculated.

TABLE 2-1. REQUIRED INPUT DATA TO SUPPORT E-CALC 2

Parameter (Monitoring Event-Specific)	Data Type (15-Minute)	
	Measured	Calculated
Global Positioning System		
TDL beam-path endpoints	✔	
Source location (including source height above grade)	✔	
Tunable Diode Laser System		
Methane attribution (path-integrated concentration)	✔	
Attribution correction (for temperature and pressure)		✔
Archived data	✔	✔
Meteorological Instrumentation		
Vector component (u,v,w) wind speed (2m)	✔	
Vector component (u, v) wind speed (5m)	✔	
Horizontal wind speed		✔
Wind direction		✔
Standard deviation of the horizontal wind direction		✔
Standard deviation of the vertical wind speed		✔
Ambient temperature (2 and 5m)	✔	
Virtual temperature		✔
Dew-point temperature (2m)		✔
Relative humidity (2m)	✔	
Barometric pressure (0 to 1m)	✔	
Friction velocity		✔
Monin-Obukhov length		✔
Sensible heat flux		✔
Archived data	✔	✔
E-Calc 2 Software		
Methane emission rate (mass-per-time)		✔
Methane plume capture		✔
Archived data (via MS Access Database Software)	✔	✔

Set-up functions for e-Calc 2 included the siting of the meteorological tower and TDL system, based on forecasted conditions, to determine the appropriate upwind-downwind orientation. A GPS unit was employed to obtain location coordinates for the TDL beam-path endpoints, meteorological instrumentation, and the suspected emissions-source location.

All monitoring events began precisely on the hour or 15 minutes thereafter (e.g., 8:00, 8:15, etc.). Raw, path-integrated TDL methane concentrations (units of ppm-m) were processed with coincident temperature and pressure measurements (15-minute-averaged) to convert these concentrations to units suitable for input into e-Calc 2 (i.e., mg/m^2). All TDL data (both measured and calculated), together with associated diagnostic data, were archived to facilitate independent validation.

The meteorological instrumentation provided direct measurements of 1-second (1 Hz) values, including vector wind components (u,v,w), temperature, relative humidity, and barometric pressure. These data were processed to calculate event-averaged meteorological values, including horizontal wind direction and speed, and standard deviations of the horizontal wind direction and vertical wind speed. Additionally, representative values of friction velocity, sensible heat flux, and Monin-Obukhov length were calculated from the appropriate covariance statistics between the vector wind components, and between the temperature and w vector wind component. Event-averaged relative humidity and atmospheric pressure measurements were also required.

The meteorological data acquisition system was programmed to archive all meteorological parameter data (measured and calculated), together with the back-up values to facilitate QC (quality control) checks, independent validation, and potential R&D studies.

For each measurement configuration, e-Calc 2 employed the source and measurement-path location information (assembled during the set-up function), and generated the meteorological control pathway for retrieval of the surface and profile meteorological data. Upon monitoring event completion, e-Calc 2 automatically assembled the event-specific "sfc" and "pfl" data files, and ran AERMOD to predict the unity-based attribution (incorporating a user-specified unity emission rate). As detailed in Section 2.2.4, the software then automatically calculated the actual emission rate by scaling the predicted unity modeling emission rate based on the measured path-integrated TDL methane concentration (see Equation 2-1) and associated plume capture (see Equation 2-2).

Results were generated (on-screen and hard copy) within 1 minute of monitoring event completion. For each event, a data-base file was generated to retain all input data and output information, together with the AERMOD input and output files supporting the unity-based attribution predictions.

SECTION 3 – ACCO MINE-FACE AND TAILINGS POND ANALYSES

The secondary goal of this ERA project was to apply e-Calc (both versions) to re-create fugitive methane and carbon dioxide emission rates from the CNRL mine-face and tailings pond operations in Fort McMurray. As discussed in Section 1.2, the intent was to use onsite, 15-minute-averaged path-integrated methane and carbon dioxide data, collected across portions of these sources in 2015 and 2016 by CNRL using a Boreal Laser TDL spectrometer, together with onsite, coincident meteorological data and contemporaneous flux-chamber sampling data (also collected by CNRL). All data supporting this secondary goal was provided by ACCO; accordingly this data is hereafter referred to as the ACCO data.

Achievement of this secondary goal has demonstrated e-Calc to be a viable and attractive alternative to the techniques currently employed for measuring GHG's from sources as large as mine faces and tailings ponds. Accordingly, the time and cost for GHG reporting from such sources can be greatly reduced.

The Major Deliverable for Milestone A was submitted to ERA on March 12, 2018; results of that analysis were based strictly on e-Calc 1. On January 1, 2019, we submitted the Major Deliverable for Milestone G, which repeated the Milestone A analysis using e-Calc 2. Because much of the information in the Milestone G Report was common to both sets of analyses, we structured the latter report to supercede the Milestone A Report.

Section 3.1 identifies the ACCO objectives. **Section 3.2** discusses the criteria developed for determining the validity of source-attribution data. **Section 3.3** presents the TDL measurement configurations and related information. **Section 3.4** presents the universe of valid "measurement event pairs." **Section 3.5** provides all e-Calc results. **Section 3.6** describes how well ACCO's objectives were achieved, including a discussion on the data quality issues adversely affecting the e-Calc results.

3.1 ACCO Objectives

ACCO identified four specific objectives (achievement of which would be of considerable value):

- To provide best estimates of methane and carbon dioxide emissions, including discernment of any diurnal trends;

- To develop methane/carbon dioxide emission-ratio profiles;

- To assess whether upwind sources had a significant effect upon the reported methane and carbon dioxide attribution from the mine face and tailings pond; and

- To provide recommendations on the type and quality of data needed to optimize e-Calc performance in the future.

Results of these analyses were presented in the context of the above ACCO objectives for e-Calc 1 and e-Calc 2. However, it is important to note that the ACCO data was collected to satisfy the input requirements of CALPUFF – a model applied by CNRL, also in its inverse form. As it turned out, while the ACCO data was voluminous (more than 2,600 combined methane and carbon dioxide 15-minute-averaged TDL measurements for both sources over the 2 years), we were able to use only a small subset of it. Still, we were able to reasonably address these objectives.

3.2 Criteria for Valid Source-Attribution Data

Selection criteria were developed and systematically applied to the universe of ACCO data to determine, for e-Calc application, the validity of a given set of coincident 15-minute-averaged upwind/downwind measurements; i.e., a valid measurement event pair (MEP). With a few caveats and exceptions, these selection criteria were:

- Contemporaneous MEP's must have existed for methane and carbon dioxide;

- Attribution must have existed for both compounds (i.e., downwind path-integrated concentrations higher than corresponding upwind path-integrated concentrations); and

- The air flow across the source must have been relatively uniform, as evidenced by the two fixed (non-mobile) meteorological towers.

  For the mine face, this last criterion translated to:

  - a wind speed equal to or greater than 3.5 meters per second (m/s) for each tower;
  - a wind direction within 20º of normal to the downwind TDL (each tower); and
  - a wind-direction difference between the two towers of 30º or less.

  For the tailings pond, this last criterion translated to:

  - a wind speed equal to or greater than 2.0 m/s (each tower);
  - a wind direction within 30º of normal to the downwind TDL (each tower); and
  - a wind-direction difference between the two towers of 30º or less.

3.3 TDL Measurement Configurations

Four TDL spectrometers were employed at each source: one each for upwind and downwind methane (CH_4) measurements, and one each for upwind and downwind carbon dioxide (CO_2) measurements.

Methane

Figures 3-1 and **3-2** present the methane TDL measurement configurations for the mine face for 2015 and 2016, respectively. In 2015, the downwind path-length was 474 meters; in 2016, the downwind path-length was 222 meters.

Figures 3-3 and **3-4** present the methane TDL measurement configurations for the tailings pond for 2015 and 2016, respectively. In 2015, the downwind path-length was 267 meters; in 2016, the downwind path-length was 242 meters.

Locations of the two fixed meteorological towers (Mine Station and Pond Station) are indicated on each figure, as well as the wind direction normal (perpendicular) to the downwind TDL measurement configuration. The upwind and downwind TDL configurations are also depicted, as well as the path-length for each TDL designated as downwind. The upwind TDL path-lengths were not important for this analysis, as the determination of attribution required the adjustment of these values to match the corresponding downwind path-lengths.

Carbon Dioxide

In 2015, downwind paths for the carbon dioxide TDL's (both sources) were coincident with (i.e., adjacent to and of the same magnitude as) the downwind paths for the methane TDL's.

In 2016, downwind carbon dioxide paths (both sources) were still adjacent to the downwind methane paths, but the magnitude was only 20 meters for each source. These paths were positioned at the western-most end of the methane path for the mine face, and the southern-most end of the methane path for the tailings pond.

FIGURE 3-1. MINE-FACE TDL MEASUREMENT CONFIGURATION FOR CH_4: 2015 (SOUTH WIND)

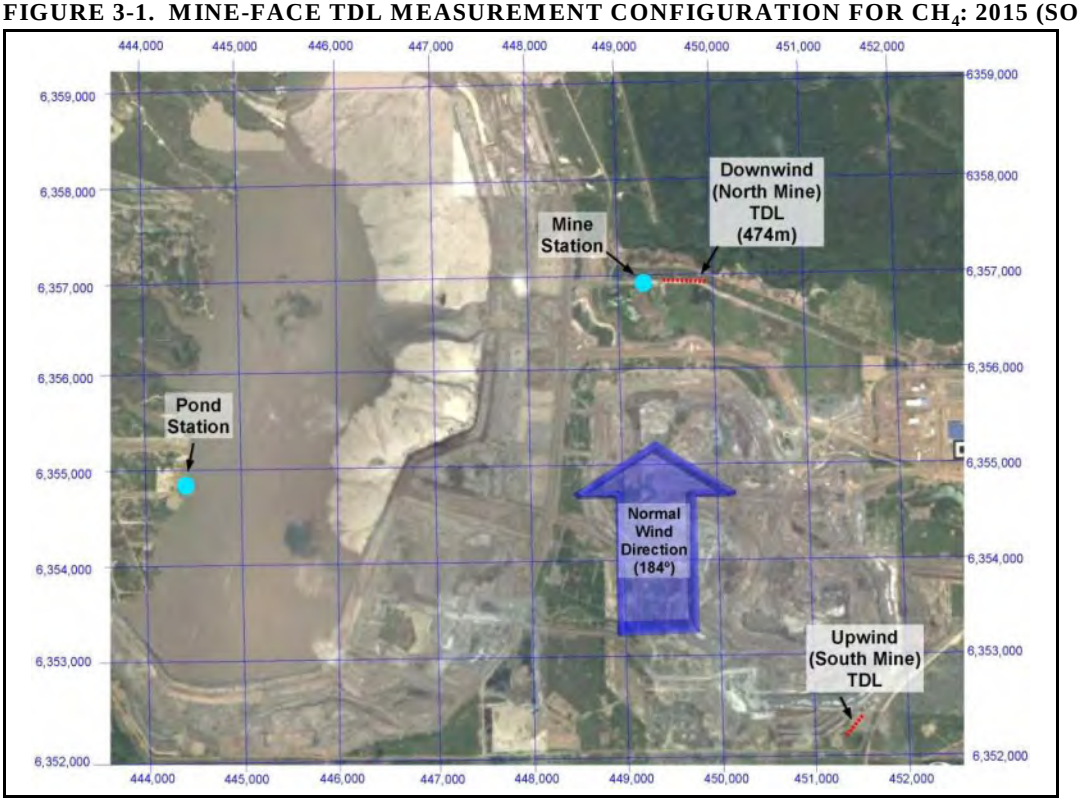

FIGURE 3-2. MINE-FACE TDL MEASUREMENT CONFIGURATION FOR CH_4: 2016 (SOUTH WIND)

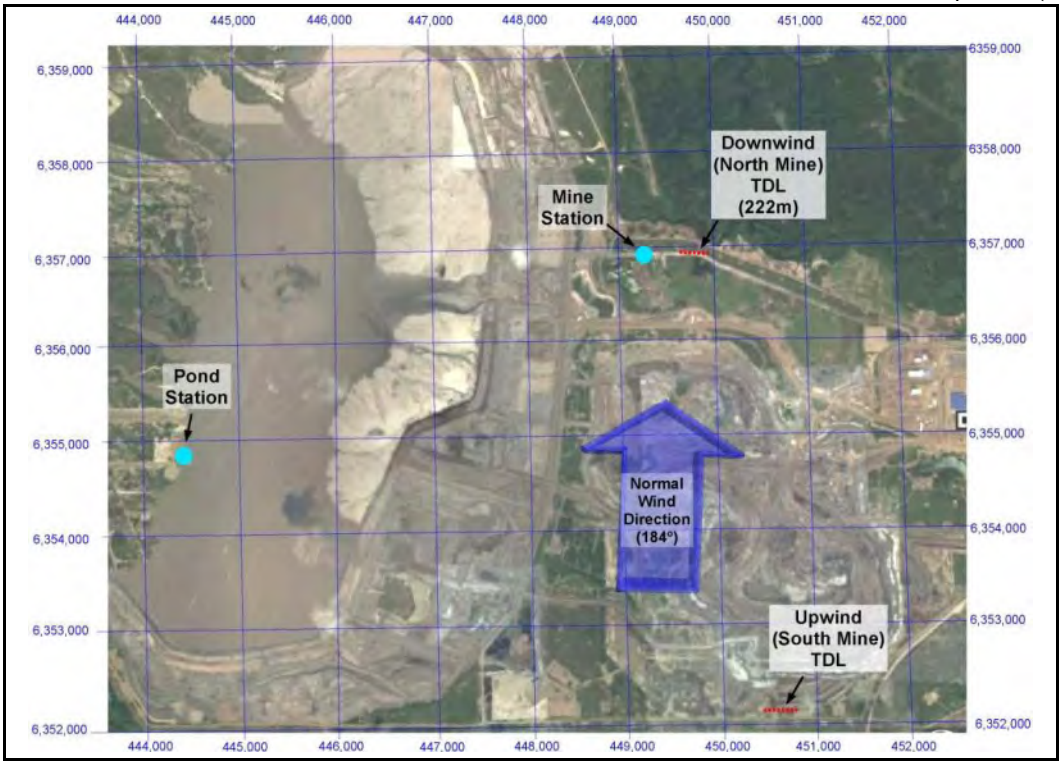

FIGURE 3-3. TAILINGS POND TDL MEASUREMENT CONFIGURATION FOR CH_4: 2015 (EAST WIND)

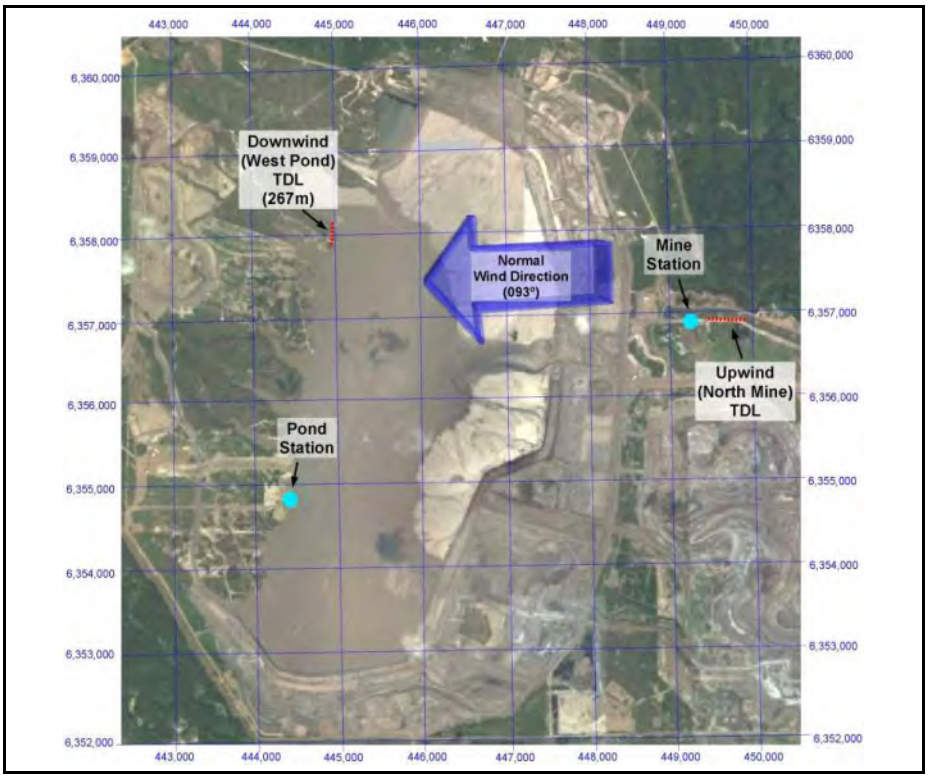

FIGURE 3-4. TAILINGS POND TDL MEASUREMENT CONFIGURATION FOR CH_4: 2016 (WEST WIND)

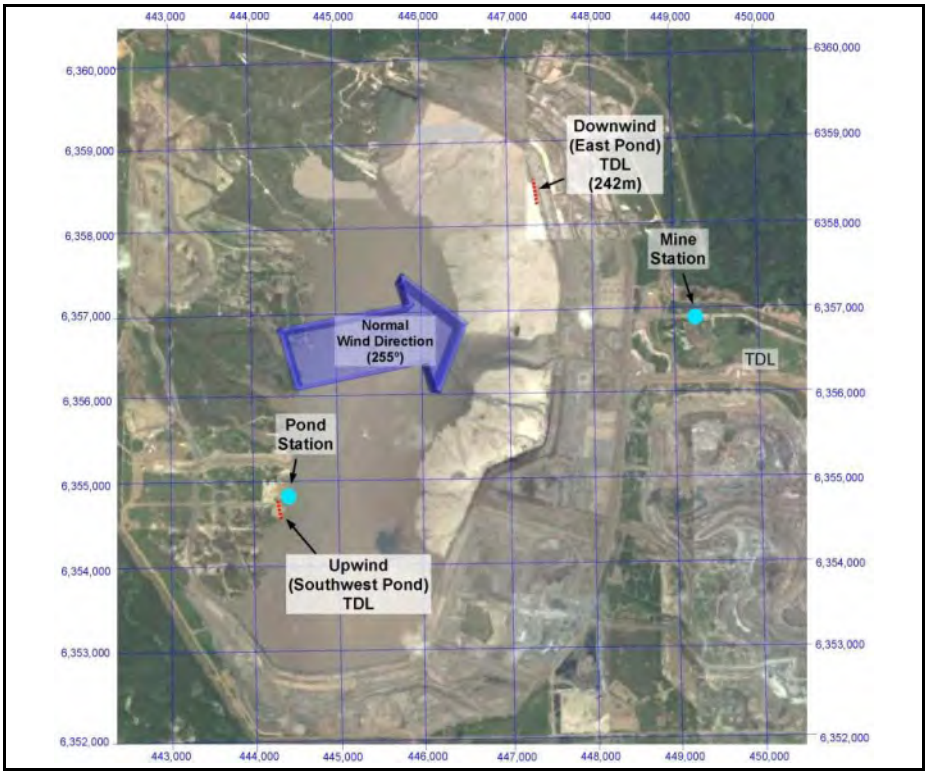

3.4 Valid Measurement Event Pairs

Table 3-1 presents the number of valid measurement event pairs for each source-year combination, where a measurement event pair is defined as a set of coincident, 15-minute-averaged upwind/downwind measurements. A total of 47 valid MEP's were identified, although four of the seven valid MEP's for the tailings pond in 2016 were nighttime events, applicable only for e-Calc 2. Accordingly, 86 individual events were modeled using e-Calc 1 (i.e., one methane and one carbon dioxide event for each valid MEP), while this number was 94 for e-Calc 2.

TABLE 3-1. NUMBER OF VALID MEASUREMENT EVENT PAIRS BY SOURCE AND YEAR

Source	Number of Valid MEPs (CH_4/CO_2)	
	2015	2016
Mine Face	25	7
Tailings Pond	8	7

Tables 3-2 and **3-3** present the valid MEP's for the mine face for 2015 and 2016, respectively. Similarly, **Tables 3-4** and **3-5** present the valid MEP's for the tailings pond for 2015 and 2016, respectively.

For each valid MEP in the following tables, the date, end-time, attribution, and mean wind speed and direction are presented; all wind data are the average of the two fixed meteorological stations. For each compound, attribution was shown as three concentration depictions: ppm, ppm-m, and mg/m^2.

In 2015 (Tables 3-2 and 3-4), the upwind and downwind TDL concentrations were reported only in units of ppm; the ppm-m attributions were derived by multiplying the subtracted ppm values (downwind minus upwind) by the downwind path-lengths.

In 2016 (Tables 3-3 and 3-5), the upwind and downwind concentrations were reported in units of both ppm and ppm-m. Shaded rows in Table 3-5 designate valid MEP's collected during the nighttime and, therefore, were usable only in e-Calc 2.

Finally, all of the carbon dioxide data for the tailings pond in 2016 exhibited anomalously high upwind concentrations, caused either by TDL instrument problems or the presence of an upwind source. For this reason, the carbon dioxide attribution (both sources and years) conservatively assumed a uniform upwind concentration of 402.8 ppm, as determined by the lower 95% confidence limit from the upwind cavity ring-down spectroscopy (CRDS) measurements taken from the southwest tailings pond location in 2016 (22 samples). This value was consistent with regional ambient background levels observed at this time.

TABLE 3-2. VALID MEASUREMENT EVENT PAIRS: 2015 MINE FACE (SOUTH WIND)

MEP ID	Date	End-Time (MDT)	Attribution						Mean Wind	
			ppm		ppm-m		mg/m^2		WD	WS
			CH_4	CO_2	CH_4	CO_2	CH_4	CO_2	(degrees)	(m/s)
Normal WD = 184º (Acceptable Range = 164º – 204º)										
Downwind TDL Path Lengths: CH_4 = 474m; CO_2 = 474m										
MF-1	09/29	09:30	1.600	35.83	758.4	16,983	497.5	30,570	171	3.64
MF-2	09/29	10:30	1.110	39.13	526.1	18,548	345.2	33,386	187	3.70
MF-3	09/29	12:45	0.137	17.63	64.9	8,357	42.6	15,042	183	3.64
MF-4	09/29	16:15	0.343	6.31	162.6	2,991	106.7	5,384	192	3.82
MF-5	09/29	16:45	0.344	7.58	163.1	3,593	107.0	6,467	187	4.09
MF-6	09/29	17:00	0.410	7.16	194.3	3,394	127.5	6,109	184	3.73
MF-7	09/29	17:15	0.431	1.69	204.3	801	134.0	1,442	189	3.72
MF-8	09/29	17:45	0.357	5.28	169.2	2,503	111.0	4,505	190	3.57
MF-9	09/30	09:15	0.973	34.02	461.2	16,125	302.6	29,026	185	3.68
MF-10	09/30	09:30	0.930	24.00	440.8	11,376	289.2	20,477	187	3.83
MF-11	09/30	09:45	0.970	21.93	459.8	10,395	301.6	18,711	185	3.80
MF-12	09/30	12:45	0.322	23.73	152.6	11,248	100.1	20,246	201	4.68
MF-13	09/30	14:30	0.338	9.05	160.2	4,290	105.1	7,721	200	4.80
MF-14	09/30	17:45	0.466	8.37	220.9	3,967	144.9	7,141	203	4.70
MF-15	09/30	18:00	0.488	8.23	231.3	3,901	151.7	7,022	204	4.22
MF-16	10/01	14:30	0.356	10.91	168.7	5,171	110.7	9,308	176	4.06
MF-17	10/01	14:45	0.368	10.46	174.4	4,958	114.4	8,924	185	4.09
MF-18	10/01	15:00	0.402	10.54	190.5	4,996	125.0	8,993	175	4.55
MF-19	10/01	15:15	0.519	11.79	246.0	5,588	161.4	10,059	179	4.15
MF-20	10/01	15:30	0.571	12.29	270.7	5,825	177.6	10,486	182	3.58
MF-21	10/01	15:45	0.558	11.93	264.5	5,655	173.5	10,179	174	4.02
MF-22	10/01	16:00	0.530	11.36	251.2	5,385	164.8	9,692	177	3.84
MF-23	10/01	16:15	0.541	9.49	256.4	4,498	168.2	8,097	178	3.92
MF-24	10/01	16:30	0.501	9.25	237.5	4,385	155.8	7,892	177	4.10
MF-25	10/01	16:45	0.531	9.43	251.7	4,470	165.1	8,046	177	3.88

TABLE 3-3. VALID MEASUREMENT EVENT PAIRS: 2016 MINE FACE (SOUTH WIND)

MEP ID	Date	End-Time (MDT)	Attribution						Mean Wind	
			ppm		ppm-m		mg/m^2		WD	WS
			CH_4	CO_2	CH_4	CO_2	CH_4	CO_2	(degrees)	(m/s)
Normal WD = 184º (Acceptable Range = 164º – 204º)										
Downwind TDL Path Lengths: CH_4 = 222m; CO_2 = 20m										
MF-26	09/06	13:45	0.100	24.88	22.2	498	14.6	896	172	3.59
MF-27	09/06	14:00	0.050	19.76	11.1	395	7.3	711	173	3.77
MF-28	09/06	16:45	0.070	20.96	15.5	419	10.2	755	177	4.16
MF-29	09/06	17:30	0.050	24.38	11.1	488	7.3	878	183	5.22
MF-30	09/09	17:45	0.050	22.76	11.1	455	7.3	819	178	3.95
MF-31	09/09	18:00	0.100	23.81	22.2	476	14.6	857	181	3.77
MF-32	09/09	18:15	0.050	25.95	11.1	519	7.3	934	180	3.76

TABLE 3-4. VALID MEASUREMENT EVENT PAIRS: 2015 TAILINGS POND (EAST WIND)

MEP ID	Date	End-Time (MDT)	Attribution						Mean Wind	
			ppm		ppm-m		mg/m^2		WD	WS
			CH_4	CO_2	CH_4	CO_2	CH_4	CO_2	(degrees)	(m/s)
Normal WD = 093º (Acceptable Range = 063º – 110º)										
Downwind TDL Path Lengths: CH_4 = 267m; CO_2 = 267m										
TP-1	10/03	15:45	0.035	9.19	9.3	2,454	6.1	4,417	91	2.75
TP-2	10/03	16:00	0.010	7.99	2.7	2,133	1.8	3,840	84	3.00
TP-3	10/03	16:15	0.037	5.74	9.9	1,533	6.5	2,759	83	2.95
TP-4	10/03	16:30	0.045	3.71	12.0	991	7.9	1,783	96	3.16
TP-5	10/03	16:45	0.062	3.60	16.6	961	10.9	1,730	93	2.76
TP-6	10/03	17:00	0.056	1.74	15.0	465	9.8	836	98	3.10
TP-7	10/03	17:15	0.059	3.79	15.8	1,012	10.3	1,821	85	2.66
TP-8	10/03	17:30	0.034	3.87	9.1	1,033	6.0	1,860	84	2.58

TABLE 3-5. VALID MEASUREMENT EVENT PAIRS: 2016 TAILINGS POND (WEST WIND)

MEP ID	Date	End-Time (MDT)	Attribution						Mean Wind	
			ppm		ppm-m		mg/m^2		WD	WS
			CH_4	CO_2	CH_4	CO_2	CH_4	CO_2	(degrees)	(m/s)
Normal WD = 255º (Acceptable Range = 225º – 285º)										
Downwind TDL Path Lengths: CH_4 = 242m; CO_2 = 20m										
TP-9	09/02	01:00	0.460	71.77	111.3	1,435	73.0	2,584	233	2.87
TP-10	09/02	01:30	0.120	68.78	29.0	1,376	19.1	2,476	248	3.25
TP-11	09/02	01:45	0.110	68.59	26.6	1,372	17.5	2,469	254	3.47
TP-12	09/02	02:00	0.120	70.05	29.0	1,401	19.1	2,522	261	3.02
TP-13	09/02	07:15	0.050	71.84	12.1	1,437	7.9	2,586	249	2.37
TP-14	09/02	08:15	0.020	72.94	4.8	1,459	3.2	2,626	257	2.79
TP-15	09/02	08:30	0.010	73.06	2.4	1,461	1.6	2,630	249	3.01

3.5 E-Calc Input

Sections 3.5.1 through **3.5.3** present the source-attribution data, the meteorological data, and the relative source-strength apportionment data, respectively, for both sources and years.

3.5.1 Source-Attribution Data

The methane and carbon dioxide attribution for both sources and years were presented in Tables 3-2 through 3-5, and are not reproduced here. E-Calc employs the mg/m^2 representation of source attribution.

3.5.2 Meteorological Data

Tables 3-6 and **3-7** present meteorological data for the mine face for 2015 and 2016, respectively, required for use with both e-Calc 1 and e-Calc 2.

Tables 3-8 and **3-9** similarly present this meteorological data for the tailings pond for 2015 and 2016, respectively, for use with both e-Calc 1 and e-Calc 2. The shaded entries in Table 3-9 depict monitoring events performed during the nighttime; accordingly, these monitoring events could be evaluated only using e-Calc 2.

In these tables, WD is wind direction, WS is wind speed, T is temperature, u* is friction velocity, z_0 is surface roughness length,

TABLE 3-6. REQUIRED MINE-FACE METEOROLOGICAL DATA: 2015 (SOUTH WIND)

			E-Calc 1					E-Calc 2										
			Mean (Both Stations)					Pond Station (2.68m sensor ht)			Mine Station (10.0m sensor ht)			Mean (Both Stations)				
Event ID	Date	End-Time (MDT)	WD (º)	WS (m/s)	T (ºC)	RH (%)	Solar Elev. Angle (º)	WD (º)	WS (m/s)	T (ºC)	WD (º)	WS (m/s)	T (ºC)	u* (m/s)	z_0 (m)	H (W/m^2)	L (m)	RH (%)
MF-1	09/29	09:30	171	3.64	5.8	78	14.1	181	3.23	6.2	160	3.59	5.3	0.18	0.004	5.9	-455.4	78
MF-2	09/29	10:30	187	3.70	6.5	78	20.7	198	3.33	6.7	175	3.60	6.2	0.29	0.031	18.4	-100.0	78
MF-3	09/29	12:45	183	3.64	10.1	70	29.6	187	3.43	10.1	178	3.37	10.1	0.23	0.022	17.0	-211.3	70
MF-4	09/29	16:15	192	3.82	18.4	46	21.2	193	3.51	17.7	190	3.63	19.1	0.31	0.062	-0.3	-14.7	46
MF-5	09/29	16:45	187	4.09	18.3	48	18.1	190	3.62	17.2	184	4.05	19.4	0.24	0.014	-12.8	-34.3	48
MF-6	09/29	17:00	184	3.73	18.3	49	16.4	192	3.15	17.1	175	3.86	19.4	0.25	0.023	-17.2	-45.7	49
MF-7	09/29	17:15	189	3.72	18.3	48	14.7	198	3.11	17.1	180	3.89	19.5	0.27	0.043	-38.3	-114.7	48
MF-8	09/29	17:45	190	3.57	18.2	49	12.9	192	3.03	16.9	188	3.69	19.5	0.27	0.069	-21.6	185.6	49
MF-9	09/30	09:15	185	3.68	7.1	94	12.1	193	3.11	7.1	176	3.81	7.0	0.29	0.041	6.9	98.0	94
MF-10	09/30	09:30	187	3.83	7.2	94	13.8	200	3.25	7.3	174	3.95	7.1	0.24	0.015	7.8	990.6	94
MF-11	09/30	09:45	185	3.80	7.5	93	15.6	200	3.08	7.6	170	4.08	7.3	0.27	0.025	14.6	-132.3	93
MF-12	09/30	12:45	201	4.68	15.5	63	29.3	198	4.49	14.8	203	4.23	16.2	0.50	0.191	37.7	395.5	63
MF-13	09/30	14:30	200	4.80	20.5	50	28.4	199	4.38	19.5	200	4.61	21.5	0.45	0.095	-6.0	-3.9	50
MF-14	09/30	17:45	203	4.70	22.9	45	10.7	207	4.53	22.0	199	4.24	23.7	0.45	0.179	-71.0	296.4	45
MF-15	09/30	18:00	204	4.22	22.7	45	8.8	204	4.16	21.7	203	3.69	23.7	0.45	0.342	-68.8	256.0	45
MF-16	10/01	14:30	176	4.06	22.2	42	28.0	176	3.94	20.9	175	3.62	23.4	0.20	0.015	14.0	-13.6	42
MF-17	10/01	14:45	185	4.09	22.3	42	27.7	180	3.97	21.0	189	3.65	23.5	0.24	0.038	8.1	-21.6	42
MF-18	10/01	15:00	175	4.55	22.5	42	26.4	171	4.51	21.4	179	3.96	23.6	0.24	0.018	4.2	-19.2	42
MF-19	10/01	15:15	179	4.15	22.4	41	25.4	185	3.54	21.2	173	4.27	23.6	0.25	0.013	-4.5	-21.3	41
MF-20	10/01	15:30	182	3.58	23.1	39	24.3	185	3.01	22.3	178	3.72	23.8	0.26	0.029	10.1	-6.7	39
MF-21	10/01	15:45	174	4.02	22.8	40	23.1	180	3.57	21.8	168	3.96	23.8	0.23	0.015	-2.7	-26.3	40
MF-22	10/01	16:00	177	3.84	22.8	40	21.8	182	3.32	21.6	172	3.90	24.0	0.27	0.066	9.2	-54.4	40
MF-23	10/01	16:15	178	3.92	22.9	40	20.4	182	3.63	21.8	173	3.70	24.0	0.24	0.046	-6.1	-52.1	40
MF-24	10/01	16:30	177	4.10	23.0	39	18.9	174	3.67	22.0	180	4.02	24.0	0.21	0.011	-18.2	-51.8	39
MF-25	10/01	16:45	177	3.88	23.0	40	17.3	178	3.55	21.9	175	3.72	24.0	0.22	0.009	3.5	-1529.2	40

TABLE 3-7. REQUIRED MINE-FACE METEOROLOGICAL DATA: 2016 (SOUTH WIND)

			E-Calc 1					E-Calc 2										
			Mean (Both Stations)					Pond Station (5.6m sensor ht)			Mine Station (5.6m sensor ht)			Mean (Both Stations)				
Event ID	Date	End-Time (MDT)	WD (º)	WS (m/s)	T (ºC)	RH (%)	Solar Elev. Angle (º)	WD (º)	WS (m/s)	T (ºC)	WD (º)	WS (m/s)	T (ºC)	u* (m/s)	z_0 (m)	H (W/m^2)	L (m)	RH (%)
MF-26	09/06	13:45	172	3.59	16.6	50	38.7	165	3.31	15.7	178	3.46	17.6	0.26	0.019	44.7	-28.9	50
MF-27	09/06	14:00	173	3.77	17.1	50	38.5	164	3.58	16.0	182	3.54	18.1	0.29	0.037	55.0	-35.1	50
MF-28	09/06	16:45	177	4.16	17.9	50	26.6	175	4.06	17.0	178	3.80	18.9	0.31	0.048	3.1	-45.6	50
MF-29	09/06	17:30	183	5.22	16.5	50	21.3	172	6.07	15.4	194	3.78	17.5	0.38	0.055	9.6	-426.1	50
MF-30	09/09	17:45	178	3.95	14.7	50	18.3	177	3.71	14.1	178	3.75	15.3	0.26	0.019	27.1	-50.3	50
MF-31	09/09	18:00	181	3.77	14.8	50	16.4	180	3.64	14.1	182	3.48	15.4	0.25	0.026	19.1	-69.9	50
MF-32	09/09	18:15	180	3.76	14.8	50	14.4	179	3.49	14.1	181	3.60	15.4	0.26	0.020	8.1	-175.3	50

TABLE 3-8. REQUIRED TAILINGS POND METEOROLOGICAL DATA: 2015 (EAST WIND)

			E-Calc 1					E-Calc 2										
			Mean (Both Stations)					Pond Station (2.68m sensor ht)			Mine Station (10.0m sensor ht)			Mean (Both Stations)				
Event ID	Date	End-Time (MDT)	WD (º)	WS (m/s)	T (ºC)	RH (%)	Solar Elev. Angle (º)	WD (º)	WS (m/s)	T (ºC)	WD (º)	WS (m/s)	T (ºC)	u* (m/s)	z_0 (m)	H (W/m^2)	L (m)	RH (%)
TP-1	10/03	15:45	091	2.75	4.0	74	22.3	091	2.40	3.9	090	2.76	4.0	0.19	0.010	47.5	-10.6	74
TP-2	10/03	16:00	084	3.00	4.1	74	21.0	073	2.53	4.0	094	3.12	4.2	0.15	0.029	43.5	-9.6	74
TP-3	10/03	16:15	083	2.95	4.1	74	19.6	096	2.88	4.0	069	2.61	4.2	0.10	0.000	33.9	-2.2	74
TP-4	10/03	16:30	096	3.16	4.1	74	18.1	107	3.10	4.1	084	2.78	4.1	0.16	0.002	29.7	-12.3	74
TP-5	10/03	16:45	093	2.76	4.1	75	16.5	095	2.27	4.1	090	2.94	4.0	0.07	0.000	31.6	-1.0	75
TP-6	10/03	17:00	098	3.10	4.0	75	14.9	106	3.01	4.0	089	2.76	3.9	0.16	0.007	32.3	-10.0	75
TP-7	10/03	17:15	085	2.66	4.0	75	13.2	091	2.77	4.0	078	2.17	3.9	0.12	0.001	40.2	-3.6	75
TP-8	10/03	17:30	084	2.58	4.1	74	11.4	086	2.40	4.0	082	2.43	4.2	0.21	0.185	46.3	-22.0	74

TABLE 3-9. REQUIRED METEOROLOGICAL DATA: 2016 TAILINGS POND (WEST WIND)

			E-Calc 1					E-Calc 2									
			Mean (Both Stations)					Pond Station (5.6m sensor ht)			Mine Station (5.6m sensor ht)			Mean (Both Stations)				
Event ID	Date	End-Time (MDT)	WD (º)	WS (m/s)	Temp (ºC)	RH (%)	Solar Elev. Angle (º)	WD (º)	WS (m/s)	Temp (ºC)	WD (º)	WS (m/s)	Temp (ºC)	u* (m/s)	z_0 (m)	H (W/m^2)	L (m)	RH (%)
TP-9	09/02	01:00	233	2.87	17.0	50	night	230	2.54	16.0	235	2.72	18.0	0.25	0.097	-5.8	296.6	50
TP-10	09/02	01:30	248	3.25	16.5	50	night	257	2.53	15.4	238	3.42	17.6	0.26	0.064	-7.9	183.2	50
TP-11	09/02	01:45	254	3.47	16.1	50	night	261	2.71	15.0	246	3.66	17.2	0.21	0.073	-11.1	64.7	50
TP-12	09/02	02:00	261	3.02	15.6	50	night	268	2.44	14.6	253	3.10	16.7	0.16	0.020	-7.2	47.4	50
TP-13	09/02	07:15	249	2.37	12.9	50	4.0	247	2.32	11.5	250	2.15	14.4	0.18	0.020	-7.4	79.0	50
TP-14	09/02	08:15	257	2.79	13.3	50	12.0	257	2.51	12.2	256	2.76	14.5	0.23	0.019	1.4	-732.5	50
TP-15	09/02	08:30	249	3.01	13.5	50	14.0	250	2.95	12.5	248	2.74	14.6	0.25	0.025	3.5	-345.7	50

3.5.3 Relative Source-Strength Apportionment Data

Table 3-10 presents the number of flux-chamber sampling locations for each source and year. Both methane and carbon dioxide were analyzed from all flux-chamber samples. The locations and concentrations of these samples formed the basis of the relative source strength, as discussed in Section 2.2.4 (Step 2).

TABLE 3-10. NUMBER OF FLUX-CHAMBER SAMPLING LOCATIONS BY SOURCE AND YEAR

Source	Number of Sampling Locations	
	2015	2016
Mine Face	4	3
Tailings Pond	9	9

Figures 3-5 and **3-6** depict the mine-face flux-chamber sampling locations and reported emission rates for 2015 and 2016, respectively. For 2016, the ACCO data included a map which graphically depicted the areal extent of each emission area or regime (reproduced herein as the base map in Figure 3-6). No such map was provided for 2015, however, and ACCO's recommendation was to use the same general layout as 2016. All emission rates (both figures) are reported in units of kilograms per square meter per year.

FIGURE 3-5. MINE-FACE FLUX-CHAMBER SAMPLING LOCATIONS AND EMISSION RATES: 2015

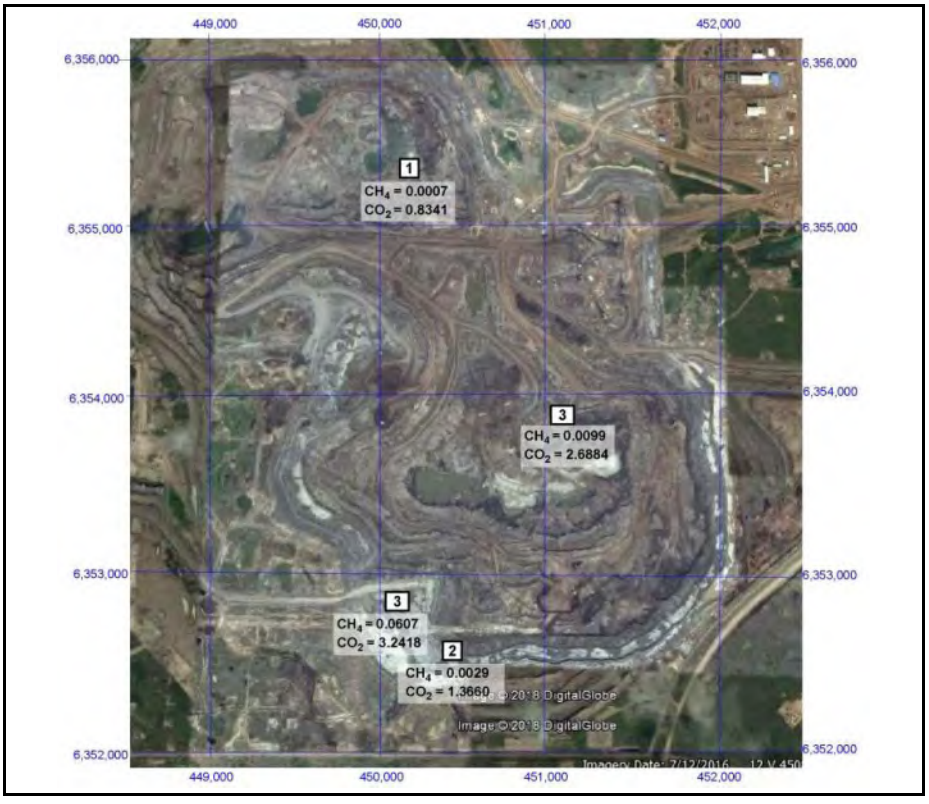

FIGURE 3-6. MINE-FACE FLUX-CHAMBER SAMPLING LOCATIONS AND EMISSION RATES: 2016

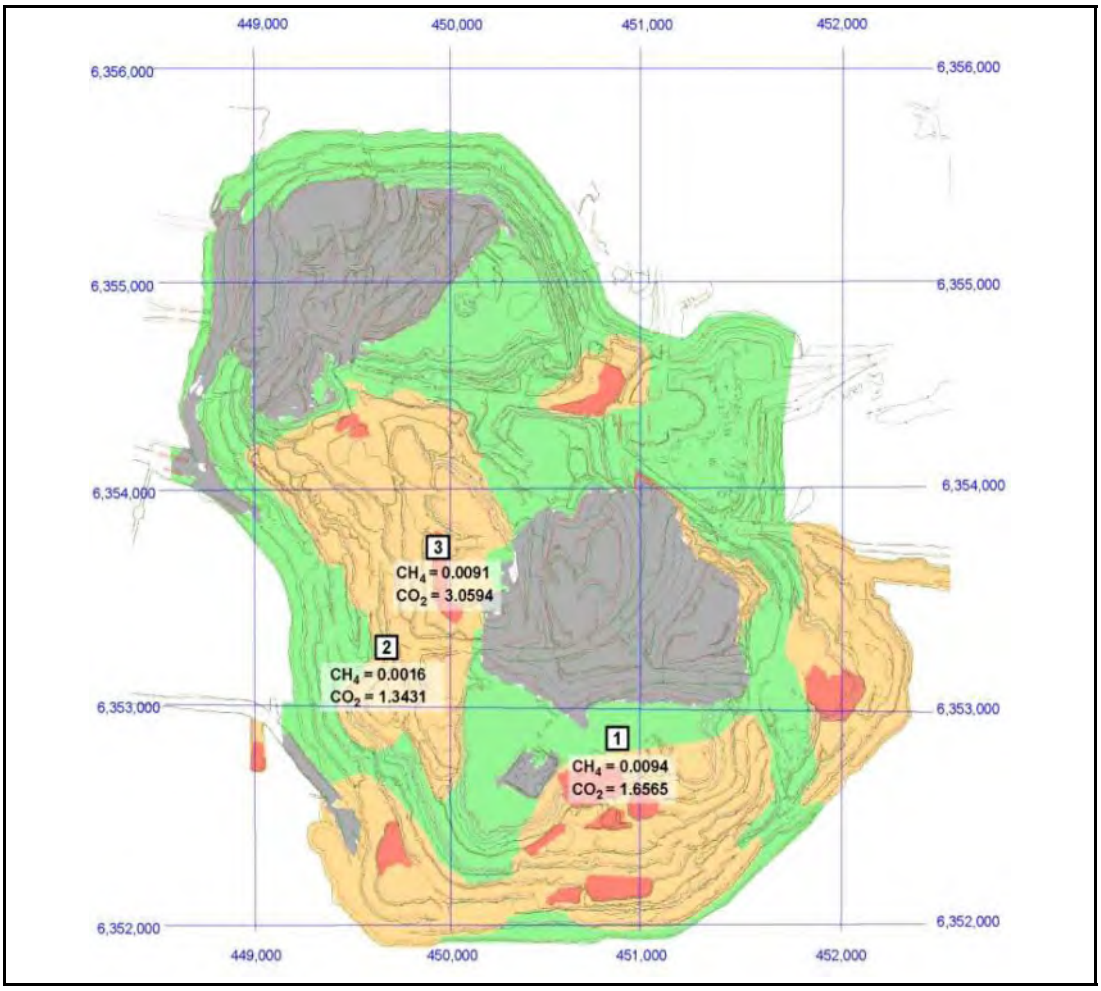

Figures 3-7 and **3-8** depict the tailings pond flux-chamber sampling locations and reported emission rates for 2015 and 2016, respectively. All emission rates (both figures) are again presented in units of kilograms per square meter per year.

FIGURE 3-7. TAILINGS POND FLUX-CHAMBER SAMPLING LOCATIONS AND EMISSION RATES: 2015

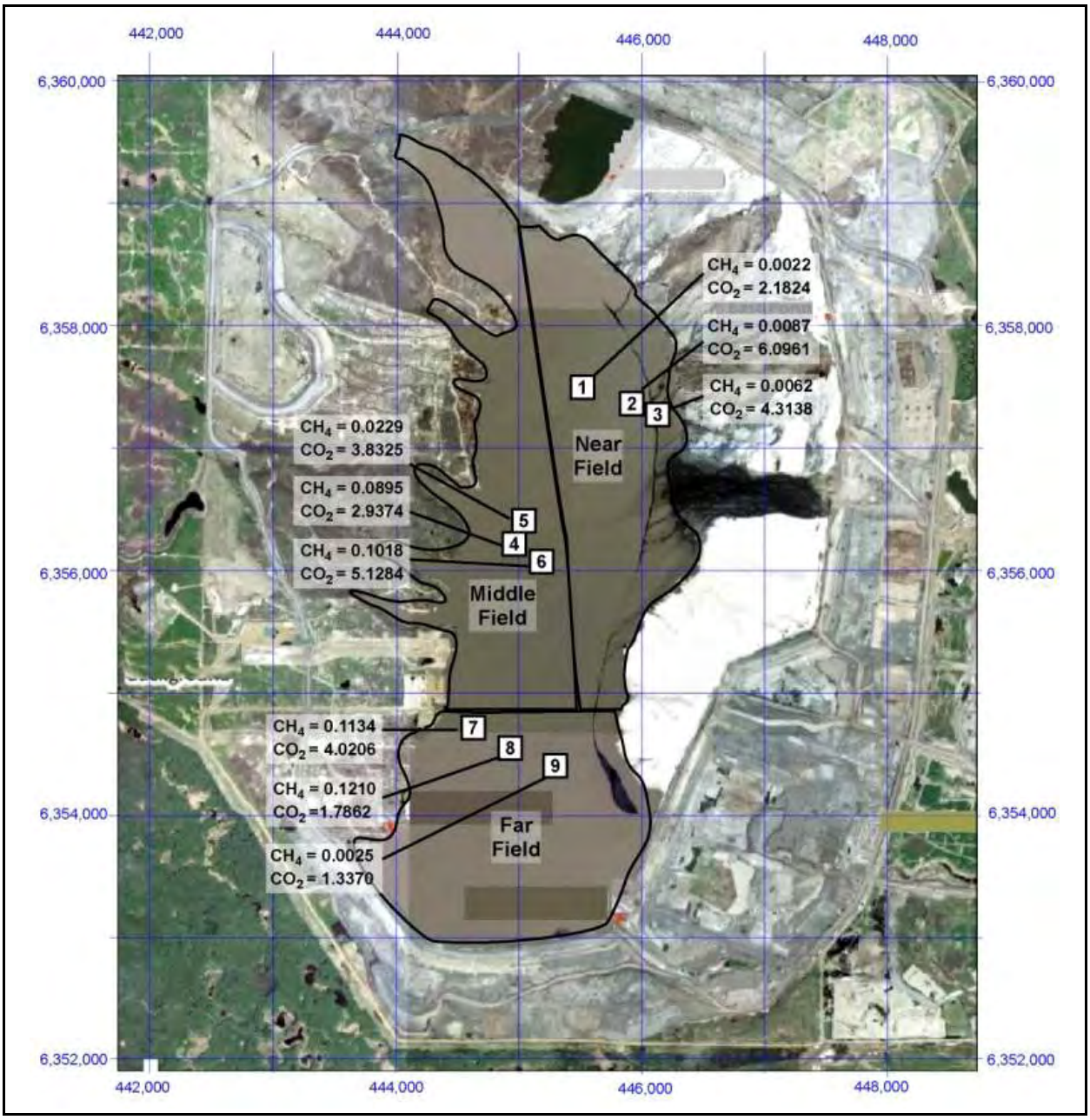

FIGURE 3-8. TAILINGS POND FLUX-CHAMBER SAMPLING LOCATIONS AND EMISSION RATES: 2016

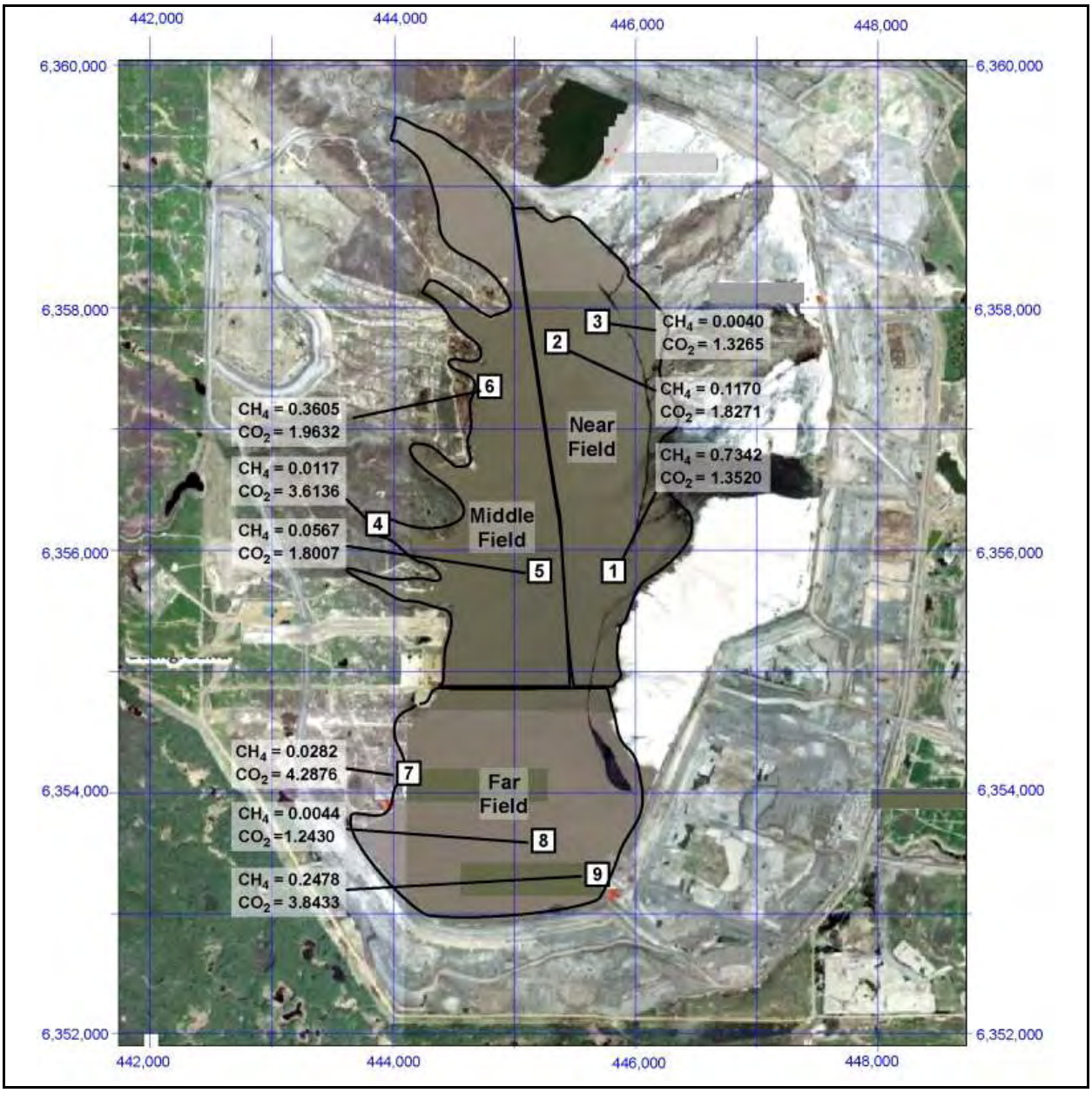

Figure 3-9 graphically depicts the mine-face relative source-strength apportionment (both methane and carbon dioxide) for 2015. The yellow, orange, and red areas correspond to previously derived emissions regimes (not shown), with the relative source strengths reproduced in the figure key (unitless dimensions). The green designation denotes areas in which the emissions were reported to be zero (although no flux-chamber sampling was performed); this is the only source and year in which any zero emissions were assumed.

FIGURE 3-9. RELATIVE MINE-FACE SOURCE-STRENGTH APPORTIONMENT FOR CH_4 AND CO_2: 2015

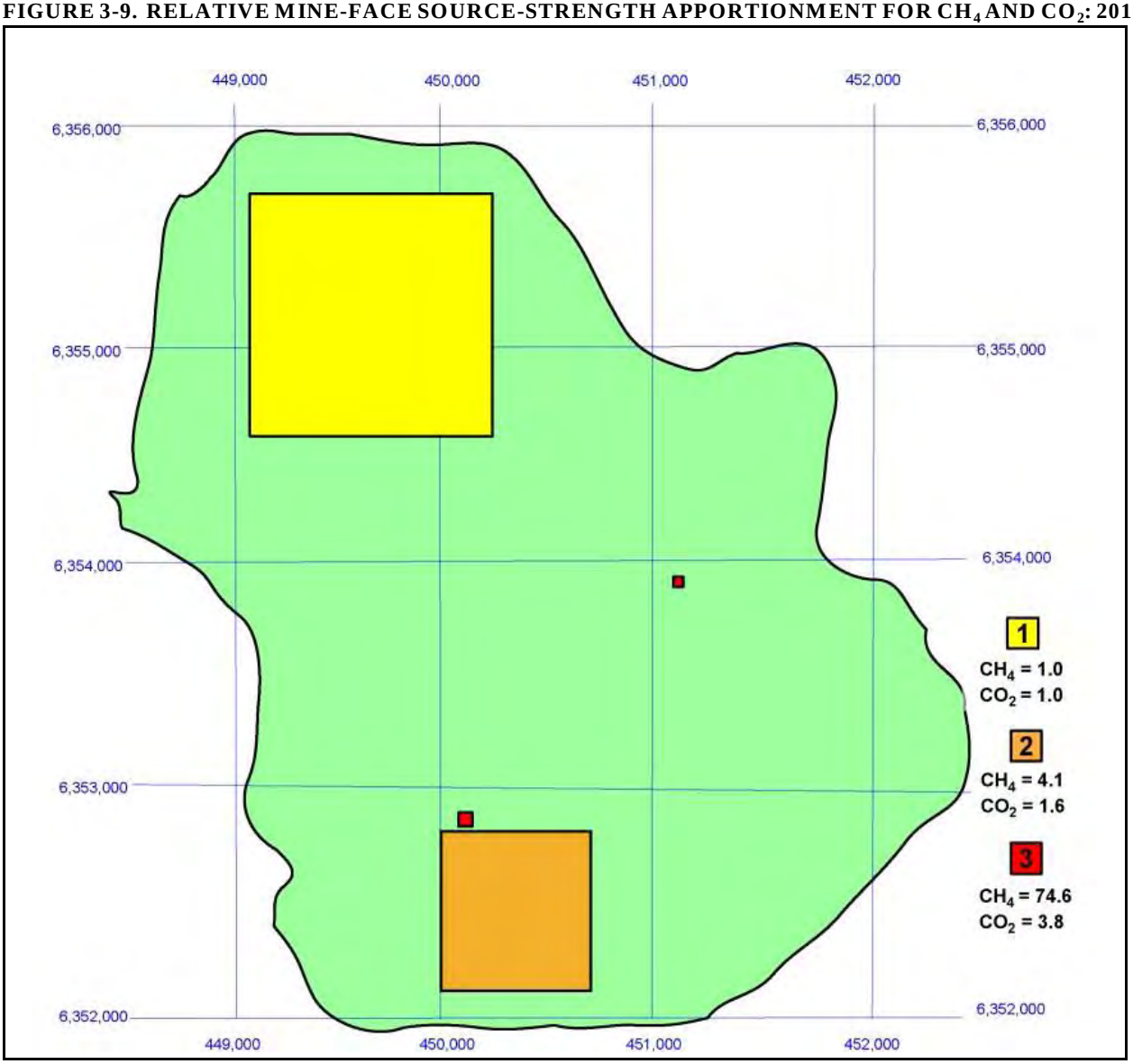

Figure 3-10 graphically depicts the mine-face relative source-strength apportionment (both methane and carbon dioxide) for 2016. As in 2015, the yellow, orange, and red areas correspond to the previously defined emissions regimes (not shown), with the relative source strengths reproduced in the figure key (unitless dimensions).

FIGURE 3-10. RELATIVE MINE-FACE SOURCE-STRENGTH APPORTIONMENT FOR CH_4 AND CO_2: 2016

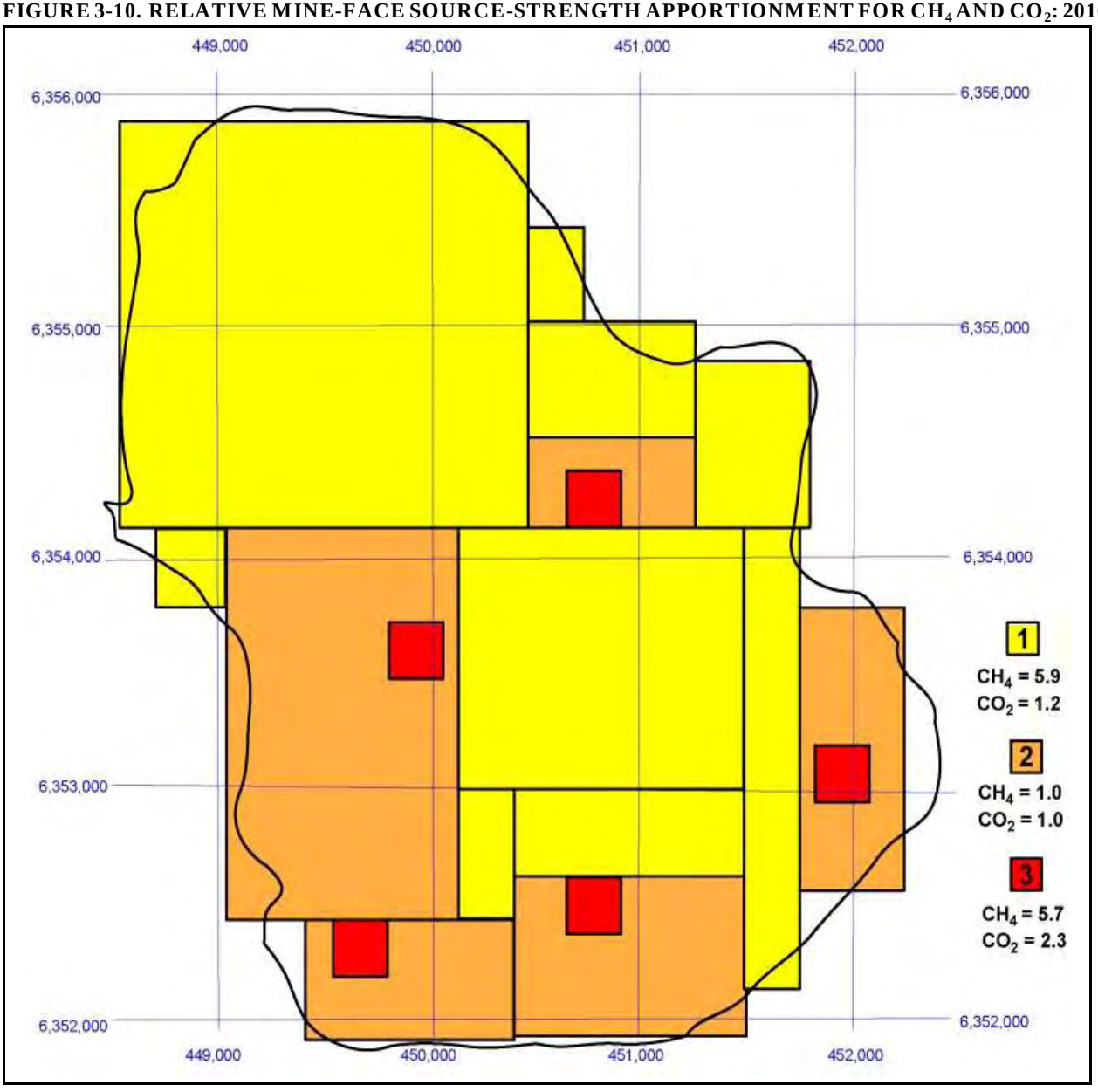

Figures 3-11 and **3-12** present the methane relative source-strength apportionment maps for the tailings pond for 2015 and 2016, respectively. The yellow, orange, and red areas correspond to the previously defined emissions regimes (not shown), with the relative source strengths reproduced in the figure key (unitless dimensions).

.

FIGURE 3-11. RELATIVE TAILINGS POND SOURCE-STRENGTH APPORTIONMENT FOR CH_4: 2015

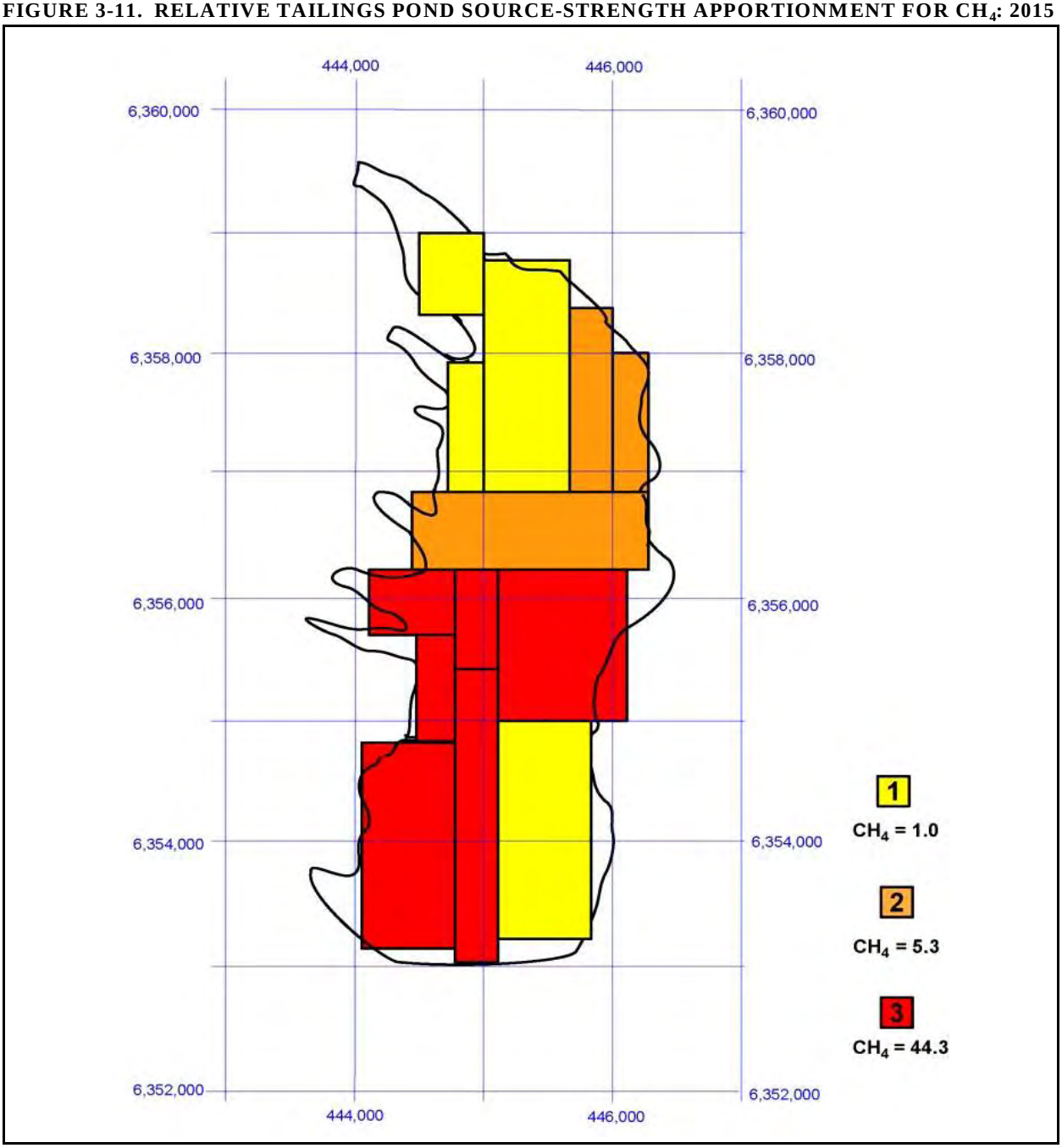

FIGURE 3-12. RELATIVE TAILINGS POND SOURCE-STRENGTH APPORTIONMENT FOR CH_4: 2016

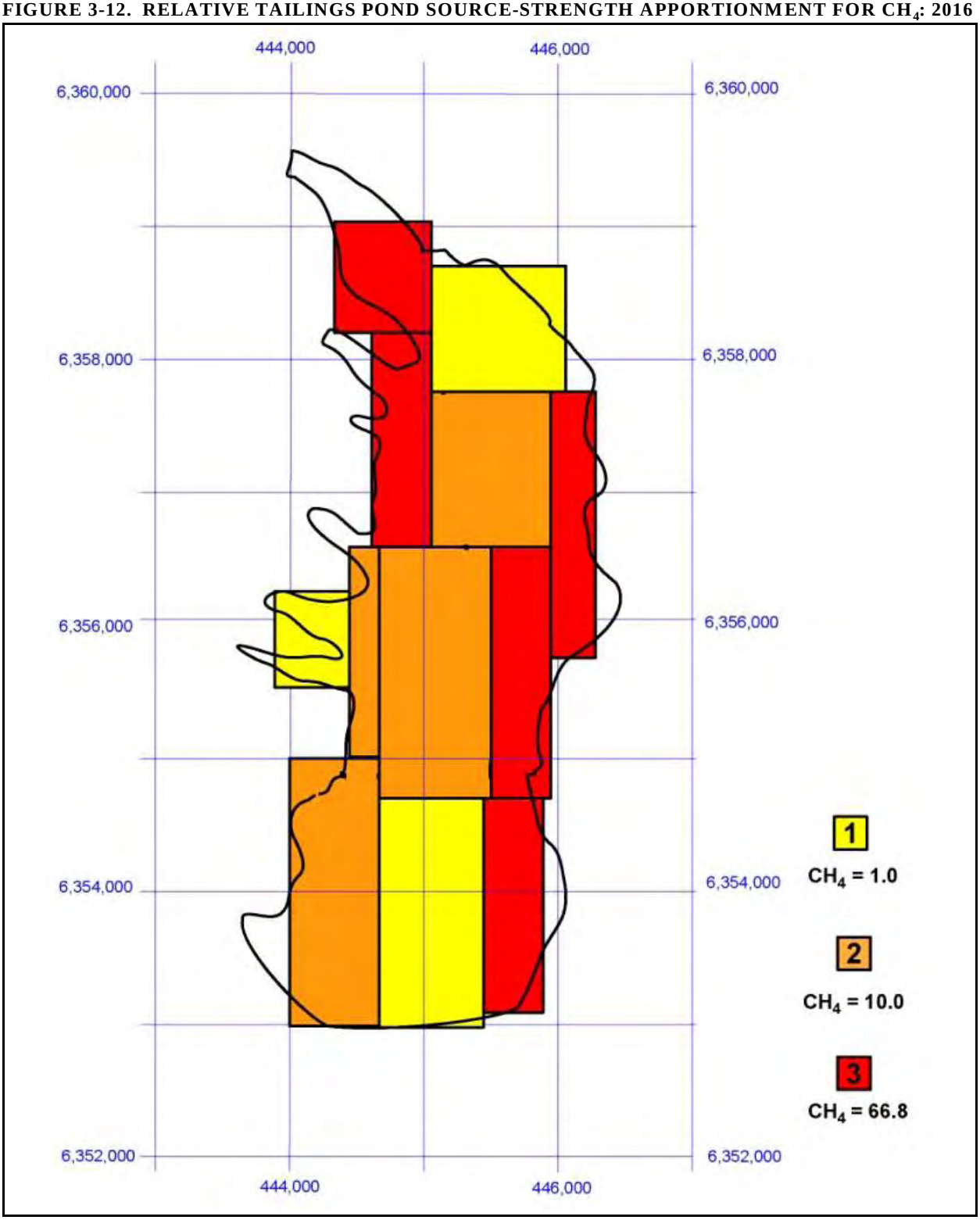

Figures 3-13 and **3-14** present the carbon dioxide relative source-strength apportionment maps for the tailings pond for 2015 and 2016, respectively. The yellow, orange, and red areas correspond to the previously defined emissions (not shown), with the relative source strengths reproduced in the figure key (unitless dimensions).

FIGURE 3-13. RELATIVE TAILINGS POND SOURCE-STRENGTH APPORTIONMENT FOR CO_2: 2015

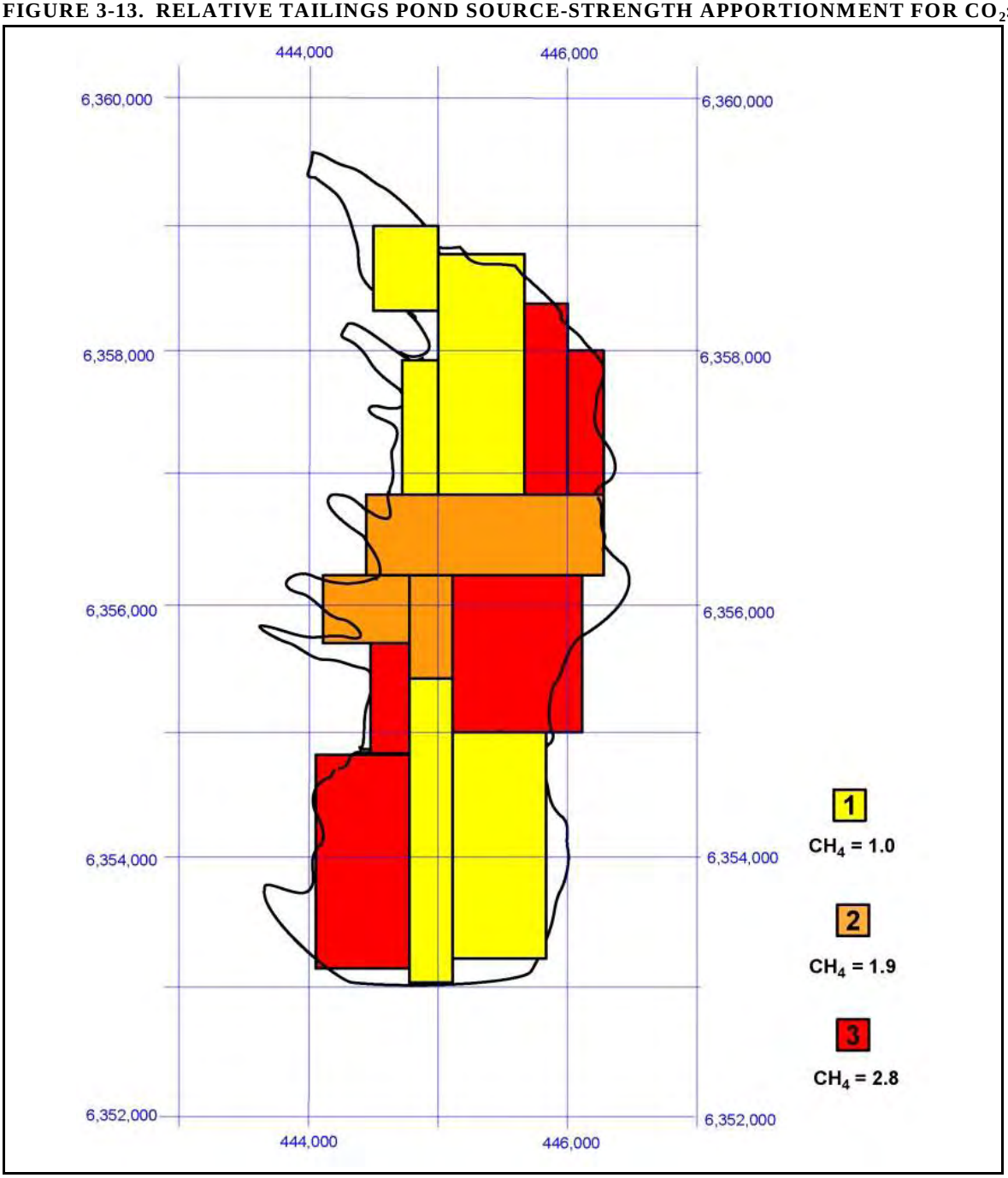

FIGURE 3-14. RELATIVE TAILINGS POND SOURCE-STRENGTH APPORTIONMENT FOR CO_2: 2016

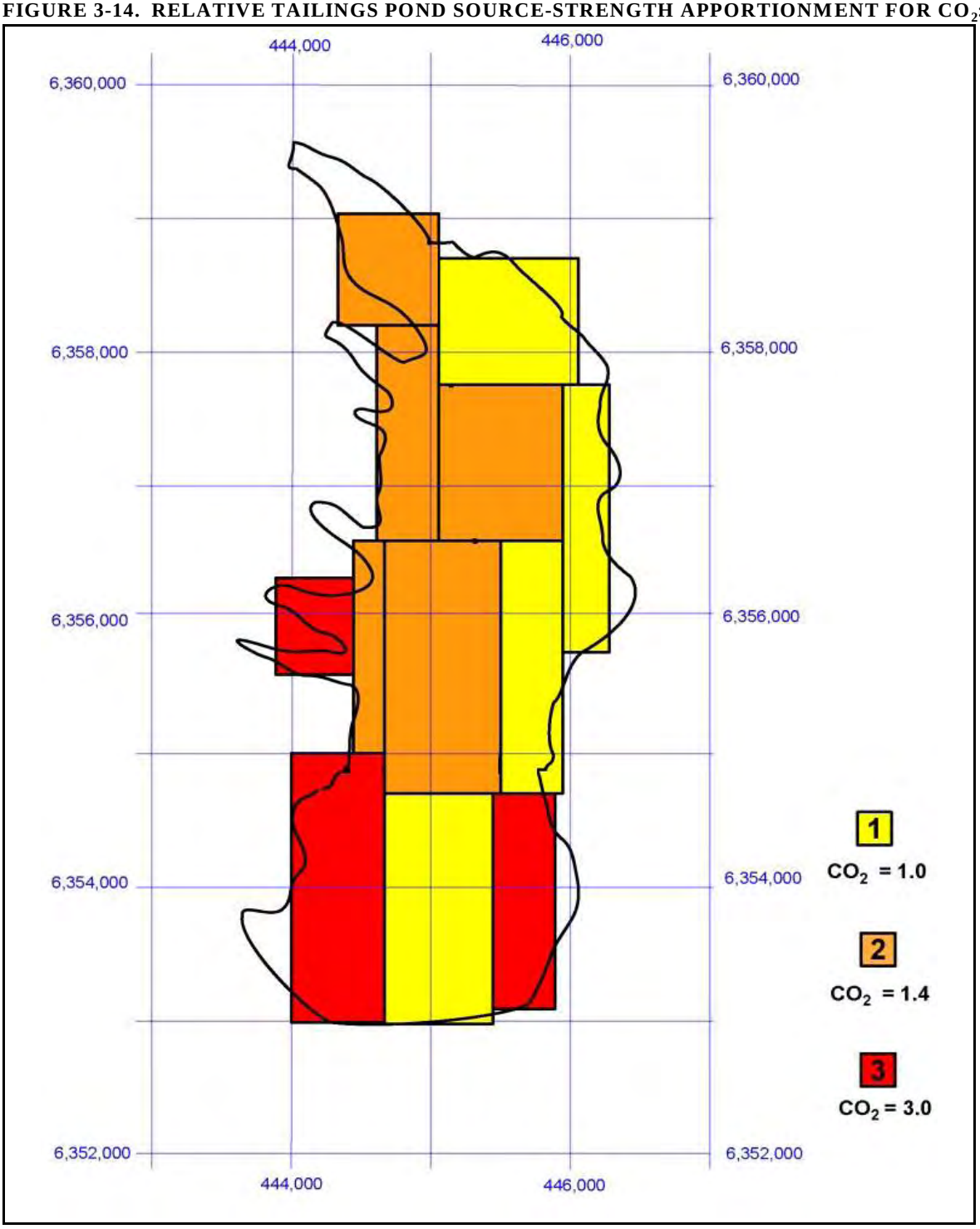

3.6 E-Calc Results

Sections 3.6.1 and **3.6.2** present tabular summaries of all daily e-Calc results (both versions) for the mine face and the tailings pond, respectively. All emission rates in these tables are presented in units of metric tons per year (mT/yr). It was assumed that all calculated 15-minute-averaged emission rates were constant for the entire year. Mean emission rates were calculated for each day, as well as the standard deviation about the mean.

Section 3.6.3 presents a comparative analysis of these results.

3.6.1 Mine Face

Tables 3-11 and **3-12** summarize the mine-face methane and carbon dioxide e-Calc results for 2015 and 2016, respectively.

TABLE 3-11. MINE-FACE E-CALC RESULTS: 2015

Event ID	Date	End-Time (MDT)	Mean Wind		Emission Rate (Metric Tons per Year)			
					Methane		Carbon Dioxide	
			WD (degrees)	WS (m/s)	E-Calc 1	E-Calc 2	E-Calc 1	E-Calc 2
MF-1	09/29	09:30	171	3.64	72,482	30,145	3,095,857	1,111,979
MF-2	09/29	10:30	187	3.70	69,265	76,176	3,785,001	3,609,693
MF-3	09/29	12:45	183	3.64	7,520	4,288	1,593,465	796,041
MF-4	09/29	16:15	192	3.82	27,369	18,940	731,045	474,178
MF-5	09/29	16:45	187	4.09	23,223	12,795	793,062	390,874
MF-6	09/29	17:00	184	3.73	22,681	17,379	642,304	414,819
MF-7	09/29	17:15	189	3.72	28,549	27,532	168,768	145,173
MF-8	09/29	17:45	190	3.57	23,585	8,760	518,990	178,294
				Daily Mean	**34,334**	**24,502**	**1,416,062**	**890,131**
				Standard Deviation (%)	**68.3**	**92.4**	**93.5**	**128.5**
MF-9	09/30	09:15	185	3.68	53,718	50,215	2,999,592	1,064,359
MF-10	09/30	09:30	187	3.83	57,900	49,197	2,316,371	1,704,613
MF-11	09/30	09:45	185	3.80	56,144	71,497	2,027,635	2,170,384
MF-12	09/30	12:45	201	4.68	50,799	25,231	5,102,027	2,505,620
MF-13	09/30	14:30	200	4.80	51,236	38,542	1,876,306	1,386,731
MF-14	09/30	17:45	203	4.70	80,106	66,688	1,949,127	1,606,832
MF-15	09/30	18:00	204	4.22	80,357	48,558	1,832,464	1,100,048
				Daily Mean	**61,466**	**49,990**	**2,586,217**	**1,648,370**
				Standard Deviation (%)	**21.3**	**31.5**	**45.6**	**32.5**
MF-16	10/01	14:30	176	4.06	18,500	6,304	1,029,403	358,747
MF-17	10/01	14:45	185	4.09	23,694	8,887	1,075,947	427,738
MF-18	10/01	15:00	175	4.55	22,787	8,404	1,097,431	436,403
MF-19	10/01	15:15	179	4.15	28,454	16,186	1,128,787	550,089
MF-20	10/01	15:30	182	3.58	29,577	18,516	1,064,032	596,981
MF-21	10/01	15:45	174	4.02	28,108	12,900	1,115,784	466,677
MF-22	10/01	16:00	177	3.84	26,047	15,643	1,001,357	539,911
MF-23	10/01	16:15	178	3.92	27,359	14,190	849,834	400,688
MF-24	10/01	16:30	177	4.10	25,832	9,029	855,379	320,402
MF-25	10/01	16:45	177	3.88	25,928	10,910	825,977	344,571
				Daily Mean	**25,629**	**12,097**	**1,004,393**	**444,221**
				Standard Deviation (%)	**12.7**	**38.0**	**11.7**	**21.1**

TABLE 3-12. MINE-FACE E-CALC RESULTS: 2016

Event ID	Date	End-Time (MDT)	Mean Wind		Emission Rate (Metric Tons per Year)			
					Methane		Carbon Dioxide	
			WD (degrees)	WS (m/s)	E-Calc 1	E-Calc 2	E-Calc 1	E-Calc 2
MF-26	09/06	13:45	172	3.59	5,021	2,997	3,812,147	2,365,615
MF-27	09/06	14:00	173	3.77	2,630	1,747	3,023,040	2,232,796
MF-28	09/06	16:45	177	4.16	4,045	2,494	3,552,436	2,381,583
MF-29	09/06	17:30	183	5.22	3,766	2,687	5,419,692	4,987,179
				Daily Mean	**3,866**	**2,481**	**3,951,829**	**2,991,793**
				Standard Deviation (%)	**25.5**	**21.4**	**26.1**	**44.5**
MF-30	09/09	17:45	178	3.95	2,732	1,498	3,640,661	2,162,306
MF-31	09/09	18:00	181	3.77	5,387	3,013	3,771,239	2,318,150
MF-32	09/09	18:15	180	3.76	2,631	1,550	4,009,550	2,579,866
				Daily Mean	**3,583**	**2,020**	**3,807,150**	**2,353,441**
				Standard Deviation (%)	**43.6**	**42.6**	**4.9**	**9.0**

3.6.2 Tailings Pond

Tables 3-13 and **3-14** summarize the tailings pond methane and carbon dioxide e-Calc results for 2015 and 2016, respectively. The shaded rows in Table 3-14 identify those events which took place during the nighttime, and could be addressed only using e-Calc 2.

TABLE 3-13. TAILINGS POND E-CALC RESULTS: 2015

Event ID	Date	End-Time (MDT)	Mean Wind		Emission Rate (Metric Tons per Year)			
					Methane		Carbon Dioxide	
			WD (degrees)	WS (m/s)	E-Calc 1	E-Calc 2	E-Calc 1	E-Calc 2
TP-1	10/03	15:45	91	2.75	2,776	3,706	247,419	355,101
TP-2	10/03	16:00	84	3.00	941	1,104	258,115	287,232
TP-3	10/03	16:15	83	2.95	3,438	2,242	182,854	128,005
TP-4	10/03	16:30	96	3.16	3,833	3,878	115,811	119,665
TP-5	10/03	16:45	93	2.76	4,755	2,694	99,558	57,520
TP-6	10/03	17:00	98	3.10	4,563	4,805	52,064	55,982
TP-7	10/03	17:15	85	2.66	4,637	4,332	105,097	101,240
TP-8	10/03	17:30	84	2.58	2,624	4,098	103,814	165,156
				Mean	**3,446**	**3,357**	**145,592**	**158,738**
				Standard Deviation (%)	**37.9**	**38.7**	**51.6**	**68.1**

TABLE 3-14. TAILINGS POND E-CALC RESULTS: 2016

Event ID	Date	End-Time (MDT)	Mean Wind		Emission Rate (Metric Tons per Year)			
					Methane		Carbon Dioxide	
			WD (degrees)	WS (m/s)	E-Calc 1	E-Calc 2	E-Calc 1	E-Calc 2
TP-9	09/02	01:00	233	2.87	–	31,501	–	9,710,846
TP-10	09/02	01:30	248	3.25	–	6,586	–	12,078,641
TP-11	09/02	01:45	254	3.47	–	4,185	–	8,476,829
TP-12	09/02	02:00	261	3.02	–	4,382	–	8,211,123
TP-13	09/02	07:15	249	2.37	2,341	1,343	10,040,075	5,611,226
TP-14	09/02	08:15	257	2.79	1,320	2,326	15,091,770	26,818,851
TP-15	09/02	08:30	249	3.01	632	1,127	13,775,174	24,949,262
				Mean	**1,431**	**7,350**	**12,969,006**	**13,693,825**
				Standard Deviation (%)	**60.1**	**147.2**	**20.2**	**62.5**

3.6.3 Comparative Analysis

Table 3-15 presents the e-Calc-derived mean methane and carbon dioxide mT/yr emissions rates by source and year, as well as the ratio between carbon dioxide and methane (CO_2/CH_4 ratio). In general, carbon dioxide emissions were much greater than methane for both sources. In each year, e-Calc 1 predicted significantly greater emission rates than e-Calc 2 for the mine face (both compounds), but similar emission rates to e-Calc 2 for the tailings pond.

TABLE 3-15. MEAN E-CALC EMISSION RATES BY SOURCE AND YEAR

	Emission Rate (Metric Tons per Year)							
	Mine Face				Tailings Pond			
	2015		2016		2015		2016	
Compound	e-Calc 1	e-Calc 2	e-Calc 1	e-Calc 2	e-Calc 1	e-Calc 2	e-Calc 1	e-Calc 2
Methane	38,449	26,676	3,745	2,284	3,446	3,357	1,431	7,350
Carbon Dioxide	1,579,038	924,074	3,889,824	2,718,214	145,592	158,738	12,969,006	13,693,825
CO_2/CH_4 Ratio	41	35	1,039	1,190	42	47	9,063	1,863

Mine-Face Methane Emissions

From Table 3-15, mean mine-face methane emissions were about 10 times greater in 2015 than 2016 for e-Calc 1, and about 12 times greater for e-Calc 2.

From Table 3-11, in 2015 (based on 25 valid events over 3 days), the methane emission rates ranged from 7,520 to 80,357 mT/yr (spanning a factor of 10.7) for e-Calc 1, and from 4,288 to 76,176 mT/yr (factor of 17.8) for e-Calc 2.

In 2016 (Table 3-12, based on seven valid events over 2 days), the methane emission rates ranged from 2,630 to 5,387 mT/yr (factor of 2.0) for e-Calc 1, and from 1,498 to 3,013 mT/yr (factor of 2.0 again) for e-Calc 2.

Mine-Face Carbon Dioxide Emissions

From Table 3-15, mean mine-face carbon dioxide emissions were about 2.5 times greater in 2016 than 2015 for e-Calc 1, and about 2.9 times greater for e-Calc 2.

From Table 3-11, in 2015 (based on 25 valid events over 3 days), the carbon dioxide emission rates ranged from 168,768 to 5,102,027 mT/yr (factor of 30.2) for e-Calc 1, and from 145,173 to 3,609,693 mT/yr (factor of 24.9) for e-Calc 2.

In 2016 (Table 3-12, based on seven valid events over 2 days), the carbon dioxide emission rates ranged from 3,023,040 to 5,419,692 mT/yr (factor of 1.8) for e-Calc 1, and from 2,162,306 to 4,987,179 mT/yr (factor of 2.3) for e-Calc 2.

Tailings Pond Methane Emissions

From Table 3-15, mean tailings pond methane emissions were about 2.4 times greater in 2015 than 2016 for e-Calc 1, but about 2.2 times greater in 2016 than 2015 for e-Calc 2.

From Table 3-13, in 2015 (based on eight valid events over 1 day), the methane emission rates ranged from 941 to 4,755 mT/yr (factor of 5.1) for e-Calc 1, and from 1,104 to 4,805 mT/yr (factor of 4.4) for e-Calc 2.

In 2016 (Table 3-14, based on three valid events over 1 day), the methane emission rates ranged from 632 to 2,341 mT/yr (factor of 3.7) for e-Calc 1, and from 1,127 to 31,501 mT/yr (factor of 28.0) for e-Calc 2 (including the four valid nighttime events).

Tailings Pond Carbon Dioxide Emissions

From Table 3-15, mean tailings pond carbon dioxide emissions were about 89.1 times greater in 2016 than 2015 for e-Calc 1, and about 86.3 for e-Calc 2.

From Table 3-13, in 2015 (based on eight valid events over 1 day), the carbon dioxide emission rates ranged from 52,064 to 258,115 mT/yr (factor of 5.0) for e-Calc 1, and from 55,982 to 355,101 mT/yr (factor of 6.3) for e-Calc 2.

In 2016 (Table 3-14, based on three valid events over 1 day), the carbon dioxide emission rates ranged from 10,040,075 to 15,091,770 mT/yr (factor of 1.5) for e-Calc 1, and from 5,611,226 to 26,818,851 mT/yr (factor of 4.8) for e-Calc 2 (including the four valid nighttime events).

Observations

The first observation (Table 3-15) was that the mean 2016 carbon dioxide emissions were much greater than those for methane (both sources), while this difference was more than 3 orders of magnitude for each source (both e-Calc versions). And yet in 2015, the e-Calc 1 and e-Calc 2 carbon dioxide emissions were only 41 and 35 times greater, respectively, for the mine face, and 42 and 47 times greater, respectively, for the tailings pond. Not being privy to any data except the raw results as described herein, we were unable to speculate on any physicochemical reasons as to why this might be so.

The second observation concerned the variability about the mean emission rates, as discussed above. Empirically, we would normally be inclined to assign a higher quality to those emissions data with less variability. This would lend the most credence to the mine-face data on October 1, 2015 (Table 3-11) and September 9, 2016 (Table 3-12).

The third observation was the lack of consistency in the overall emissions behavior between the two years (both sources). For example, from Table 3-15, the mean mine-face methane emission rate was

10.3 times greater in 2015 than in 2016 for e-Calc 1, and 11.7 times greater for e-Calc 2. Conversely, for the tailings pond, the mean carbon dioxide emission rate was 89.1 times greater in 2016 than in 2015 for e-Calc 1, and 86.3 times greater for e-Calc 2.

Conclusion

While it might have been tempting to conclude, based on the second observation, that the mine-face emissions data were of a quality higher than the tailings pond data, we asserted that such was not the case. Instead, on a more fundamental level, we believed this observation and the overall lack of reproducibility in the individual events were due primarily to insufficient TDL path-lengths, and that inadequate relative source-strength apportionments and likely problems with the TDL instruments (or their operation) only served to exacerbate the situation.

The quality issues in the ACCO data (in the context of e-Calc) are discussed next.

3.7 Achievement of ACCO Objectives

Before discussing achievement of ACCO's objectives, it is important to identify the quality issues affecting this data in the context of the area-source technique (and, thus, e-Calc). Despite these limitations, we concluded that enough usable data still remained to infer some meaningful results with respect to these objectives.

It should be noted that little can be said whether employment of e-Calc 2 resulted in a material improvement over e-Calc 1 in achieving the ACCO objectives; the quality issues associated with the ACCO data (with respect to e-Calc needs) were overriding.

3.7.1 Data-Quality Issues

For each source (both years), in the context of e-Calc input needs, two basic factors significantly affected the quality of the ACCO data. These factors precluded achievement of the minimum spatial data-representativeness criteria for both: (a) determination of source attribution (the downwind TDL path-lengths); and (b) identification and quantification of the relative source-strength apportionment (the flux-chamber sampling configurations).

Downwind TDL Path Lengths

The first (and primary) quality-affecting issue was that the downwind TDL path-lengths, in all cases, were far too short relative to the downwind source dimensions, thus significantly compromising accuracy in the predicted e-Calc emission rates.

Ideally, the path-integrated concentration should be measured along the entire crosswind dimension of the source plume. In this case, the downwind measurement paths spanned distances of some 3.5 kilometers for the mine face and 7 kilometers for the tailings pond. Even the longest path-lengths (474 meters for the mine face and 267 meters for the tailings pond) were only a small fraction of these distances, resulting in very small plume-capture percentages. Accordingly, our confidence in the overall quality of the e-Calc results was substantially compromised.

Flux-Chamber Sampling Configurations

The second quality-affecting issue was that the flux-chamber data was too sparse to be able to confidently assess the relative source strength across each source subarea. Although especially true for the mine face (see Figures 3-5 and 3-6), this factor was judged overall to be not nearly as important as the downwind TDL path-lengths.

3.7.2 Emission Rates and Ratios

In the Major Deliverable for Milestone G, a total of 28 individual graphs compared and contrasted the carbon dioxide and methane emission rates and emission ratios for the mine face and tailings pond (not reproduced herein). All emission rates were plotted from daily means based on the event emission rates in Tables 3-11 and 3-12. Generally, the mine face emissions rates and emissions

ratios (both compounds) tracked fairly well between e-Calc 1 and e-Calc 2. There was little consistency between the emission rates and ratios, however, on a day-to-day or even an event-to-event basis.

3.7.3 Diurnal Emission Trends

No diurnal emission trends could be discerned, as the only valid nighttime ACCO data in terms of e-Calc was limited to four tailings pond events (September 2, 2016), and then only for e-Calc 2. It is interesting to note that the CO_2/CH_4 ratio was reasonably uniform during these four events, but that was about all which could be said for this extremely limited set of nighttime data.

3.7.4 Impacts of Upwind Sources

Following is a discussion on whether there were upwind sources which could have had an effect upon the reported carbon dioxide and methane attributions.

Carbon Dioxide

As discussed in Section 3.4, because all upwind carbon dioxide TDL measurements for the tailings pond were anomalously high in 2016, we believed it reasonable to conservatively assign the upwind concentrations (both sources and years) a fixed value of 402.8 ppm as measured by the CRDS instrument, consistent with the regional ambient background for this non-reactive compound.

We re-examined the upwind carbon dioxide TDL data for all valid MEP's in light of the possibility that these upwind readings were real (i.e., there were no instrument problems), caused by a source further upwind. However, the only source-year combination where the data suggests there could have been an upwind attribution of carbon dioxide was the tailings pond in 2016.

The upwind TDL for the tailings pond in 2016 was located on the southwest shore (Southwest Pond site in Figure 3-4); the upwind TDL value was greater than the corresponding downwind value for all seven valid measurement event pairs. Assuming the TDL was operating properly, this evidences the possibility of a nearby upwind interfering carbon dioxide source, likely originating along or just inland of the southern-most portion of the tailings pond western shoreline.

Methane

Upwind TDL concentrations of methane, on the other hand, were reasonably uniform for the duration of each measurement day for both sources (i.e., no anomalously high readings). In our opinion, the event-to-event differences in upwind concentrations were consistent with the spatial and diurnal variability in ambient background levels typically associated with this compound. Therefore, no upwind source of methane was evidenced for either source.

3.7.5 Recommendations for Future Use of E-Calc

Following are specific recommendations concerning data collection for future e-Calc use at very large sources, such mine faces and tailings ponds. If these recommendations were to be followed, we stated confidently that accurate emission rates could be generated in a highly cost-effective manner with minimal difficulty.

Source-Attribution

The path-length necessary to capture a sufficient portion of the downwind plume is greater than can be achieved by a TDL (or any other optical remote sensing instrument). This does not even consider the insurmountable problems caused by measurement-path obstructions, especially for sources with complex terrain such as a mine face.

The only practical means of measuring the downwind plume for such sources is a rapid-sampling, point-monitoring system configured to generate path-averaged concentrations. A continually sampling CRDS system, driven along the downwind source perimeter at a uniform speed, is ideal for generating such data, and was strongly recommended.

Relative Source-Strength Apportionment

One means of determining relative source-strength apportionment across a mine face or a tailings pond is by collecting samples at the center points of uniformly spaced grids, immediately above the source surface. It is feasible to collect such data by directing a drone (close to the surface during calm or light winds), upon which is mounted a real-time sampling device (such as a closed-cell TDL), and to transmit these results, together with sample coordinates, to an onsite command center.

Perhaps an easier approach is to employ a motor boat for collecting the hot-spot data via a hand-held instrument positioned just above the pond surface during reasonable calm conditions. These readings would be taken at the center-point of each subarea determined by a similar grid to be established atop the source. A total of about 24 square subareas should be sufficient to provide a reasonable level of model accuracy. Ideally, the emissions-characterization study should be performed twice: prior to and upon completion of all monitoring events. However, in this case, for a source this large, once was judged satisfactory.

Meteorological Measurements

E-Calc 1. E-Calc 1 simulates the wind profile in the vertical dimension and the atmospheric turbulence by calculating dispersion coefficients based on wind speed, land use, solar insolation, and statistical data treatments, such as the standard deviations of the horizontal wind direction and vertical wind speed. Boundary layer parameters (e.g., friction velocity, sensible heat flux, and Monin-Obukhov length) are required in the surface meteorological file input to AERMOD. E-Calc 1 simulates these parameters in the AERMET preprocessor based on the *flux-gradient approach*.

The onsite wind data used e-Calc 1 is collected via standard cup-and-vane sensors. Wind direction, wind speed, sigma theta or σ_θ (standard deviation of the horizontal wind direction), and sigma W or σ_W (standard deviation of the vertical wind speed) are collected (or calculated) from an appropriately configured 3-meter meteorological tower. Air temperature is measured using a portable hand-held instrument, and cloud cover (in tenths) is observed and recorded; the solar elevation angle is derived in accordance with the U.S. National Oceanic and Atmospheric Administration (NOAA) Solar Calculator. E-Calc 1 cannot be applied at night without a 10-meter meteorological tower.

E-Calc 2. E-Calc 2 employs dual 3D and 2D ultrasonic anemometers (plus a temperature sensor) at two heights. This method of profiling wind speed and atmospheric turbulence, referred to as the *eddy-correlation (or covariance) approach*, allows for the direct measurement of boundary layer parameters, resulting in a more accurate assessment of emission rates – at least in theory. This approach also obviates the need for the AERMET preprocessor, thereby simplifying the e-Calc logic, and can be applied at night.

In this approach, both the friction velocity and the Monin-Obukhov length are calculated using the covariance statistic between the u (east-west) and w (up-down) wind components and the v (north-south) and w wind components; sensible heat flux is calculated using the covariance between the w wind component and the temperature. The 3D ultrasonic anemometer and temperature sensor measures 1-second orthogonal wind and temperature, from which the covariance values are generated. Sigma theta is calculated from wind direction data generated by the 2D ultrasonic anemometer. (It should be noted that a simpler meteorological configuration is described in Section 6.2 of this Final Project Report.)

SECTION 4 – FIELD-WORK PLANNING

The project Work Plan described all planning and logistical aspects of those activities leading to System development. A Quality Assurance Project Plan (QAPP), included as an appendix to the Work Plan, set forth specific procedures to ensure that all data generated was of a quality sufficient to achieve the project objectives.

The Work Plan was prepared in accordance with the U.S. EPA DQO process. Its application represents the first step in the successful planning of any project involving the measurement of environmental data.

The QAPP was prepared consistent with U.S. EPA guidance provided in "EPA Requirements for Quality Assurance Project Plans, EPA QA/R-5," EPA/240/B-01/003, March 2001, and its companion document, "Guidance for Quality Assurance Project Plans, EPA QA/G-5," EPA/240/R-02/009, December 2002.

Section 4.1 presents an overview of each planning element contained in the Work Plan. **Section 4.2** presents an overview of each procedure forth in the QAPP. The reader is urged to consult the Major Deliverable for Milestone B for specific planning and procedural details.

4.1 Work Plan Requirements

The DQO Process and Statement of the Problem

The DQO process is an iterative, seven-step planning approach used for the collection of high-quality environmental data. This process is best described as a systematic strategy for defining the criteria that design of an effective data-collection program should satisfy, including: when, where, and how to collect samples or measurements; determination of tolerable decision-error rates; and the number of samples or measurements which should be collected.

The DQO process is described in the U.S. EPA document, *Data Quality Objectives Process for Hazardous Waste Investigations (EPA QA/G-4HW)*, Office of Environmental Information, Washington, DC, EPA/600/R-00/007, January 2000. Although this DQO guidance document was revised in 2006, this earlier version is still applicable and was followed herein as it is judged superior for applied research projects.

A step-by-step overview of the DQO process was presented, as well as the way it would be applied to the controlled methane-release component of this project. For each step, a generic statement of purpose and resultant outputs were identified, and the means of achieving these outputs were presented throughout the remainder of the Work Plan.

Management and Responsibilities

Figure 4-1 depicts the overall management organization for this project.

FIGURE 4-1. PROJECT MANAGEMENT

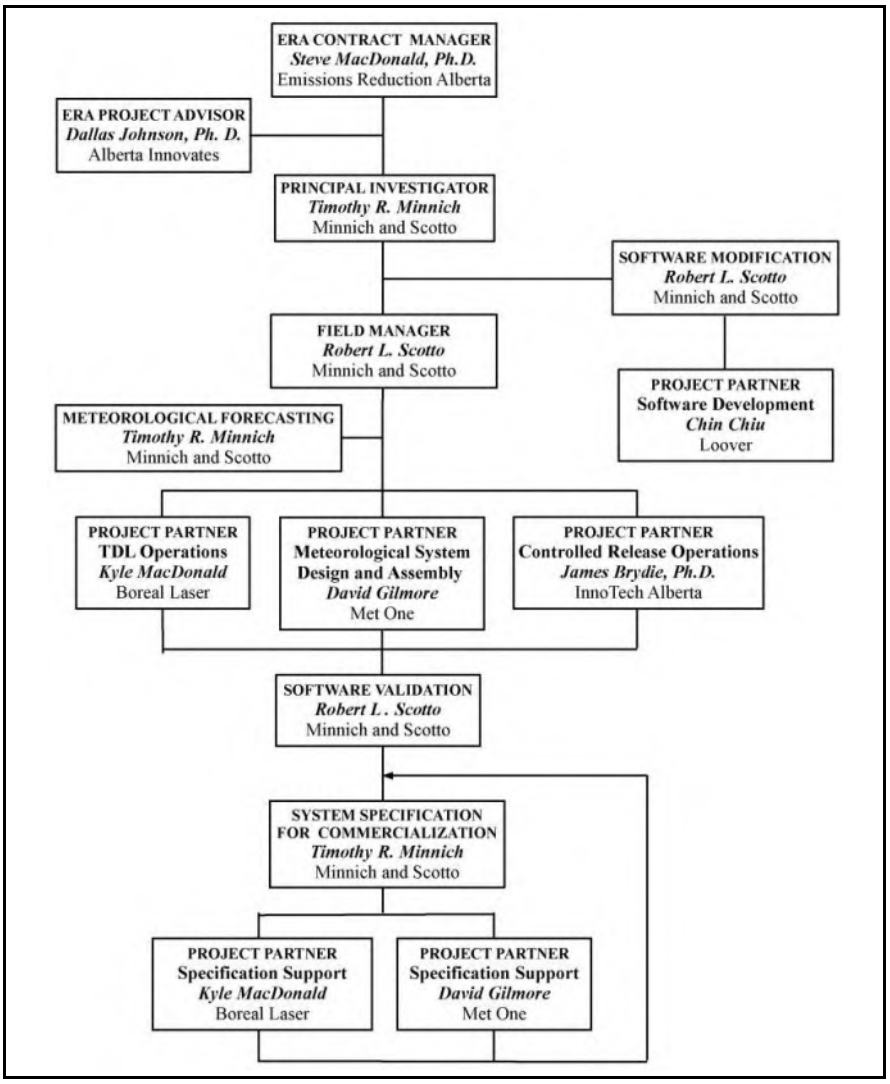

Experimental Design

The experimental design was described in terms of the sources to be simulated for controlled methane releases, as construction of these sources was part of the Project itself. Also described were the TDL measurement configurations to be employed (depending on the wind direction).

Source Simulation

Figures 4-2 through **4-5** presented the simulated process sources. These were: a production pad (well-head leak, where the pipes emerge from the ground); a gas-gathering pipeline assembly (valve

or flange leak); a gas transmission line (flange or rupture leak); and a boosting station (ruptured compressor-engine seal leak or condensate tank thief hatch or pressure-relief valve leak).

FIGURE 4-2. SIMULATED METHANE SOURCE: PRODUCTION PAD

FIGURE 4-3. SIMULATED METHANE SOURCE: GAS-GATHERING PIPELINE ASSEMBLY

FIGURE 4-4. SIMULATED METHANE SOURCE: GAS TRANSMISSION LINE

FIGURE 4-5. SIMULATED METHANE SOURCE: BOOSTING STATION

Potential Measurement Configurations

Figure 4-6 presents a schematic illustration of the experimental design. The TDL and retroreflector were moved, as needed, based on the mean wind direction. The meteorological tower was sited at a location representative of the plume dispersion and transport conditions between the controlled-release location and the TDL measurement path, in accordance with applicable U.S. EPA siting criteria. The distance between the simulated source and the measurement path was be between 20 and 50 meters. The lower limit ensured the methane plume was well-mixed by the time it reached the beam. The upper limit ensured the above plume capture is always achieved.

FIGURE 4-6. EXPERIMENTAL DESIGN: SCHEMATIC ILLUSTRATION

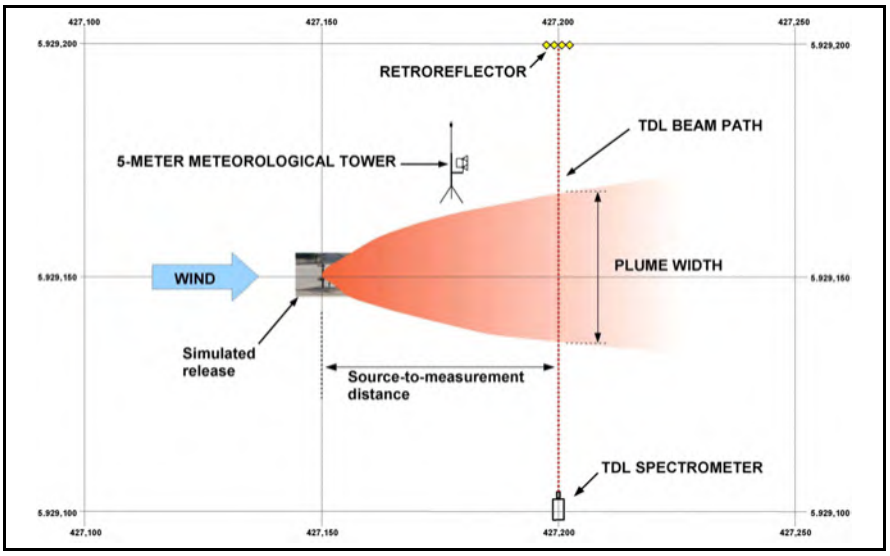

Source-Receptor Input Data

Information required for implementing the unity-based modeling included the emission source (location coordinates, orientation, booster-station dimensions, grade elevation, and release height above grade) and the measurement path (grade elevation of the TDL beam-path and coordinates of the beam endpoints).

Overview of the Data-Collection Component

A total of 8 days of controlled-release measurements were budgeted. Two full days were allocated for each of the four sources (or source groups). Additionally, 2-hour nighttime measurement "add-ons" (before sunrise or after sunset) were included in two of the measurement days. The intent was to collect, for each source, a sufficient number of measurement events within both unstable (daytime) and stable (nighttime) atmospheric regimes.

An average of twenty-four, 15-minute-averaged emission rate "snapshots" (i.e., monitoring events) was expected to be completed during each measurement day, for an anticipated project total of 192 daytime snapshots; i.e., 48 per each source (or source group). Each nighttime add-on was expected to yield a additional eight snapshots.

Data-Collection Needs

Data-collection needs required as input to e-Calc 2 were presented in terms of the measured data and the subsequent reduced data.

Measured Data

Table 4-1 identifies all data which were measured directly. The path-integrated TDL measurements were collected and generated as 1-second averages. A uniform methane mass flow rate was set for

each measurement day (blind to the Field Manager), and was checked for drift (and recorded) approximately every hour. The meteorological measurements were generated both as 1-second values and 15-minute block averages.

TABLE 4-1. DATA MEASURED DIRECTLY

Measurement
Path-Integrated Measurements
methane
Mass-Flow Measurements
methane
Direct Meteorological Measurements
wind speed vectors u, v, and w at 2 meters
wind speed vectors v and w at 5 meters
ambient temperature at 2 and 5 meters
atmospheric pressure at 2 meters

Reduced Data

Table 4-2 identifies the meteorological parameters needed to support e-Calc. These input parameters were derived from measurements made directly in the field.

TABLE 4-2. DERIVED METEOROLOGICAL PARAMETERS AND ASSOCIATED RAW MEASUREMENTS

Derived 15-Minute Parameter for E-Calc Input									Raw 1-Second Measurement
Horiz. Wind (Speed & Dir.)	Sigma Theta	Sigma Phi	Friction Velocity	Rough-ness Length	Sensible Heat Flux	Monin-Obukhov Length	Temperature		
							Amb.	2-5m Profile	
x			x	x		x			2m u-comp. 3D wind vector
x			x	x		x			2m v-comp. 3D wind vector
		x	x		x	x			2m w-comp. 3D wind vector
x	x			x					5m v-comp. 2D wind vector
x	x			x					5m w-comp. 2D wind vector
					x	x	x	x	2m ambient temperature
								x	5m ambient temperature

Field Logistics and Sequence of Activities

The start-time for each monitoring event was synchronized with the clock governing collection of the meteorological data. All monitoring events began precisely at the quarter hour; i.e., at the top of the hour or 15, 30, or 45 minutes past. All meteorological data was recorded onto a data logger which was periodically downloaded onto a flash drive (memory stick) in order to minimize the chances of data loss. The sequence of each day's field activities was:

1. Select Measurement Configuration and Perform Equipment Set-Up and Start-Up
    - Finalize the go/no-go decision; if a go, continue
    - Determine the source location and measurement configuration
    - Provide the monitoring event identification sequencing numbers for the day
    - Perform meteorological system check-out and start-up
    - Set up the controlled release apparatus, and site and power-up the TDL system

2. Conduct Data Collection
    - Commence data collection, once the TDL and controlled release systems have stabilized (uniform controlled release rate for each field day)
    - Perform documentation of all data-collection activities, including anything which may affect data quality

3. Perform Post-Data-Collection Tasks
    - Electronically back up all TDL and meteorological data, using high-capacity memory sticks
    - Prior to equipment shut-down and/or breakdown, identify and document any issue or concern potentially adverse to the quality of the data collected
    - Review all documentation

4. Conduct Planning Meeting for Next Day's Activities
    - Review meteorological forecast to support a go/no-go decision
    - Select the source type to be monitored
    - Identify any technical and logistical problems, either having occurred or anticipated, and a plan of action for their resolution
    - Decide whether to perform nighttime testing

Figure 4-7 presents the field data-collection form filled out by the Field Manager after each monitoring event.

FIGURE 4-7. FIELD DATA-COLLECTION FORM

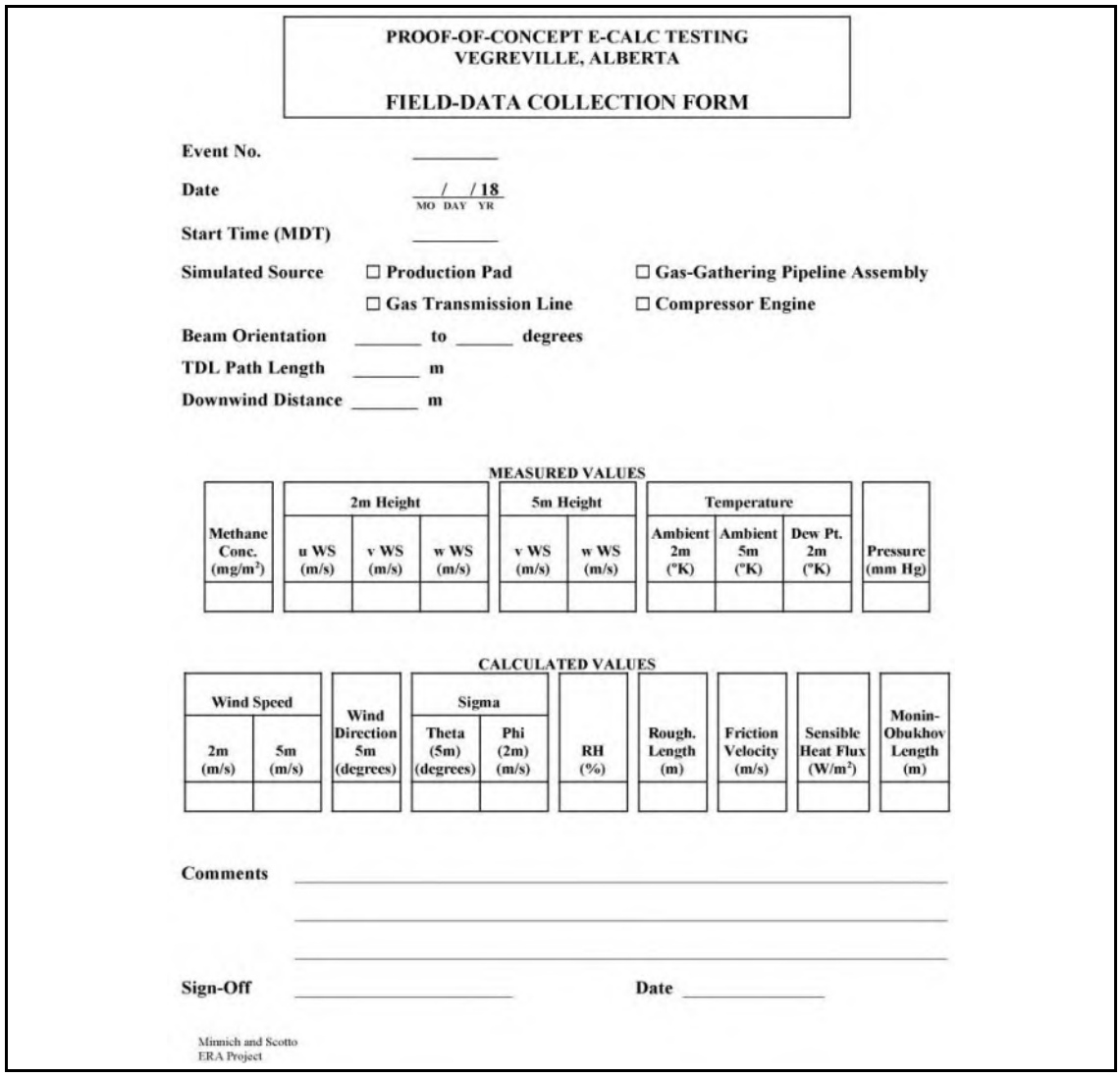

PROOF-OF-CONCEPT E-CALC TESTING
VEGREVILLE, ALBERTA

FIELD-DATA COLLECTION FORM

Event No. _____

Date ___/___/18 (MO DAY YR)

Start Time (MDT) _____

Simulated Source ☐ Production Pad ☐ Gas-Gathering Pipeline Assembly ☐ Gas Transmission Line ☐ Compressor Engine

Beam Orientation _____ to _____ degrees

TDL Path Length _____ m

Downwind Distance _____ m

MEASURED VALUES

Methane Conc. (mg/m^2)	2m Height			5m Height		Temperature			Pressure (mm Hg)
	u WS (m/s)	v WS (m/s)	w WS (m/s)	v WS (m/s)	w WS (m/s)	Ambient 2m (°K)	Ambient 5m (°K)	Dew Pt. 2m (°K)	

CALCULATED VALUES

Wind Speed		Wind Direction 5m (degrees)	Sigma		RH (%)	Rough. Length (m)	Friction Velocity (m/s)	Sensible Heat Flux (W/m^2)	Monin-Obukhov Length (m)
2m (m/s)	5m (m/s)		Theta (5m) (degrees)	Phi (2m) (m/s)					

Comments _____

_____

_____

Sign-Off _____ Date _____

Minnich and Scotto
ERA Project

Documentation and Record-Keeping

The documentation and records generated in the field were sufficiently comprehensive to ensure the technical validity of the data collected, and to support independent validation of the project findings.

Meteorological Measurement System

Meteorological data was collected, processed, and stored using a Met One IMP-865 programmable data logger. The data logger had the capability of storing the directly measured, 1-second (1 Hz) raw values, together with internally tabulated, 15-minute-averaged measured and derived values. All data was stored in a ASCII CSV text file format.

Tunable Diode Laser System

Path-integrated methane data was collected each second. The data was processed on an internal data logger (4 GB capacity), designed to allow for data transfer and downloading as needed. Stored as 1-second raw values in ASCII CSV format, all data was copied daily onto a flash drive for transfer to a separate field PC, from which 15-minute values were tabulated for each monitoring event.

Controlled-Release System

A spreadsheet detailing all controlled-release rate data was prepared. This included the mean release rate for each monitoring event, together with all supporting QC information, including tabulation of the total precision and accuracy (i.e., the mass flow controller plus the natural gas composition analysis) for each release rate.

Reporting

A comprehensive report detailing all data-collection and analysis activities was prepared upon field-work completion (Major Deliverable for Milestone F). This report included:

- test-design description
- a narrative on all field activities, including problems identified and corrective action taken
- a presentation of all data collected and generated
- the statistical analysis methods employed to assess method accuracy as functions of source type, meteorology, and emission rate
- the statistical analysis results
- identification of any bias in predicted-to-actual emission rates
- any recommendations on e-Calc software improvements; e.g., use of empirical correction factors

4.2 Quality Assurance Project Plan Requirements

QC Organization

Figure 4-8 presents the QC organization for those activities governing field data collection.

FIGURE 4-8. QC ORGANIZATION

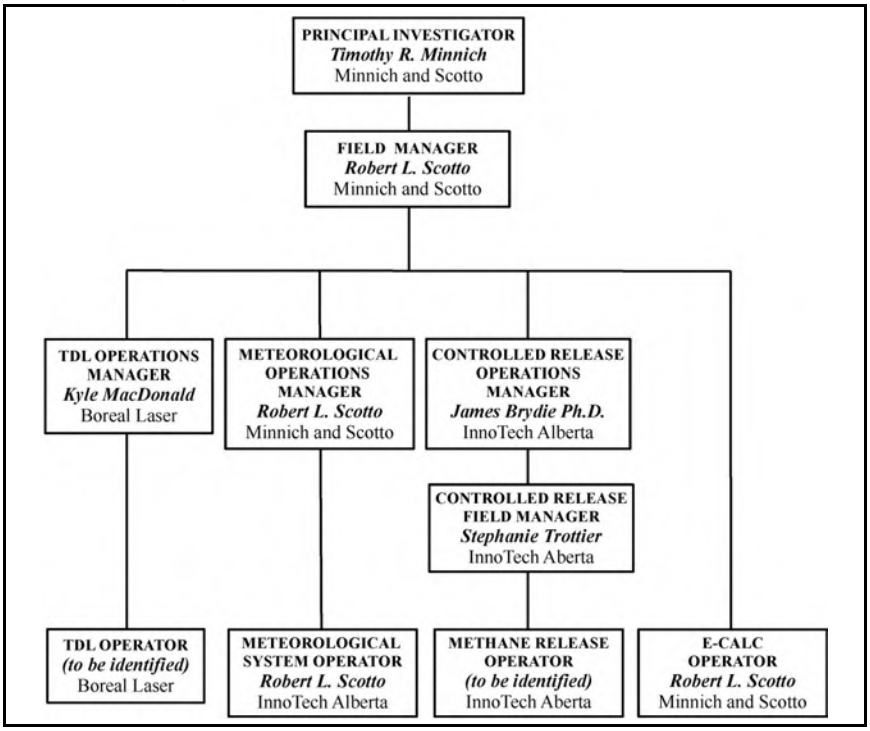

E-Calc Application

A sample Standard Operating Procedure (SOP) for e-Calc, prepared as part of a project in 2016 to assess downwind community impact from a contaminated body of water (the Newtown Creek, in Brooklyn, New York) was presented as Attachment A to the QAPP. This SOP is substantially similar to the one which would have been prepared for this Project, had e-Calc 2 already existed.

Application of the Area-Source Technique

Information presented in the corresponding section of the QAPP is substantially similar to Section 2.2.4 of this report, and is not reproduced here.

Measurement Quality Objectives

As discussed in the Work Plan, measurement and performance criteria are typically expressed in terms of Data Quality Indicators, while Measurement Quality Objectives (MQO's) are established to set the acceptance thresholds or goals which must be achieved for the measurement data collected. Both quantitative and qualitative MQO's are presented next.

Quantitative

Tables 4-3 through **4-5** present the MQO's for precision, accuracy, sensitivity, and completeness, respectively, for the TDL measurement, methane controlled release, and meteorological system.

TABLE 4-3. TDL MQO's

PRECISION, ACCURACY, AND SENSITIVITY

Measured Parameter	MQO [a]		
	Precision (ppm-m)	Accuracy (%)	Sensitivity (PQL) [b] (ppm-m)
methane	0.5	±2	0.011

COMPLETENESS

Number of Valid 15-Minute Monitoring Events (over eight days)	
Daytime	Nighttime
192	16

_____

Notes to Table 4-3:

(a) Precision and accuracy were calculated in accordance with U.S. EPA methods, as presented in 40 CFR 53.23. Accuracy assumed that methane concentrations were measured at levels 5 times the TDL PQL or greater.

(b) Assumed a path length of 45 meters.

TABLE 4-4. CONTROLLED METHANE RELEASE SYSTEM MQO's

PRECISION, ACCURACY, AND SENSITIVITY

Measured Parameter	MQO	
	Precision	Accuracy
Omega mass flow controller, Model FMA 2600A	± 0.2% full scale	± 0.8% plus 0.2% full scale

COMPLETENESS

Duration of Controlled Releases [a]		
Number of Working Days	Daytime Hours	Nighttime Hours
6	7	0
2	5	2

_____

Notes to Table 4-4:

(a) Assumed 7.5 hours of continuous release during each of eight daytime periods, and 2 hours during each of two nighttime periods.

TABLE 4-5. METHANE GAS ANALYSIS MQO's

Gas Chromatography [(a)] (Flame Ionization Detection) (%)	
Expected Precision	**Expected Accuracy**
2	2

_____

Note to Table 4-5:

(a) Expected MQO's were derived from instrument performance details InnoTech Alberta's analytical laboratory:

	Methane Concentration		
	% (v/v)	**% (v/v)**	**% (v/v)**
Expected	100.00	50.00	25.00
Average (n=8)	100.01	49.61	25.47
Standard Deviation	0.93	1.63	1.66

TABLE 4-6. METEOROLOGICAL SYSTEM MQO's

PRECISION, ACCURACY, AND SENSITIVITY

	MQO		
Measured Parameter	**Precision**	**Accuracy**	**Sensitivity (threshold)**
RM Young 3D Ultrasonic Anemometer, Model 81000			
vector components u and v	0.001 m/s	0.01 m/s	0.01 m/s
vector component w	0.0005 m/s	0.01 m/s	0.01 m/s
RM Young 2D Ultrasonic Anemometer, Model 86000			
horizontal wind speed	0.01 m/s	0.1 m/s	0.01 m/s
horizontal wind direction	0.1 degrees	2.0 degrees	0.01 m/s
Met One Air Temperature Sensors, Model 064			
ambient temperature	0.02º C	0.05º C	NA
Met One Air Barometric Pressure Sensor, Model 092			
atmospheric pressure	0.10 hPa	0.35 hPa	NA

COMPLETENESS

Number of Valid 15-Minute Monitoring Events (over 8 days)	
Daytime	**Nighttime**
192	16

Qualitative

Qualitative MQO's consisted of data representativeness (spatial and temporal) and data comparability. Achievement of these MQO's was demonstrated via strict adherence to the strategies and procedures detailed in the Work Plan. This ensured the collection of measurement data was consistent in type and quality, at all times.

Representativeness

Achievement of both spatial and temporal representativeness was inherent in the sampling design.

Spatial representativeness was achieved for each monitoring event, as long as: (a) the TDL measurement path encompassed the entire downwind, cross-plume dimension; and (b) meteorological measurements were representative of the microscale region between the methane emissions source and the TDL measurement path.

Temporal representativeness was achieved by ensuring that each 15-minute monitoring event was synchronized to begin precisely at top of the hour (or 15, 30, or 45 minutes past).

Comparability

Comparability between any given set of monitoring events was achieved, given that all other MQO's were achieved (both quantitative and qualitative) for each data measurement.

Equipment Inventory, Calibration, and Maintenance

The following components comprised the equipment inventory for the controlled-release program. Brochures and product sheets were included in the QAPP, but are not reproduced herein.

Inventory

Tunable Diode Laser

- one spectrometer
- one retroreflector
- one PC

Meteorological Sensors

- one RM Young Ultrasonic 3D Anemometer, Model 81000
- one RM Young Ultrasonic 2D Anemometer, Model 86000
- two Met One Ambient Temperature Sensors, Model 064
- one Met One Barometric Pressure Sensor, Model 092

Meteorological Data Logger and Software

- one Climatronics IMP-865 data logger
- one LoggerNet software package

Meteorological Tower

- one Will-Burt Mast Tower (extendable up to 6 meters)

Controlled Methane Release System

- a methane gas supply
- an apparatus to provide single- and multipoint releases
- one Omega Mass Flow Controller, Model FMA-2600A

Calibration and Maintenance

Table 4-7 presents the calibration procedures and frequency for all measurement equipment employed in the field. Visual inspections were performed on a daily basis to evidence any equipment damage or defects; no such conditions were identified.

TABLE 4-7. MEASUREMENT EQUIPMENT CALIBRATION PROCEDURES AND FREQUENCY

Measurement Type	Measurement System	Calibration Frequency	Method / Type of Standard
Open-Path TDL Spectrometer			
methane concentration	Boreal GasFinder3-OP	every 5 years	none (recommended check-up calibration once every 5 years)
Controlled Methane Release System			
methane release	Omega mass flow controller, Model FMA-2600A (or equiv.)	annually	NIST-traceable volume standard
Meteorological System			
vector components u, v, and w	RM Young 3D ultrasonic anemometer, Model 81000	annually	RM Young factory wind tunnel
horizontal wind speed and direction	RM Young 2D ultrasonic anemometer, Model 86000	annually	RM Young factory wind tunnel
ambient temperature	Met One ambient temperature sensor, Model 064	annually	NIST-traceable temperature standard
atmospheric pressure	Met One barometric pressure sensor, Model 092	annually	NIST-traceable aneroid barometer

Data Validation

The functionality of the TDL, meteorological, and controlled methane release systems was checked on an ongoing basis, in accordance with manufacturer's specifications and the application methods.

Data Control and Management

All data generated by the TDL, meteorological, and controlled methane systems was controlled via PC interface and manufacturer's DAS (data acquisition system) software. Specific data control and management activities for each system were detailed in the QAPP, but are not reproduced herein.

Statistical Assessment of Measured Emission Rates

A statistical assessment e-Calc's performance in predicting the controlled methane release rate was made, based on source type and category of meteorological conditions (e.g., day vs. night, strong vs. light winds). For each source type and set of meteorological conditions, statistical analyses were performed to determine the degree to which the predicted tracer-gas emission rates conformed to the actual or "true" emissions (i.e., the controlled emission rates).

More sophisticated correlation tests between actual and predicted source-specific emission rates were envisioned, but some had to be abandoned as issues with background methane concentrations introduced a high level of uncertainty into the collected data (discussed in subsequent sections of this report).

SECTION 5 – CONTROLLED-RELEASE PROGRAM

The Milestone F Report evaluated the performance of e-Calc 2 in addressing the primary project goal. The metric for this statistical performance assessment was how well the predicted methane emission rate compared to the controlled (or actual) release rate. This P/A comparison was expressed throughout as a percent ratio, and assessed largely as functions of meteorology.

Table 5-1 presents a summary of the field testing each measurement day. Tests were conducted between August 14 and 23, 2018. A total of 211 daytime and 16 nighttime, 15-minute-averaged monitoring events were completed for the four simulated sources.

The controlled emissions were constant over each measurement day (one exception), but at differing rates as selected by InnoTech Alberta (unknown to the e-Calc 2 operator).

TABLE 5-1. SUMMARY OF DAILY FIELD TESTING

Day	Date (2018)	Day of the Week	Simulated Source	Release Ht. Above Grade (m)	# of Valid Events		# of Background Readings
					Daytime	Nighttime	
1	Aug. 14	Tuesday	booster station (BS)	3.0	29	0	2
2	Aug. 15	Wednesday	booster station	3.0	26	0	4
3	Aug. 16	Thursday	gas-gathering pipeline (GGP)	1.0	26	0	6
4	Aug. 17	Friday	gas-gathering pipeline	1.0	24	0	6
5	Aug. 18	Saturday	gas-transmission line (GTL)	0.4	24	0	4
6	Aug. 20	Monday	gas-transmission line	0.4	25	0	6
7	Aug. 21	Tuesday	production pad (PP)	0.4	23	0	8
8	Aug. 22	Wednesday	production pad	0.4	20	0	8
9	Aug. 23	Thursday	gas-gathering pipeline	1.0	14	16	10
				Total	**211**	**16**	**54**

Section 5.1 addresses assignment of the methane background values. **Section 5.2** presents composite results for the entire nine-day measurement program. **Section 5.3** presents an analysis of the results by simulated source. **Section 5.4** presents conclusions of this statistical data analysis. **Section 5.5** describes subsequent analyses that we committed to perform as part of this Final Project Report.

5.1 Assignment of Methane Background Values

E-Calc (versions 1 and 2) predicts an emission rate based on the attribution from a fugitive ground-level source. In general, source attribution is determined by subtracting the background (or upwind) concentration from the downwind concentration for each monitoring event – 15 minutes, in this case. When the background concentration is negligible, the source attribution can be ascribed solely to the downwind value (i.e., background measurements are not required).

For this project, however, treatment of the background methane concentration required special attention, as the background was shown to be: (a) variable over the measurement day; and (b) quite significant, relative to the source attribution. Several-minute background measurements were made immediately before and after each data "block," in which a block was defined as a continuous (uninterrupted) series of monitoring events. The background value assigned to each monitoring event was then linearly interpolated between the two actual measurements.

Table 5-2 presents the background methane concentrations assigned to each monitoring event over the entire nine days of measurements. Also depicted are the measurement day and date, the simulated source, and the local end-time of each event. The bolded numbers represent background values, measured during times when the controlled methane-release system was turned off. All other numbers (i.e, not bolded) represent the interpolated background values, as discussed above.

The greatest source of analysis uncertainty (and, therefore, potential error) was the inability to "ground-truth" these interpolated background methane concentrations. In general, the confidence in the background value assigned to any particular monitoring event was roughly proportional both to the rate of change of the interpolated value from one event to the next, and to the closeness between the event and the nearest background measurement (i.e., forward or backward in time).

TABLE 5-2. BACKGROUND METHANE CONCENTRATIONS FOR EACH BLOCK OF DATA (ppm)

End-Time (Local)	Day 1 Aug. 14 BS	Day 2 Aug. 15 BS	Day 3 Aug. 16 GGP	Day 4 Aug. 17 GGP	Day 5 Aug. 18 GTL	Day 6 Aug. 20 GTL	Day 7 Aug. 21 PP	Day 8 Aug. 22 PP	Day 9 Aug. 23 GGP
9:00		**2.136**							
9:15		2.149							
9:30		2.161							
9:45		2.174							
10:00	**1.976**	2.186							
10:15	1.972	**2.199**		**2.201**					
10:30	1.968			2.181					
10:45	1.965			2.161					
11:00	1.961			2.141					
11:15	1.957			2.121		**1.834**			
11:30	1.953			2.101		1.832			
11:45	1.949		**2.090**	2.081		1.830			
12:00	1.945		2.087	2.061		1.827		**2.049**	
12:15	1.942	**2.077**	**2.084 / 2.056**	2.041		1.825		2.042	
12:30	1.938	2.071	2.040	2.021		1.823		2.035	
12:45	1.934	2.066	2.024	2.001	**1.888**	1.821	**1.947**	2.027	
13:00	1.930	2.060	2.008	1.981	1.887	1.818	1.941	2.020	
13:15	1.926	2.055	**1.992**	1.961	1.886	**1.816 / 1.808**	1.934	2.013	
13:30	1.922	2.049	**1.960**	**1.941 / 1.909**	1.885	1.810	1.928	2.006	
13:45	1.919	2.043	1.960	1.912	1.883	1.811	1.921	1.998	
14:00	1.915	2.038	1.959	1.916	1.882	1.813	**1.915**	**1.991/1.993**	
14:15	1.911	2.032	1.959	1.919	1.881	1.814		1.998	
14:30	1.907	2.027	1.958	1.923	1.880	1.816	**1.726**	2.003	**2.728**
14:45	1.903	2.021	1.958	1.926	1.879	1.817	1.723	**2.008/1.928**	2.557
15:00	1.899	2.015	1.957	1.930	1.878	1.819	1.720	1.926	**2.386**
15:15	1.896	2.010	1.957	**1.933**	1.877	1.820	1.717	1.923	
15:30	1.892	2.004	1.956	**1.915**	1.876	**1.822 / 1.819**	1.715	1.921	
15:45	1.888	1.998	1.956	1.934	1.874	1.820	1.712	1.918	
16:00	1.884	1.993	1.955	1.953	1.873	1.820	1.709	1.916	**2.446**
16:15	1.880	1.987	1.955	1.972	1.872	1.821	1.706	1.913	2.361
16:30	1.876	1.982	1.954	1.992	**1.871 / 1.873**	1.822	**1.706/1.706**	1.911	2.276
16:45	1.873	1.976	1.954	2.011	1.874	1.822	1.705	**1.908/1.906**	2.191
17:00	1.869	1.970	1.953	2.030	1.875	1.823	1.704	1.915	**2.106/2096**
17:15	1.865	1.965	1.953	**2.049**	1.875	1.823	1.702	1.923	2.107
17:30	**1.861**	1.959	1.952		1.876	1.824	1.701	1.932	2.108
17:45		1.954	1.952		1.877	1.825	1.700	1.940	2.110
18:00		**1.948**	1.951		1.878	1.825	1.699	**1.949**	2.111
18:15			1.951		1.879	**1.826**	1.697		2.112
18:30			1.950		1.880		**1.696/1.694**		2.113
18:45			1.950		1.880		1.701		2.115
19:00			1.949		1.881		1.708		2.116
19:15			**1.949**		**1.882**		1.715		**2.117/2.109**
19:30							1.721		2.110
19:45							1.728		2.111
20:00							**1.735**		2.112
20:15									2.113
20:30									2.115
20:45									2.116
21:00									2.117
21:15									2.118
21:30									**2.119/2.114**
21:45									2.113
22:00									2.112
22:15									2.111
22:30									2.110
22:45									2.109
23:00									2.109
23:15									2.108
23:30									2.107
23:45									2.106
0:00									2.105
0:15									**2.104**

5.2 Composite Results

In this section, the predicted-to-actual emission rates are shown for the nine days of measurements, as a whole. The statistics presented are: P/A relative standard deviation (RSD) vs. block number, wind speed, and standard deviation of the horizontal wind direction (sigma theta or σ_θ); and P/A bias vs. block number. The P/A statistics are analyzed in greater detail, on a source-by-source basis, in Section 5.3.

Table 5-3 presents an overall statistical analysis summary. For each measurement day, presented are the simulated source, the data blocks and associated monitoring events (data blocks are numbered sequentially), and, for each block, the closest separation between the controlled release and the downwind TDL beam. Also presented for each data block are the predicted and actual emission rates (mg/s), as well as the statistics identified above. In general, the P/A bias and relative standard deviation were determined to be the best measures of assessing the block-to-block e-Calc 2 performance.

TABLE 5-3. OVERALL STATISTICAL ANALYSIS SUMMARY

Day	Source	Data Block	Events	Separation Distance (m)	Predicted (P) (mg/s)	Actual (A) (mg/s)	P/A Bias (%)	P/A RSD (%)	2m Wind Speed (m/s)	2m Sigma Theta (degrees)
1	Booster Station	1	1-29	20.4	663.1	403.4	65.2	25.0	3.45	13.08
2	Booster Station	2	1-4	20.4	1658.9	322.7	414.1	364.0	1.16	19.72
		3	5-26	23.1	480.3	322.7	48.8	65.4	2.70	11.41
3	Gas-Gathering Pipeline	4	1	42.5	506.6	443.7	14.2	n/a	2.50	12.23
		5	2-4	42.5	347.0	443.7	-21.8	14.4	1.73	22.49
		6	5-26	42.5	475.1	443.7	7.1	29.0	3.22	13.49
4	Gas-Gathering Pipeline	7	1-12	29.6	560.4	403.4	38.9	11.8	3.21	14.59
		8	13-18	29.6	539.9	403.4	33.8	9.2	3.21	15.22
		9	19-24	29.6	490.8	403.4	21.7	12.5	2.98	18.04
5	Gas-Transmission Line	10	1-14	75.0	754.5	645.4	16.9	24.4	6.79	12.46
		11	15-24	75.0	834.6	645.4	29.3	20.4	4.91	12.12
6	Gas-Transmission Line	12	1-7	54.5	534.8	726.0	-26.3	21.6	2.62	30.52
		13	8-15	54.5	650.6	726.0	-10.4	23.6	3.33	23.58
		14	16-25	54.5	709.3	726.0	-2.3	24.9	2.67	22.93
7	Production Pad	15	1-4	43.9	263.2	363.0	-27.5	29.0	2.57	25.71
		16	5-11	43.2	362.1	363.0	-0.3	17.7	2.80	26.89
		17	12-18	43.2	386.4	363.0	6.5	17.4	2.33	21.30
		18	19-23	43.2	402.8	363.0	11.0	29.3	1.25	10.23
8	Production Pad	19	1-7	57.6	391.1	484.0	-19.2	19.1	2.02	17.01
		20	8-9	57.6	456.8	484.0	-5.6	39.0	3.26	15.60
		21	10-16	31.0	505.3	484.0	4.4	11.1	3.23	11.65
		22	17-20	31.0	631.6	484.0	-30.5	10.4	1.30	12.88
9	Gas-Gathering Pipeline	23	1	52.0	2256.8	1613.4	39.9	n/a	2.98	13.91
		24	2-4	31.1	1324.5	726.0	82.4	9.0	5.25	12.08
		25	5-12	31.1	1193.5	726.0	64.4	13.2	5.49	9.90
		26	13-20	31.1	1359.1	726.0	87.2	12.2	4.34	12.91
		27	21-30	31.1	1154.7	726.0	59.0	27.2	3.82	9.16

Figure 5-1 presents the P/A relative standard deviation vs. block number over all nine measurement days. Excluded from this graph are Block 2 (booster station, Day 2), Block 4 (gas-gathering pipeline, Day 3), and Block 23 (gas-gathering pipeline, Day 9). Block 2 was designated as a statistical outliner in this and the three subsequent figures (discussed in Section 5.3.1). Blocks 4 and 23 each consisted of a single monitoring event, thereby precluding RSD calculation.

In general, the P/A relative standard deviation decreased with increasing block number, as indicated by the best-fit line. This improvement over time was likely due to the increased number of background measurements with latter measurement days, as can be seen from Table 5-1.

FIGURE 5-1. P/A RELATIVE STANDARD DEVIATION VS. BLOCK NUMBER

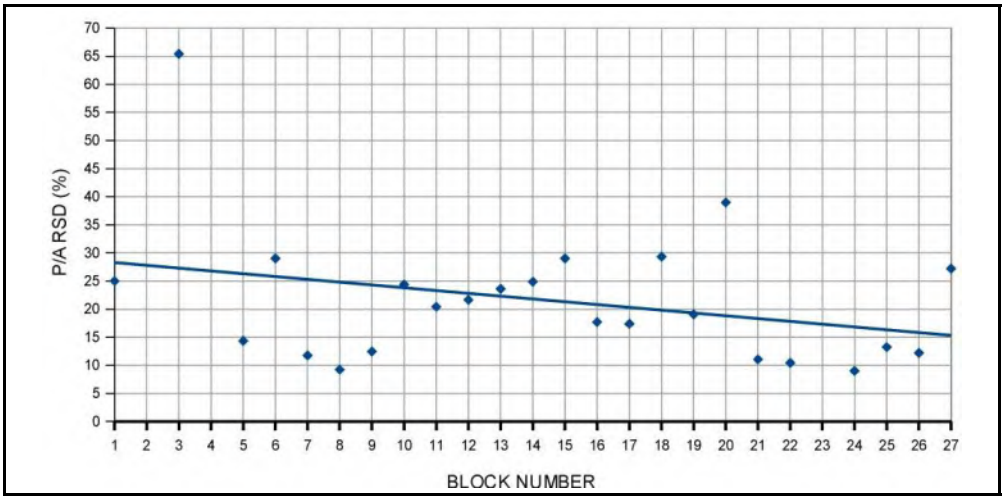

Figure 5-2 presents the P/A bias vs. block number over the nine measurement days. Except for Block 1 (booster station, Day 1), Block 3 (booster station, Day 2), and Blocks 24 through 27 (gas-gathering pipeline, Day 9), the bias was within about 40 percent (+/−) for all of these 20 remaining blocks, and within about 20 percent for 13 of those.

FIGURE 5-2. P/A BIAS VS. BLOCK NUMBER

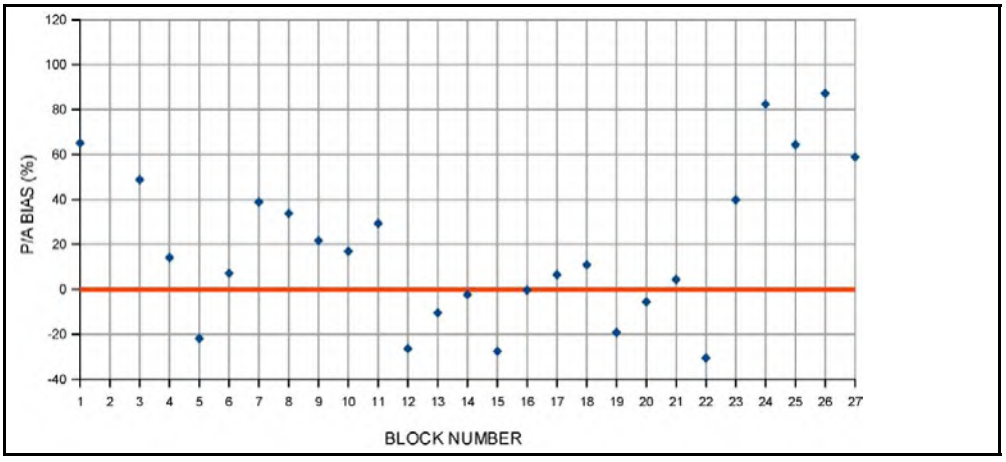

Figure 5-3 presents the P/A relative standard deviation vs. wind speed at 2 meters. There appeared to be little correlation between the P/A relative standard deviation and mean 2-meter wind speed, as indicated by the best-fit line and a correlation coefficient (r^2) of 0.013 (not shown).

FIGURE 5-3. P/A RELATIVE STANDARD DEVIATION VS. WIND SPEED (2m)

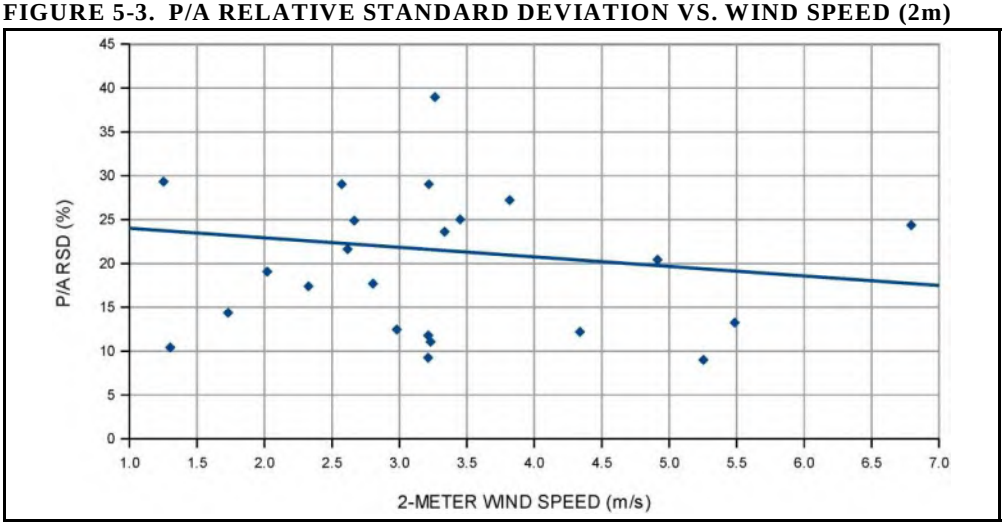

Figure 5-4 presents the P/A relative standard deviation vs. sigma theta at 2 meters. The standard deviation of the horizontal wind direction is generally a measure of atmospheric stability, whereas the lower the value, the less horizontal dispersion and the greater stability. While one might expect a direct correlation between sigma theta and the P/A relative standard deviation, such was not the case ($r^2 = 0.005$). The likely reason for this lack of correlation was the fact that the plume capture was generally at (or close to) 100 percent for most monitoring events, indicating that the horizontal dispersion was properly accounted for in the e-Calc software.

FIGURE 5-4. P/A RELATIVE STANDARD DEVIATION VS. SIGMA THETA (2m)

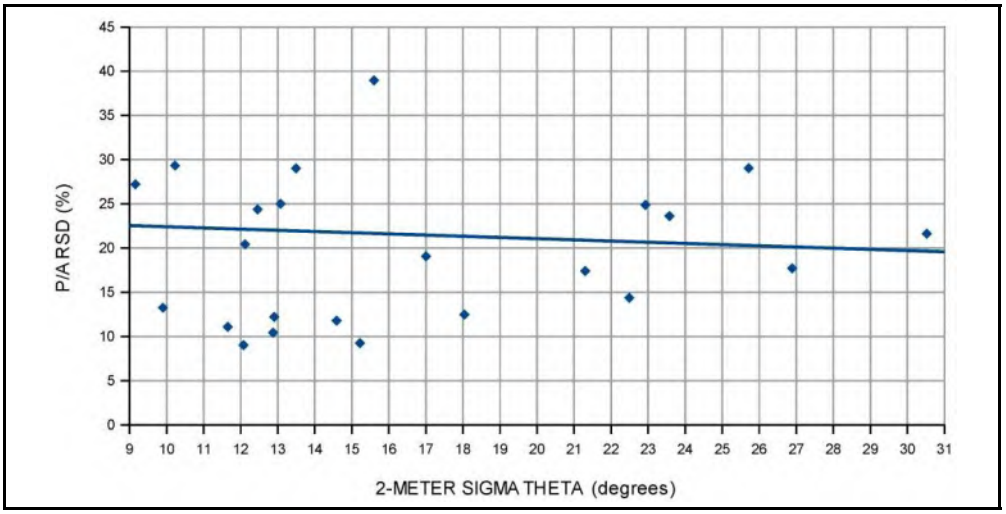

5.3 Analysis of Results by Simulated Source

Sections 5.3.1 through **5.3.4** present analysis results for the booster station, the gas-gathering pipeline, the gas transmission line, and the production pad, respectively. Each measurement day is discussed within the corresponding section.

For each measurement day, a table was introduced in the Milestone F Report which detailed, for each monitoring event: the TDL attribution; the predicted e-Calc 2 methane emission rate and the associated plume capture; the actual (or controlled) methane release rate; the 2- and 5-meter meteorological sensor height information (wind speed, wind direction, actual temperature, and sigma theta); the turbulence parameters consisting of the standard deviation of the vertical wind speed, friction velocity, Monin-Obukhov length, and sensible heat flux; the relative humidity; and the atmospheric pressure. These tables are not reproduced herein.

5.3.1 Booster Station – Days 1 and 2

The simulated booster station, a wooden box (length 16.5 meters, width 3.1 meters, and height 3.0 meters), was constructed to represent a typical enclosure which might house a compressor engine within a condensate-tank complex. The separation distance between the controlled release and the TDL beam was 20.4 meters. The controlled methane was released via Tygon tubing which extended the height of the enclosure, centered on the rooftop.

Day 1 – August 14

Figure 5-5 presents, for Day 1, the P/A bias vs. event end-time for the booster station simulation. From Table 5-3, the Day 1 actual emission rate was 403.4 mg/s, and the mean P/A bias for the Block 1 (Events 1 through 29) was +65.2 percent.

FIGURE 5-5. DAY 1 – BOOSTER STATION: P/A BIAS VS. EVENT END-TIME

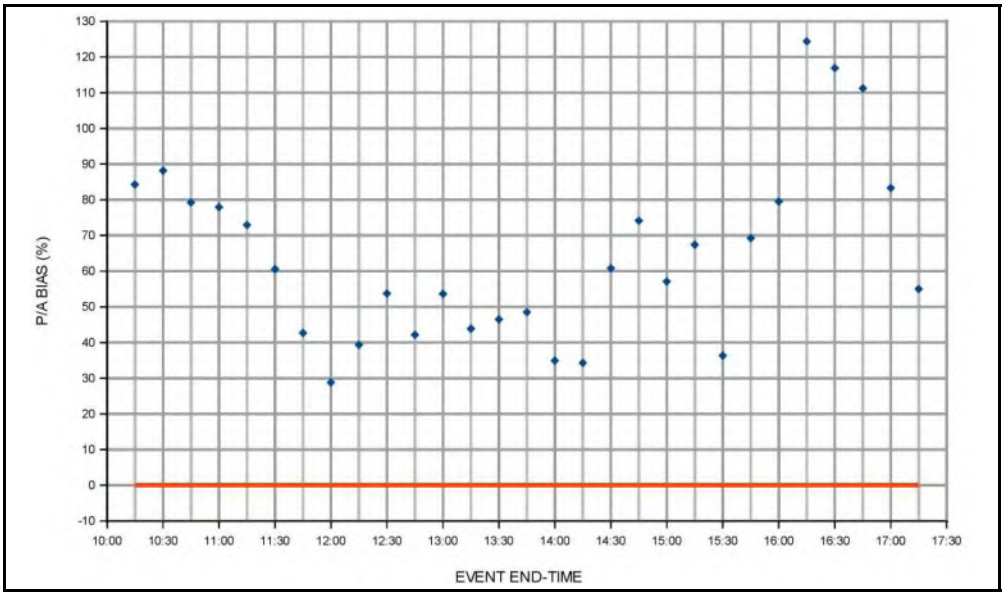

All of the 29 individual, Day 1 monitoring events had a positive P/A bias of about 30 percent or greater, with 15 of those greater than 60 percent. The fact that only two background measurements were made (i.e., Day 1 had only a single block of data) certainly contributed to the data scatter, but it clearly could not account for all of it. This was evidenced by the first and last few monitoring events, when the duration between each of these events and the nearest background measurement was relatively short, yet the biases were still very significant.

Instead, we felt that the scatter in this data was predominantly the result of the downwind TDL beam being positioned too close to the controlled release (separation distance 20.4 meters) for this elevated source (3.0 meters above grade), under the observed wind (3.45 m/s mean speed) and atmospheric stability (13 degrees mean sigma theta). Specifically, our hypothesis was that the wind created a "rotor" – a commonly observed downwash phenomenon occurring in the lee side of a structure which, under sufficiently strong winds and reasonably stable atmospheric conditions, induces a circulation. Rotors cause the contaminant plume to become trapped and concentrated close to the ground, in the lee of the structure. Here, this phenomenon resulted in an artificially high attribution, thus yielding a substantial emission-rate over-prediction (discussed further in Section 7).

Figure 5-6 presents, for Day 1, the P/A bias vs. wind speed (Block 1, Events 1 through 29) for the booster station simulation (see Table 5-3). The increase in P/A bias with wind speed supported the hypothesis that the TDL beam was not positioned far enough downwind on this day. This hypothesis was further supported by data collected for this source on Day 2 (see below).

FIGURE 5-6. DAY 1 – BOOSTER STATION: P/A VS. WIND SPEED (2m)

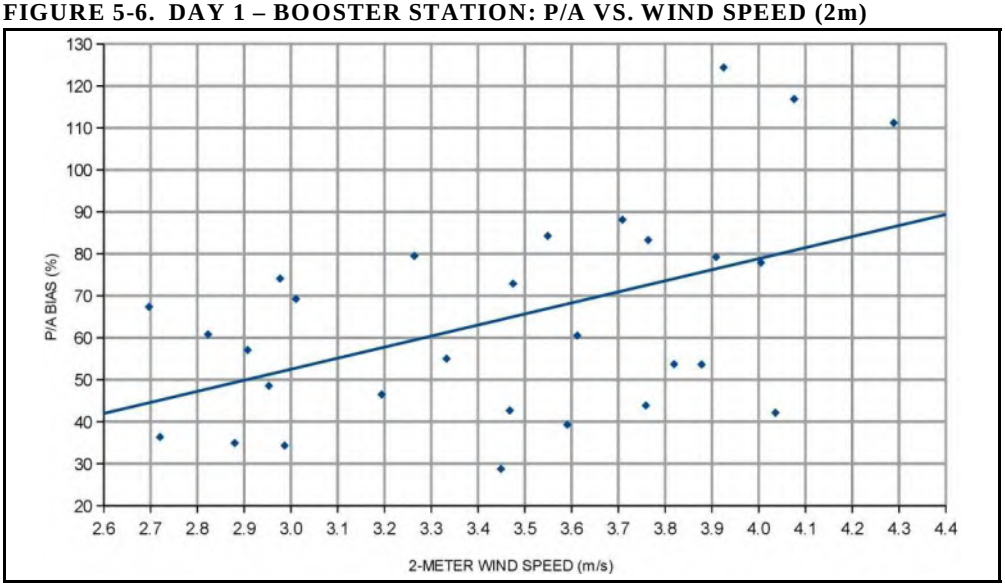

Day 2 – August 15

On this day, there were two blocks of data: Block 2, consisting of Events 1 through 4 (end-times 09:15 – 10:00); and Block 3, consisting of Events 5 through 26 (end-times 12:30 – 17:45). The separation distance between the controlled release and the downwind TDL beam was still 20.4 meters during Block 2, but was extended to 23.1 meters prior to initiation of Block 3. All other booster station conditions were identical to Day 1.

Figure 5-7 presents, for Day 2, the P/A bias vs. event end-time for the booster station simulation. From Table 5-3, the Day 2 actual emission rate was 322.7 mg/s, and the mean P/A biases were: Block 2 (Events 1 through 4), +414.1 percent; and Block 3 (Events 5 through 26), +48.8 percent.

FIGURE 5-7. DAY 2 – BOOSTER STATION: P/A BIAS VS. EVENT END-TIME

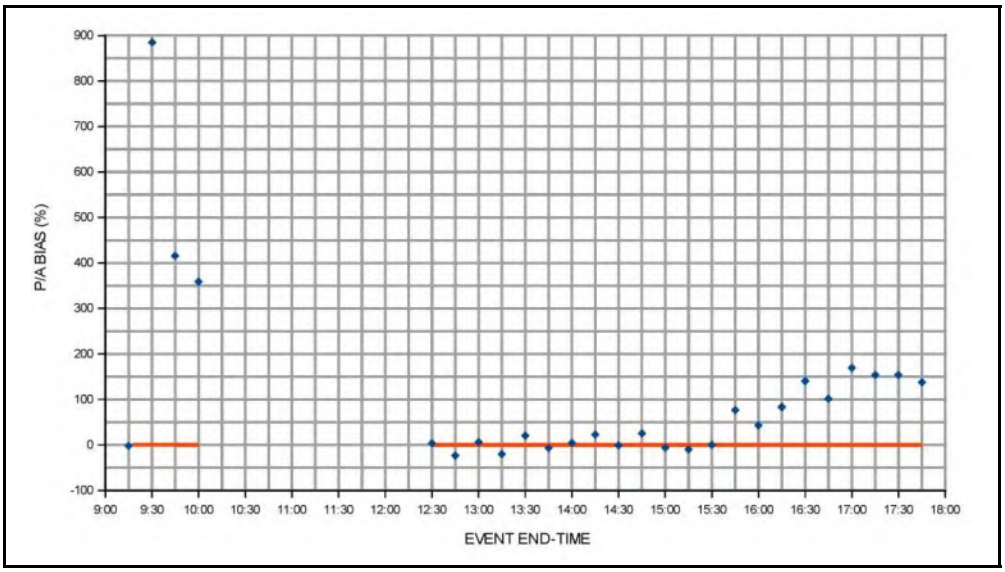

For Block 2, the P/A bias as a whole was clearly quite poor (despite Event 1 being very good). Even though the per-event rate of change of the interpolated background value for this block was the third greatest of all 27 blocks for the entire study (Table 5-2), we believe the primary reason for this unacceptably poor bias was found in the 2-meter wind-speed data for these four events (0.979 to 1.364 m/s). The relatively stable conditions of the early to mid-morning (09:00 to 10:00) and the very light winds probably led to significant "pooling," in which concentrated pockets of stagnant methane likely accumulated near the TDL beam, leading to the very high P/A biases for Events 2 through 4. This is the reason for designating Block 2 a statistical outlier, and was why field operations were suspended on this day until a stronger wind took hold.

For Block 3 (separation distance 23.1 meters), the P/A bias as a whole was much better (+48.8 percent), but still not good. However, as shown in this figure, there was a period of 13 consecutive monitoring events in the afternoon, beginning at 12:15 and ending at 15.30 (Events 5 through 17), when the individual P/A biases were actually quite good, as discussed next.

Figure 5-8 presents, for Day 2, the P/A bias vs. event time for the booster station simulation, but only for Events 5 through 17 of this block (Block 3). Of these 13 events, ten had a P/A bias within about 20 percent, and eight within 10 percent. The PA relative standard deviation for this subset of events was 15.2 percent, with a P/A bias of just +1.17 percent.

Although e-Calc is designed only for ground-level sources, it is apparent that under these particular meteorological conditions, the software performance was very good for this somewhat elevated source.

FIGURE 5-8. DAY 2 – BOOSTER STATION (EVENTS 5-17 ONLY): P/A BIAS VS. EVENT END-TIME

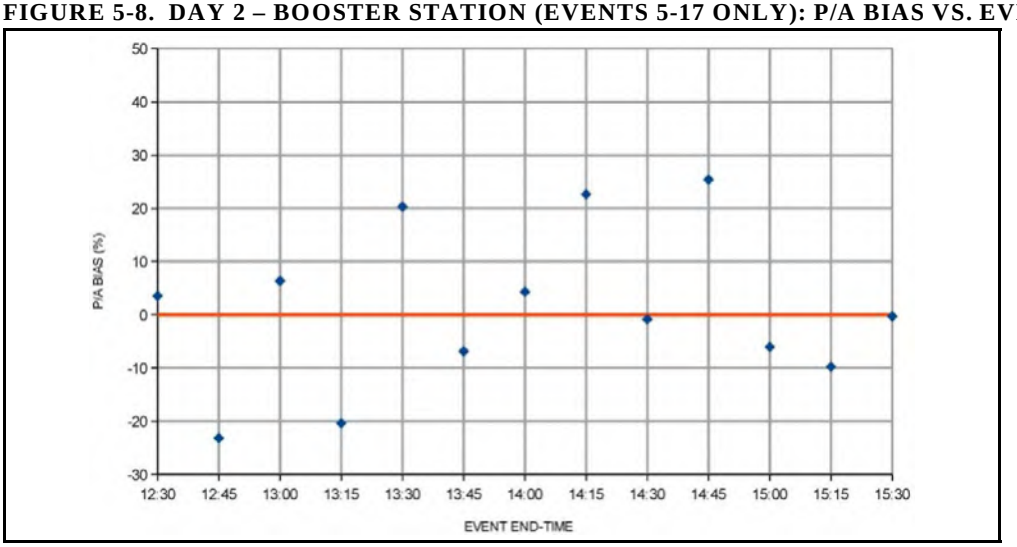

The statistics for the final nine events of Block 3 (Figure 5-7), while better than Block 2, are still not considered to be satisfactory. We believe this was due primarily to the onset of a more stable atmospheric regime owing to the time of the day (15:30 to 17:45), and the possible re-establishment of the downwash rotor (or possibly to some other phenomenon related to an increased atmospheric stability).

5.3.2 Gas-Gathering Pipeline – Days 3, 4, and 9

The gas-gathering pipeline leaks were simulated using a small, rectangular lattice-type array of 2.5-centimeter-diameter copper piping. The pipes were pierced with about 70 or 80 small holes in order to distribute the methane flow to the ambient air. The piping array was about 1.8 meters by 0.9 meters in size, and was positioned 1.0 meters above the ground.

Day 3 – August 16

Figure 5-9 presents, for Day 3, the P/A bias vs. event end-time for the gas-gathering pipeline simulation. From Table 5-3, the Day 3 actual emission rate was 443.7 mg/s, and the mean P/A biases were: Block 4 (Event 1), +14.2 percent, Block 5 (Events 2 through 4), −21.8 percent, and Block 6 (Events 5 through 26), +7.1 percent.

FIGURE 5-9. DAY 3 – GAS-GATHERING PIPELINE: P/A BIAS VS. EVENT END-TIME

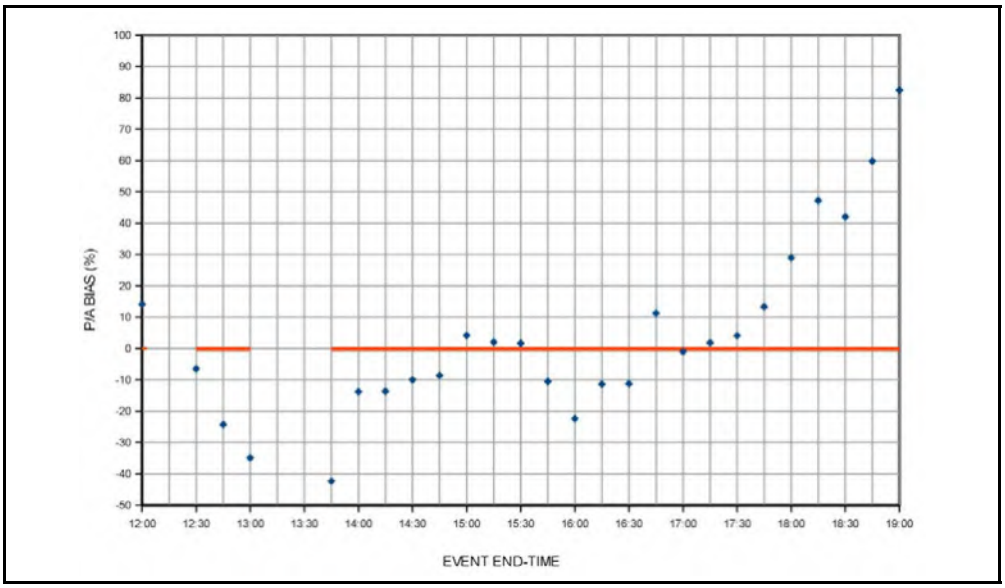

For Block 4 (Event 1, end-time 12:00), the P/A bias was reasonably good (better than +15 percent).

For Block 5 (Events 2 through 4 end-times 12:30 – 13:00), the P/A bias began quite good (better than –8 percent), but increased to about –35 percent by Event 4. The per-event rate of change of the interpolated background methane values for Block 5 was the sixth greatest, lending considerable uncertainty to any conclusions drawn for these four events.

However, for Block 6 (Events 5 through 26, end-times 13:45 – 19:00), the interpolated background values were much more uniform (Table 5-2), adding more overall confidence in the data. The P/A biases were quite good from Events 6 through 21 (end-times 14:00 – 17:45), with values less than 15 percent for all but one of these 16 events. After that, however, the P/A biases exhibit a sharp increase, coinciding with a more stable atmospheric regime (event ending at 18:00). We hypothesized that the poor biases of these last five events (Events 22 through 26) were again related to the increase in atmospheric stability (likely associated with a declining sun angle and the subsequent onset of nighttime).

Day 4 – August 17

Figure 5-10 presents, for Day 4, the P/A bias vs. event end-time for the gas-gathering pipeline simulation. From Table 5-3, the Day 4 actual emission rate was 403.4 mg/s, and the mean P/A biases were: Block 7 (Events 1 through 12), +38.9 percent; Block 8 (Events 13 through 18), +33.8 percent; and Block 9 (Events 19 through 24), +21.7 percent.

FIGURE 5-10. DAY 4 – GAS-GATHERING PIPELINE: P/A BIAS VS. EVENT END-TIME

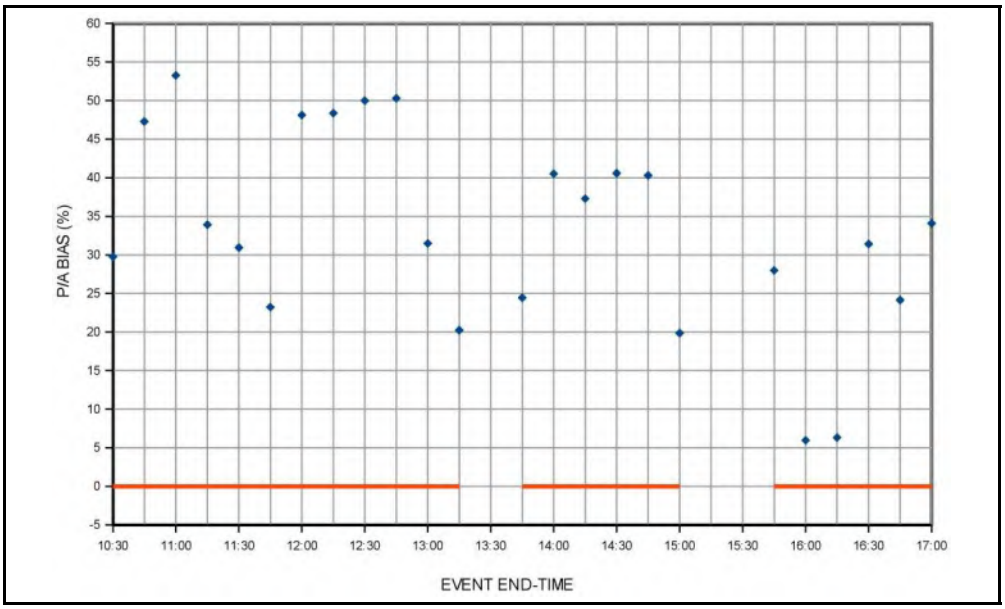

In general, a large, systematic positive bias was observed for nearly all events on this day. For Block 7 (Events 1 through 12, end-times 10:30 – 13:15), the P/A bias was greater than +30 percent for 10 of the 12 events, and greater than +40 percent for six of those 10. For Block 8 (Events 13 through 18, end-times 13:45 – 15:00), the P/A bias was greater than about +20 percent for all six events. For Block 9 (Events 19 through 24, end-times 15:45 – 17:00), the P/A bias was somewhat better, generally within +30 percent for the six events, with two less than +10 percent.

As for the interpolated background values, Table 5-2 shows that Block 7 and Block 9 had the fourth and fifth greatest per-event rates of change, respectively. Troubling was the disparity between the methane background concentrations measured at the beginning and end of the 15-minute period from 13:15 to 13:30, and again at the beginning and end of the 30-minute period from 15:00 to 15:30. While this does not explain the systematic positive bias, we believe the uncertainty in the interpolated background values precluded having any confidence in the emission measurements for this entire day.

Day 9 – August 23

Figure 5-11 presents, for Day 9, the P/A bias vs. event end-time for the gas-gathering pipeline simulation. From Table 5-3, the Day 9 actual emission rate was 1,613.4 mg/s for Block 23, and 726.0 mg/s for Blocks 24 thorough 27. The mean P/A biases were: Block 23 (Event 1), +39.9 percent; Block 24 (Events 2 through 4), +82.4 percent; Block 25 (Events 5 through 12), +64.4 percent; Block 26 (Events 13 through 20), +87.2 percent; and Block 27 (Events 21 through 30), +59.0 percent. The final 16 events (beginning with the end-time of 20:00) were the only events performed during nighttime conditions for the entire study.

FIGURE 5-11. DAY 9 – GAS-GATHERING PIPELINE: P/A BIAS VS. EVENT END-TIME

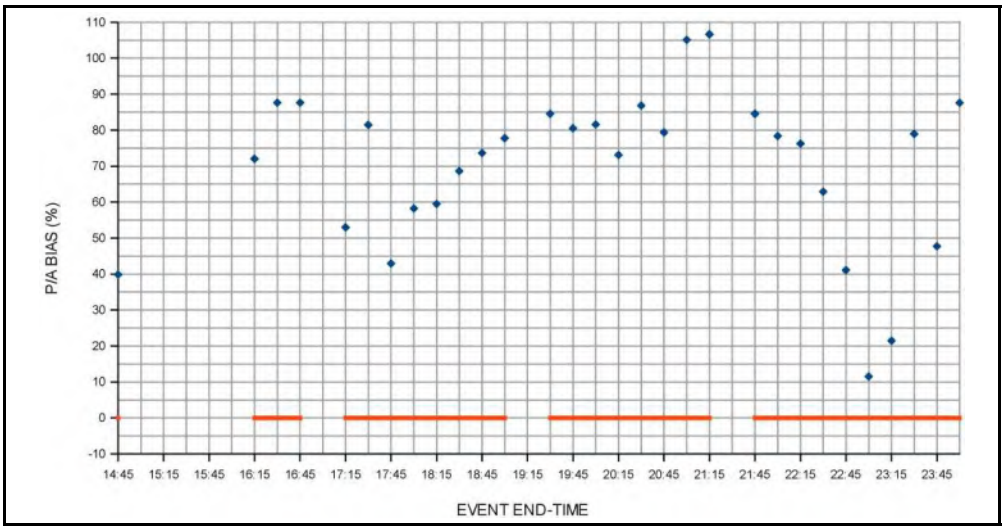

As for the interpolated background values, for Block 23 (Event 1, end-time 14:45), the background methane measurements were made immediately before and after this single event, and still the rate of change for this interpolated value was the greatest of all blocks over the entire study (Table 5-2).

For Block 24 (Events 2 through 4, end-times 16:15 – 16:45), the per-event rate of change of interpolated background methane value, while somewhat less, was still very significant – the second greatest of all blocks.

However, for Block 25 (Events 5 through 12, end-times 17:15 – 19:00), Block 26 (Events 13 through 20, end-times 19:30 – 21:15), and Block 27 (Events 21 through 30, end-times 21:45 – 00:00), the per-event rates of interpolated background methane values were much less, better than almost any other data block.

Day 9 was the only day characterized by overcast, relatively windy conditions. During the first two blocks (Blocks 23 and 24), although not shown herein, the mean 2-meter wind direction (2m) was 036 and 042 degrees, respectively (i.e., generally blowing from the northeast), while the final three blocks (Blocks 25 through 27) had a mean 2-meter wind direction of 023, 022, and 360 degrees, respectively (i.e., generally blowing from between the north and the north-northeast).

Based on the above wind-direction data, we hypothesized that there might have been an unknown, local source of methane to the northeast of the work area. If so, the stable atmospheric conditions could well have inhibited the dilution of this methane plume as it impacted the TDL measurement path during the first two data blocks. By the latter blocks, even though the atmosphere remained stable, the more northerly winds would have directed this methane plume to the east of the measurement path, thus allowing for the far more uniform interpolated background values.

Even taking into account this explanation of the background for Blocks 23 and 24, however, the overall P/A bias was disappointingly poor for this entire day (and night). Of the 26 events comprising Blocks 25 through 27, the individual P/A biases for all but two were greater than +40 percent.

For the nighttime events (i.e., all but the first two events of Block 26 plus all of Block 27, or Events 15 through 30), the individual P/A biases were even more inconsistent.

We believe the meteorological phenomenon that we hypothesized was partially responsible for the large variability in the earlier background measurements (Blocks 23 and 24), and also played a major role in the very poor P/A biases for Blocks 25 through 27. Not only was Day 9 the only measurement day which remained heavily overcast throughout, it also had the second-highest mean 2-meter wind speed (4.49 m/s for Blocks 25 through 27) behind Day 5 (6.01 m/s).

In terms of predicted emission rates, we believe that the controlled-release methane plume was more intact (i.e., less vertically dispersed) as it reached the TDL beam under these atmospheric conditions than was simulated by e-Calc 2 (and thus AERMOD). This artificially high concentration at the beam height would cause a corresponding over-prediction of the emission rate. This theory is consistent with the interpolated background values in Blocks 23 and 24, in that the set of atmospheric conditions unique to this measurement day helps explain both the large variability in the background measurements for these blocks, and the substantial over-prediction for Blocks 25 through 27.

5.3.3 Gas-Transmission Line – Days 5 and 6

An underground gas-transmission line leak was simulated by placing a bucket (0.4 meters tall and 0.4 meters in diameter) placed on the ground, and introducing the methane into the center of the bucket bottom. The overlying soil through which the methane had to flow to escape through the top of the bucket was simulated by adding some 200 small, cylindrical stainless steel pall rings (height and diameter approximately 2.5 centimeters), filling the entire bucket.

Day 5 – August 18

Figure 5-12 presents, for Day 5, the P/A bias vs. event end-time for the gas-transmission line simulation. From Table 5-3, the Day 5 actual emission rate was 645.4 mg/s, and the mean P/A biases were: Block 10 (Events 1 through 14, end-times 13:00 – 16:15), +16.9 percent; and Block 11 (Events 15 through 24, end-times 16:45 – 19:00), +29.3 percent.

FIGURE 5-12. DAY 5 – GAS-TRANSMISSION LINE: P/A BIAS VS. EVENT END-TIME

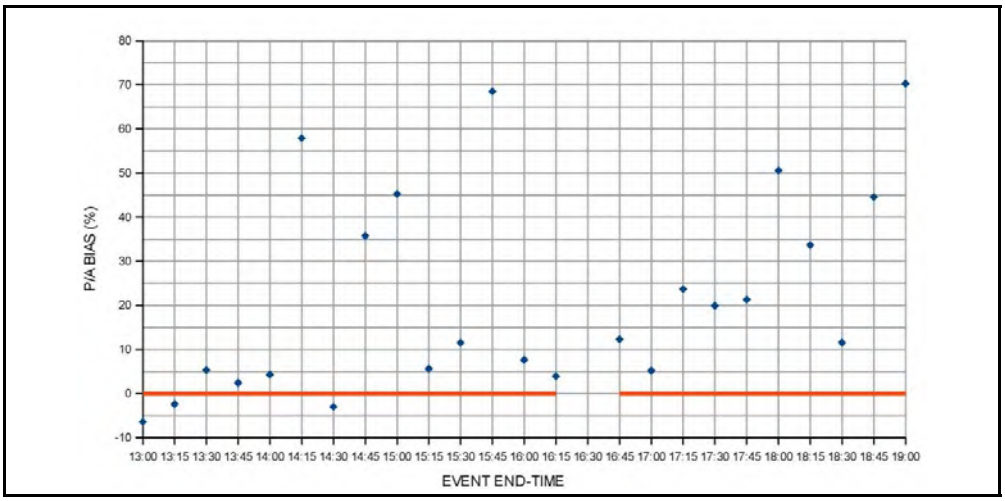

The per-event rate of change for the interpolated background values for Day 5 was the best of any measurement day as a whole, as indicated by (Table 5-2).

For Block 10 (Events 1 through 14), the P/A bias was very good (within about 12 percent), excluding four outlier events (Events 6, 8, 9, and 12). The 2-meter wind direction was very consistent for this entire block (range 313.1 to 330.4 degrees), as was the wind speed (range 6.025 to 7.401 m/s). Therefore, we could only hypothesize that there was some intermittent background source of methane for these four events.

For Block 11 (Events 15 through 24), the P/A bias was not as good (within 25 percent), again excluding four outlier events (Events 20, 21, 23, and 24). The increasingly poor P/A bias as it got later in the day again was likely caused by some intermittent background source (Block 11 wind-direction range 311.9 to 332.9 degrees), or evidenced our hypothesis put forth for Block 3 (Day 2) and Block 6 (Day 3) relating to e-Calc's (and thus AERMOD's) inability to adequately handle the increase in atmospheric stability, as the sun was declining and the wind speed decreasing (e.g., 3.159 m/s at Event 24).

Day 6 – August 20

Figure 5-13 presents, for Day 6, the P/A bias vs. event end-time for the gas-transmission line simulation. From Table 5-3, the Day 6 actual emission rate was 726.0 mg/s, and the mean P/A biases were: Block 12 (Events 1 through 7, end-times 11:30 through 13:00), −26.3 percent; Block 13 (Events 8 through 15 end-times 13:30 – 15:15), −10.4 percent; and Block 14 (Events 16 through 25, end-times 15:45 – 18:00), −2.3 percent.

FIGURE 5-13. DAY 6 – GAS-TRANSMISSION LINE: P/A BIAS VS. EVENT END-TIME

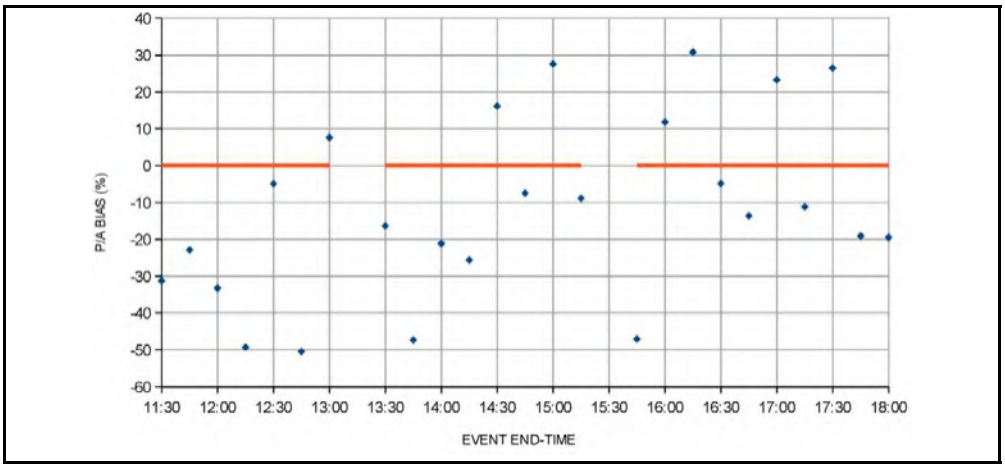

The per-event rate of change for the interpolated background values for Day 6 was the second best of any measurement day as a whole, as indicated by Table 5-2.

Although the mean P/A bias for Block 12 was −26.3 percent, the mean P/A bias improved for Block 13 (−10.4 percent) and Block 14 (−2.3 percent). Still, from Figure 5-13, the P/A values for individual events exhibited a lot of scatter, generally ranging from about −50 percent to +30 percent for the two latter blocks.

Smoke from historic western forest fires impacted the study on most measurement days but, with one exception, we believe the impact was not a significant factor in the performance of e-Calc 2, except on Day 6 when the smoke was by far the greatest. In fact, the sky was so dark in the middle of the day that some of the outside building lights went on automatically. We believe the decreased solar radiation and the presence of a large amount of smoke particles may have been responsible for the large scatter in the data above, but the precise mechanism involved remains unclear.

5.3.4 Production Pad – Days 7 and 8

A production pad will typically leak at the well head. This type of leak was simulated using an empty bucket (0.4 meters tall and 0.4 meters in diameter) placed on the ground, and introducing the methane into the center of the bucket bottom. This approach was similar to the underground gas-transmission pipeline simulation (Days 5 and 6), except that the bucket remained empty.

Day 7 – August 21

Figure 5-14 presents, for Day 7, the P/A bias vs. event end-time for the production pad simulation. From Table 5-3, the Day 7 actual emission rate was 363.0 mg/s, and the mean P/A biases were: Block 15 (Events 1 through 4, end-times 13:00 – 13:45), −27.5 percent; Block 16 (Events 5 through 11, end-times 14:45 – 16:15), −0.3 percent; Block 17 (Events 12 through 18, end-times 16:45 – 18:15), +6.5 percent; and Block 18 (Events 19 through 23, end-times 18:45 – 19:45), +11.0 percent.

FIGURE 5-14. DAY 7 – PRODUCTION PAD: P/A BIAS VS. EVENT END-TIME

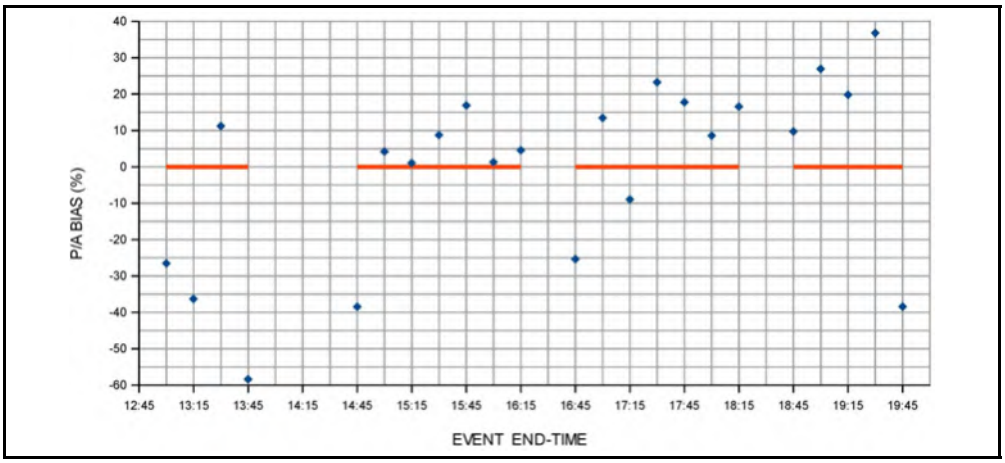

As indicated in Table 5-2, the per-event rate of change for the interpolated background values for Day 7 were relatively poor for Blocks 15 and 18, but relatively good for Blocks 16 and 17.

The individual P/A biases were generally poor for all four data blocks, with the greatest spreads during Block 15 (about −60 to +10 percent) and Block 18 (about −40 to +35 percent). The spread was a bit less on Block 16 (about −40 to +15 percent) and Block 17 (about −25 to +25 percent).

Day 8 – August 22

Figure 5-15 presents, for Day 8, the P/A bias vs. event end-time for the production pad simulation. From Table 5-3, the Day 8 actual emission rate was 484.0 mg/s, and the mean P/A biases were: Block 19 (Events 1 through 7, end-times 12:15 – 13:45), −19.2 percent; Block 20 (Events 8 and 9, end-times 14:15 – 14:30), −5.6 percent; Block 21 (Events 10 through 16, end-times 15:00 – 16:30), +4.4 percent; and Block 22 (Events 17 through 20, end-times 17:00 – 17:45), −30.5 percent.

FIGURE 5-15. DAY 8 – PRODUCTION PAD: P/A BIAS VS. EVENT END-TIME

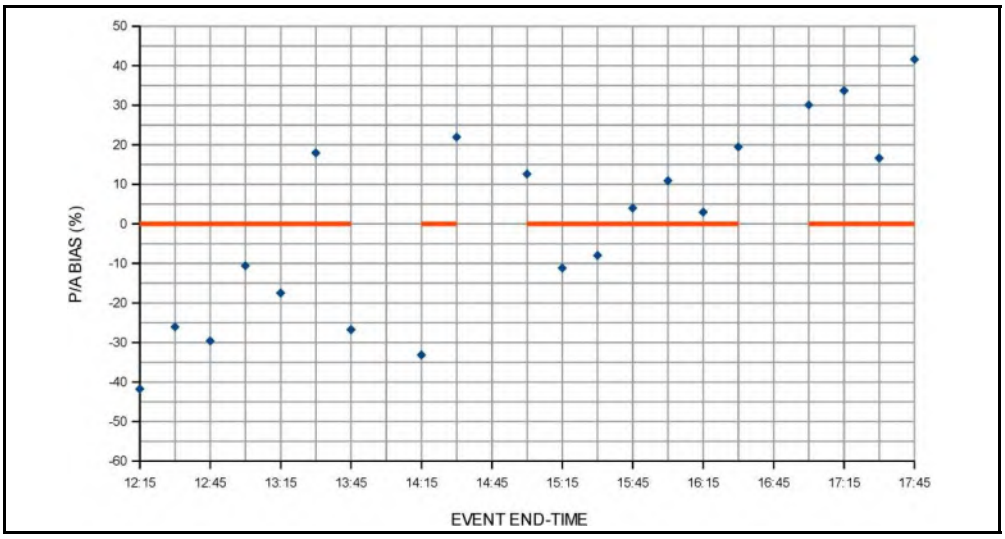

As indicated in Table 5-2, the per-event rate of change for the interpolated background values for Day 8 was relatively poor for Blocks 19 and 22, fair for Block 20, and good for Block 21.

For Block 19, the individual P/A biases were poor (about –40 to +20 percent). For Block 20, the individual P/A biases were poor (about –35 to +20 percent). For Block 21, the individual P/A biases were fairly good (about –10 to +20 percent). For Block 22, the individual P/A biases were poor (about +15 to +40 percent). These results were generally consistent with the interpolated background data quality.

5.4 Conclusions

The primary project goal was generally achieved. An exception, however, was that we were unable to develop source-specific empirical correction factors, despite the fact a general systematic bias was observed in the P/A results. The large scatter of the P/A data and the confounding issue concerning assignment of monitoring event background values precluded our ability to develop these empirical adjustments to e-Calc 2.

Background issues notwithstanding, the statistical performance of e-Calc 2 in addressing the project goal was still somewhat disappointing overall. Although a major reason for the less-than satisfactory P/A results was the inability to assign an accurate methane background concentration to each monitoring event, it was evident there were other factors at play as well. Presented next are considerations with respect both to the model (i.e., AERMOD), and to the interpolated background methane concentrations.

5.4.1 AERMOD Considerations

For the booster-station simulation, e-Calc 2 clearly over-predicted during Day 1, likely owing to the establishment of a rotor downwind of this somewhat elevated source (see the discussion in Section 5.3.1). On the other hand, once the TDL beam was moved further downwind on Day 2 (Block 3), the software performed quite well. The exception to this, however, was when the wind was very light (less than about 1.4 m/s at 2 meters), resulting in methane pooling which, in turn, led to a breakdown of the model and anomalously high emission-rate predictions. It should be noted that the AERMOD Implementation Guide cautions model users about prediction inaccuracies under very light wind conditions (less than 1 m/s at a height of 10 meters), due to plume meander.

Another problem primarily affecting the booster station was the fact that, for small, slightly elevated non-buoyant sources such as this, under most conditions, the model holds constant the elevation of the plume centerline within about 50 meters downwind of the source (beyond which it tends to mix uniformly in the vertical dimension). In this case, therefore, the model positioned the plume centerline at the booster station's methane release height (3 meters above the ground). However, we were able to demonstrate that for these days (Days 1 and 2), the plume centerline, in actuality, was brought closer to the ground (to within about 1 or 1.5 meters, depending on the data block) before reaching the TDL beam-path. In summary, the model "thought" that the plume centerline was higher than it actually was and, accordingly, the concentration measured at the beam-path height (1 meter) was less than the predicted concentration. The result, therefore, was that the model erroneously corrected (i.e., over-predicted) the subsequent emission rate.

For the other simulated sources, (the gas-gathering pipeline, gas-transmission line, and production pad), the biggest problem appeared to be associated with emission-rate over-predictions as the atmosphere became more stable during the late afternoon. This was especially evident during Day 3 (gas-gathering pipeline), and to a lesser degree to Day 5 (gas-transmission line). It appeared that

the eddy-correlation (or covariance) approach employed in the new AERMOD version (and, therefore, e-Calc 2), under these conditions, was unable to properly simulate the vertical wind-speed profile below the height of the lowest wind-speed measurement, i.e., 2 meters.

5.4.2 Background Methane Considerations

As discussed in Section 5.1, background methane was shown to be variable over each measurement day, and quite significant relative to the source attribution. The value assigned to each monitoring event was derived by linear interpolation based on the two actual background measurements made just prior to and after each block of data.

Table 5-4 presents, for each data block, the mean interpolated background methane concentration (IB), the mean methane source attribution (SA), and the ratio of these values (IB/SA). Source attribution was derived by subtracting the mean background concentration from the mean downwind concentration for each data block (in much the way it was derived for the individual monitoring events). These ratios illustrate the necessity of having an accurate background concentration to assign to each monitoring event.

TABLE 5-4. RATIO OF INTERPOLATED BACKGROUND METHANE TO SOURCE ATTRIBUTION

Day	Source	Data Block	Events	Mean Methane Concentration (ppm)		Ratio (IB / SA)
				Interpolated Background (IB)	Source Attribution (SA)	
1	Booster Station	1	1-29	1.919	0.333	5.8
2	Booster Station	2	1-4	2.168	1.193	1.8
		3	5-26	2.013	0.287	7.0
3	Gas-Gathering Pipeline	4	1	2.087	0.338	6.2
		5	2-4	2.024	0.285	7.1
		6	5-26	1.955	0.284	6.9
4	Gas-Gathering Pipeline	7	1-12	2.071	0.371	5.6
		8	13-18	1.921	0.377	5.1
		9	19-24	1.982	0.355	5.6
5	Gas-Transmission Line	10	1-14	1.880	0.154	12.2
		11	15-24	1.878	0.208	9.0
6	Gas-Transmission Line	12	1-7	1.825	0.195	9.4
		13	8-15	1.815	0.206	8.8
		14	16-25	1.823	0.282	6.5
7	Production Pad	15	1-4	1.931	0.148	13.1
		16	5-11	1.715	0.360	4.8
		17	12-18	1.701	0.463	3.7
		18	19-23	1.715	1.286	1.3
8	Production Pad	19	1-7	2.020	0.471	4.3
		20	8-9	2.001	0.201	9.9
		21	10-16	1.918	0.670	2.9
		22	17-20	1.928	2.051	0.9
9	Gas-Gathering Pipeline	23	1	2.557	1.152	2.2
		24	2-4	2.276	0.783	2.9
		25	5-12	2.112	0.697	3.0
		26	13-20	2.114	0.917	2.3
		27	21-30	2.109	0.901	2.3

Although not of use directly in this project, we chose to plot the entire set of measured background readings (all days) as a function of the time of day, in order to explore the premise that background concentrations are higher in the morning due to the establishment of nighttime temperature inversions.

Figure 5-16 depicts the measured background (methane) concentration vs. the time of day, for all measurement days (total of 54 readings per Table 5-1).

Figure 5-17 depicts the same information, except for elimination of the Day 9 results (for reasons discussed in the context of the daily results, Section 5.3.2). The best-fit curve illustrates how the background concentration was generally highest in the early part of the day, then leveled off or slowly declined as the day wore on (r^2 = 0.418). We believe, in general, that the higher concentrations earlier in the day were indeed the result of temperature inversions (normally occurring during many nights), which acted to inhibit vertical dispersion and hence served as a methane "lid." These inversions then dissipated during the daytime under the destabilizing influence of the sun.

FIGURE 5-16. MEASURED BACKGROUND CONCENTRATION VS. TIME (ALL DAYS)

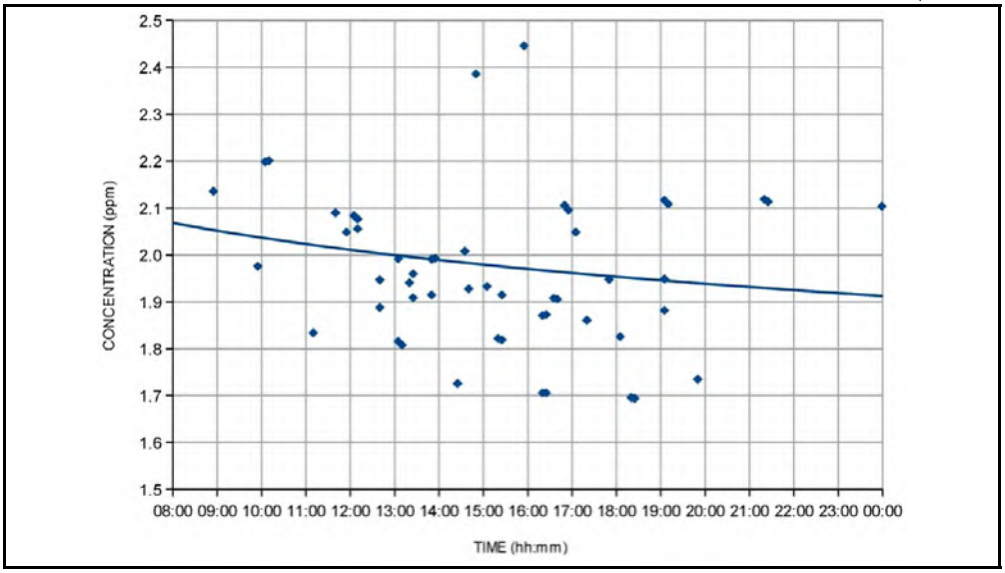

FIGURE 5-17. MEASURED BACKGROUND CONCENTRATION VS. TIME (DAYS 1-8 ONLY)

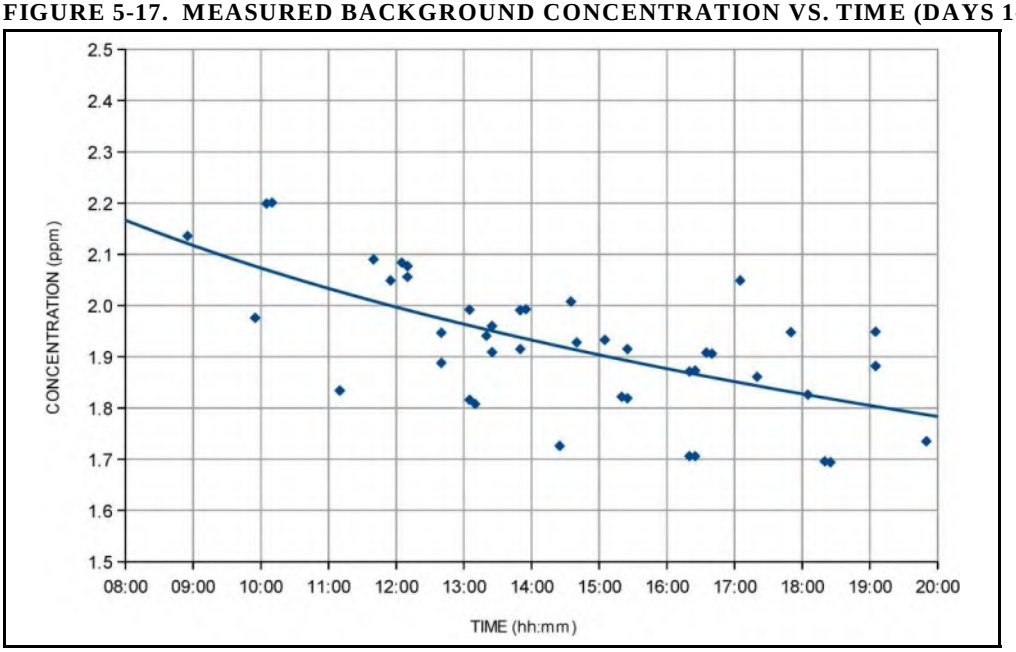

The periodic background methane measurements evidenced that the background was generally changing over the course of each measurement day. Although a linear interpolation was judged the best means of assigning a background value to each monitoring event, there was no assurance that this assumption reflected reality. In fact, there was no way of knowing whether some of these high P/A biases weren't caused by a background spike at some point during a particular data block.

Similarly, from Table 5-4, since the mean background concentration was generally quite large compared to the mean source attribution, there was a practical limit in our ability to discern, for any given monitoring event, how much of the P/A bias could be attributed to the performance of e-Calc 2 (as opposed to the error in the assigned background value). Still, subsequent analyses were identified and performed to improve the e-Calc 2 performance (discussed next).

5.5 Subsequent Analyses

The practical implications of the background methane issue notwithstanding, further examination of the program results led us to believe that we had isolated a significant source of P/A error, related to employment of the eddy-correlation (or covariance) approach.

As mentioned in Section 5.4, we suspected that the model, as configured, was unable to properly simulate the vertical wind-speed profile in the lowest few meters of the atmosphere. The eddy-correlation approach constructs this profile based solely on wind-sensor measurements at two heights. For this project, these heights (2.0 and 5.0 meters) were selected based on an exhaustive literature survey and on recommendations from one of the leading researchers in the field. Initial examination confirmed that the lower height (2 meters) was not ideal, and that model performance would likely be improved if the wind sensor were lowered.

The following subsequent analyses were explored, prior to finalizing the System specification:*

- Confirmation of the covariance algorithm employed;
- A more refined treatment of background methane data; and
- Assessment of whether a single wind sensor was satisfactory.

An approach was developed and implemented to address these issues, which: (a) was focused and technically sound; and (b) involved performance of extensive additional dispersion modeling employing both e-Calc 1 and e-Calc 2.

_____

* At the time, we committed to perform a detailed analysis on this error source for inclusion in this Final Project Report. However, in retrospect, we decided to incorporate the results of these subsequent analyses into the Set of Specifications (the Major Deliverable for Milestone H); therefore, the results of these analyses are included in Section 6.

SECTION 6 – INITIAL SYSTEM SPECIFICATION

The Major Deliverable for Milestone H provided the initial System specification, based largely on the statistical performance assessment of e-Calc 2 as presented in the Milestone F Report. As mentioned, the metric for this statistical performance assessment was how well the predicted methane emission rate compared to the controlled (or actual) release rate.

Section 6.1 summarizes the requisite follow-up analyses (detailed in Appendix A to the Milestone H Report). **Section 6.2** presents an overview of the System and identifies the essential components. **Section 6.3** presents the initial System recommendations and limitations.

6.1 Requisite Follow-Up Analyses

These follow-up analyses were successful in removing most of the P/A emission-rate inconsistency. There was an additional opportunity to explore whether and to what degree these results would be compromised should the meteorological instrumentation requirements of e-Calc 2 be simplified by eliminating the upper-most wind sensor (5-meter height). Three analyses were performed sequentially:

- Analysis #1: Covariance Algorithm Confirmation
  The purpose of this analysis was to confirm that the covariance algorithms employed to support the eddy-correlation approach were correctly implemented in the field. Before beginning additional background variability work (which would reduce even further the amount of data upon which to base the specifications), an approach was designed to verify that these algorithms were implemented correctly. The logic was that if there had been a problem, the P/A results would have been compromised, irrespective of the background issues.

- Analysis #2: Further Treatment of Background Data
  Through further examination of the background data, the purpose of this analysis was to improve the P/A emission-rate ratios until there was sufficient confidence in these results to: (a) justify moving forward with the specification development; and (b) confirm the original positioning of the bottom wind sensor (2-meter height).

- Analysis #3: Assessment of Whether a Single Wind Sensor was Satisfactory
  The purpose of this analysis was to assess whether satisfactory P/A emission-rate results could be obtained using a single wind sensor, which would simplify the field logistics. E-Calc 2 was re-run using the meteorological data from the single sensor (2-meter height) for the P/A results remaining from Analysis #2, and these results were compared to those for the same data set using both sensors (2- and 5-meter heights).

6.1.1 Covariance Algorithm Confirmation

E-Calc 2 employs the eddy-correlation (or covariance) approach, which typically requires the measurement of wind at two heights above the ground – in this case, 2 and 5 meters. Covariance statistics, calculated from the lower of these two sensors, are then used to determine the friction velocity. Friction velocity (units of meters-per-second) is a stability parameter used in AERMOD to characterize atmospheric turbulence. It is a measure of mechanical effects alone, i.e., wind sheer at ground-level.

In the flux-gradient approach (e-Calc 1), friction velocity is calculated from the surface roughness length, which characterizes the roughness of the terrain. The roughness length is obtained from published tables as part of the pre-field activities. AERMOD uses the friction velocity, together with surface characterization pre-processing software and a wind measurement from a single height, to generate the vertical wind-speed profile, which primarily governs the predicted (back-calculated) emission rate in e-Calc 1 (and e-Calc 2).

In the eddy-correlation approach (e-Calc 2), the friction velocity is instead derived using the time-averaged fluctuations of the horizontal and lateral vectors from the lower of the two wind sensors. The power-law equation is used to generate the vertical wind-speed profile based on the calculated friction velocity and the wind measurements from both sensor heights.

The current version of AERMOD employs the flux-gradient approach to calculate friction velocity. This approach has been extensively evaluated in model-validation studies performed by the U.S. EPA over the years. As mentioned in Section 2.1 of this report, the U.S. EPA is planning to update AERMOD based on the eddy-correlation approach, but has yet to release the software coding for this version.

After much deliberation, we concluded that the most viable means of determining whether the eddy-correlation approach had been correctly implemented in the field was to repeat the e-Calc 2 modeling using e-Calc 1, and then compare the friction-velocity values calculated as part of the two software versions. The close tracking of these two friction-velocity depictions (graphs not reproduced herein) provided ample evidence that the covariance algorithms employed to support the eddy-correlation approach were correctly implemented, and we were able to move forward with the next analysis.

6.1.2 Further Treatment of Background Data

The background methane concentrations assigned to each monitoring event were presented in Table 5-2. In each case, this value was derived by linear interpolation of the actual background measurements made just prior to and after each block of data. While this approach for assigning background concentrations to individual monitoring events appeared sound, the results were only marginally satisfactory. Therefore, we had to acknowledge the likelihood that there were other factors governing the quality of the interpolated background data, which needed to be explored.

In order to identify an additional criterion for background "acceptance," the refined Milestone H analysis focused on those situations where two consecutive background measurements were made. The logic was that the quality of the background depiction would be in question if these readings varied too much, as it was unlikely that the actual background concentration would change significantly over such a short duration. From Table 5-2, it can be seen that consecutive background readings were taken a total of 15 times over the nine days of measurements. In 13 of these instances, the measurements comprising these background "pairs" were taken at the beginning and end of a single 15-minute period; in the remaining two instances, they were taken over consecutive 15-minute periods.

The additional criterion was that any set of consecutive background readings had to be within 3 ppb of each other, or the adjacent blocks of data were rejected. Only five such sets of background data met this 3-ppb threshold: one each on Days 3, 5, and Day 6, and two on Day 7. We accepted interpolated concentrations from a maximum of four events either side of each acceptable background pair, as long as the per-event rate of change of the interpolated value was less than 2 ppb. For example, on Day 7, both consecutive background readings met the 3-ppb threshold, but the per-event rate of change for the final block of data was more than 6 ppb (due to the high final background measurement for the day), thereby causing elimination of the entire block.

Table 6-1 presents the initial universe of acceptable monitoring events based on the above refined background criteria. The mean 2-meter wind speed, the actual and predicted emission rate, and the P/A bias are shown for each of the 31 events identified. The mean P/A biases for the seven groups of continuous events ranged between 2.4 and 22.9 percent. By comparison, the U.S. EPA considers any emission-rate measurement system to be excellent if it can consistently be within 30 percent of the actual emissions.

TABLE 6-1. INITIAL UNIVERSE OF ACCEPTABLE MONITORING EVENTS

Monitoring Event		Mean 2m	Emission Rate (mg/s)		
No.	End-Time (MDT)	Wind Speed (m/s)	Actual (A)	Predicted (P)	P/A Bias (%)
Day 3 (August 16, 2918) – Gas-Gathering Pipeline					
5	13:45	2.74	443.7	256.2	-42.3
6	14:00	2.77	443.7	383.0	-13.7
7	14:15	2.82	443.7	383.7	-13.5
8	14:30	2.57	443.7	399.7	-9.9
	Mean	**2.73**	**443.7**	**355.7**	**-19.9**
Day 5 (August 18, 2018) – Gas-Transmission Line					
11	15:30	7.23	645.4	720.0	11.6
12	15:45	6.36	645.4	1,087.7	68.5
13	16:00	6.33	645.4	695.0	7.7
14	16:15	6.03	645.4	670.9	3.9
	Mean	**6.49**	**645.4**	**793.4**	**22.9**
15	16:45	6.09	645.4	724.8	12.3
16	17:00	5.05	645.4	679.1	5.2
17	17:15	5.51	645.4	798.1	23.7
18	17:30	5.53	645.4	774.0	19.9
	Mean	**5.55**	**645.4**	**744.0**	**15.3**
Day 6 (August 20, 2018) – Gas-Transmission Line					
12	14:30	3.75	726.0	843.4	16.2
13	14:45	3.06	726.0	672.1	-7.4
14	15:00	3.36	726.0	926.2	27.6
15	15:15	3.15	726.0	661.6	-8.9
	Mean	**3.33**	**726.0**	**775.8**	**6.9**
16	15:45	2.74	726.0	384.2	-47.1
17	16:00	2.75	726.0	811.6	11.8
18	16:15	3.23	726.0	949.5	30.8
19	16:30	2.97	726.0	690.6	-4.9
	Mean	**2.92**	**726.0**	**709.0**	**-2.4**
Day 7 (August 21, 2018) – Production Pad					
8	15:30	3.17	363.0	394.8	8.8
9	15:45	3.02	363.0	424.3	16.9
10	16:00	2.91	363.0	367.7	1.3
11	16:15	2.85	363.0	379.5	4.6
	Mean	**2.99**	**363.0**	**391.6**	**7.9**
12	16:45	2.18	363.0	270.9	-25.4
13	17:00	2.51	363.0	411.8	13.4
14	17:15	2.61	363.0	330.5	-9.0
15	17:30	2.48	363.0	447.3	23.2
16	17:45	2.38	363.0	427.5	17.8
17	18:00	2.13	363.0	394.1	8.6
18	18:45	2.00	363.0	423.1	16.6
	Mean	**2.33**	**363.0**	**386.5**	**6.5**

Because of random phenomena affecting short-term application of AERMOD, the initial System specification included the recommendation that an average of four successive measurements (monitoring events) be used to create an hourly emission rate.

As to the suggestion that the P/A results might have been improved had the bottom sensor been repositioned lower, we believe that the Table 6-1 results based on the 2-meter sensor height were sufficiently acceptable. This issue, however, is one of several which might merit consideration in any future field-testing studies.

6.1.3 Assessment of Whether a Single Wind Sensor was Satisfactory

The purpose of this analysis was to assess whether satisfactory P/A results could be obtained using a single wind sensor (3D sonic anemometer), positioned at a height of 2 meters. This assessment was performed because, if successful, the System specifications and field logistics would be simplified (i.e., the 5-meter sensor would no longer be required).

Table 6-2 presents, for the 31 high-quality monitoring events from Analysis #2, a comparison of the e-Calc 2 P/A emission rates with both wind sensors vs. the single wind sensor. Shown for each monitoring event are:

- the event number and end-time;
- the mean 2-meter wind speed;
- the actual emission rate;
- the predicted emission rate and the relative difference (both sensor scenarios); and
- the P/A bias and the arithmetic difference (both sensor scenarios).

The thick horizontal lines separating monitoring events (Days 5, 6, and 7) signify the 15-minute period during which the dual background measurements were made (see Table 5-2).

In general, the consistency between the two wind-sensor scenarios was judged excellent, and provided ample justification for preparing the System specifications based on the single-sensor scenario.

These results appeared to be somewhat dependent upon wind speed, in which slightly higher (or more conservative) emissions rates were predicted for Days 5 and 6 under the single-sensor scenario, when the wind speed was generally greater than 3 m/s. On the other hand, on Day 7 when the wind speed was generally less than 3 m/s, the predicted emission rates for single-sensor scenario were slightly lower (or less conservative). Still, for purposes of developing the System specification, these differences are extremely minor and are of largely academic interest only.

TABLE 6-2. E-CALC 2 COMPARISON: TWO WIND SENSORS VS. A SINGLE WIND SENSOR

Monitoring Event		Mean	Emission Rate (ER) (mg/s)			ER Relative	P/A Bias (%)		
No.	End-Time (MDT)	2m WS (m/s)	Actual	Predicted 2 Sensors	Predicted 1 Sensor	Difference (%)	2 Sensors	1 Sensor	Difference (2 - 1)
Day 3 (August 16, 2018) – Gas-Gathering Pipeline									
5	13:45	2.74	443.7	256.2	279.3	(9.0)	(42.3)	(37.1)	(5.2)
6	14:00	2.77	443.7	383.0	415.0	(8.4)	(13.7)	(6.5)	(7.2)
7	14:15	2.82	443.7	383.7	432.0	(12.6)	(13.5)	(2.6)	(10.9)
8	14:30	2.57	443.7	399.7	423.2	(5.9)	(9.9)	(4.6)	(5.3)
Daily Mean		**2.73**	**443.7**	**355.7**	**387.4**	**(9.0)**	**(19.9)**	**(12.7)**	**(7.2)**
Day 5 (August 18, 2018) – Gas-Transmission Line									
11	15:30	7.23	645.4	720.0	744.6	(3.4)	11.6	15.4	(3.8)
12	15:45	6.36	645.4	1,087.7	1,107.5	(1.8)	68.5	71.6	(3.1)
13	16:00	6.33	645.4	695.0	708.7	(2.0)	7.7	9.8	(2.1)
14	16:15	6.03	645.4	670.9	684.3	(2.0)	4.0	6.0	(2.0)
15	16:45	6.09	645.4	724.8	759.6	(4.8)	12.3	17.7	(5.4)
16	17:00	5.05	645.4	678.9	699.6	(3.0)	5.2	8.4	(3.2)
17	17:15	5.51	645.4	798.1	815.4	(2.2)	23.7	26.3	(2.6)
18	17:30	5.53	645.4	774.0	798.0	(3.1)	19.9	23.6	(3.7)
Daily Mean		**6.02**	**645.4**	**768.7**	**789.7**	**(2.8)**	**19.1**	**22.4**	**(3.2)**
Day 6 (August 20, 2018) – Gas-Transmission Line									
12	14:30	3.75	726.0	843.4	851.1	(0.9)	16.2	17.2	(1.0)
13	14:45	3.06	726.0	672.1	673.6	(0.2)	(7.4)	(2.2)	(5.2)
14	15:00	3.36	726.0	926.2	931.6	(0.6)	27.6	28.3	(0.7)
15	15:15	3.15	726.0	661.6	665.1	(0.5)	(8.9)	(8.4)	(0.5)
16	15:45	2.74	726.0	384.2	386.5	(0.6)	(47.1)	(46.8)	(0.3)
17	16:00	2.75	726.0	811.6	819.5	(1.0)	11.8	12.9	(1.1)
18	16:15	3.23	726.0	949.5	950.8	(0.1)	30.8	31.0	(0.2)
19	16:30	2.97	726.0	690.6	703.1	(1.8)	(4.9)	(3.2)	(1.7)
Daily Mean		**3.13**	**726.0**	**742.4**	**747.7**	**(0.7)**	**2.3**	**3.6**	**(1.3)**
Day 7 (August 21) – Production Pad									
8	15:30	3.17	363.0	394.8	407.4	(3.2)	8.8	12.2	(3.4)
9	15:45	3.02	363.0	424.3	402.6	5.1	16.9	10.9	6.0
10	16:00	2.91	363.0	367.7	366.1	0.4	1.3	0.9	0.4
11	16:15	2.85	363.0	379.5	382.0	(0.7)	4.6	5.2	(0.6)
12	16:45	2.18	363.0	270.9	265.7	1.9	(25.4)	(26.8)	1.4
13	17:00	2.51	363.0	411.8	415.6	(0.9)	13.4	14.5	(1.1)
14	17:15	2.61	363.0	330.5	327.2	1.0	(9.0)	(9.9)	0.9
15	17:30	2.48	363.0	447.3	443.4	0.9	23.2	22.2	1.0
16	17:45	2.38	363.0	427.5	426.9	0.1	17.8	17.6	0.2
17	18:00	2.13	363.0	394.1	392.1	0.5	8.6	8.0	0.6
18	18:15	2.00	363.0	423.1	422.8	0.1	16.6	16.5	0.1
Daily Mean		**2.39**	**363.0**	**385.6**	**384.5**	**0.4**	**6.2**	**5.9**	**0.3**

6.2 System Overview and Components

Overview

Figure 6-1 is a System block diagram. Measured data from the TDL spectrometer, the GPS unit, and the meteorological instrumentation feed into a data-processing computer. The processed data streams then feed into the e-Calc 2 software, and the 15-minute-averaged methane emission rates are generated, in real-time.

FIGURE 6-1. SYSTEM BLOCK DIAGRAM

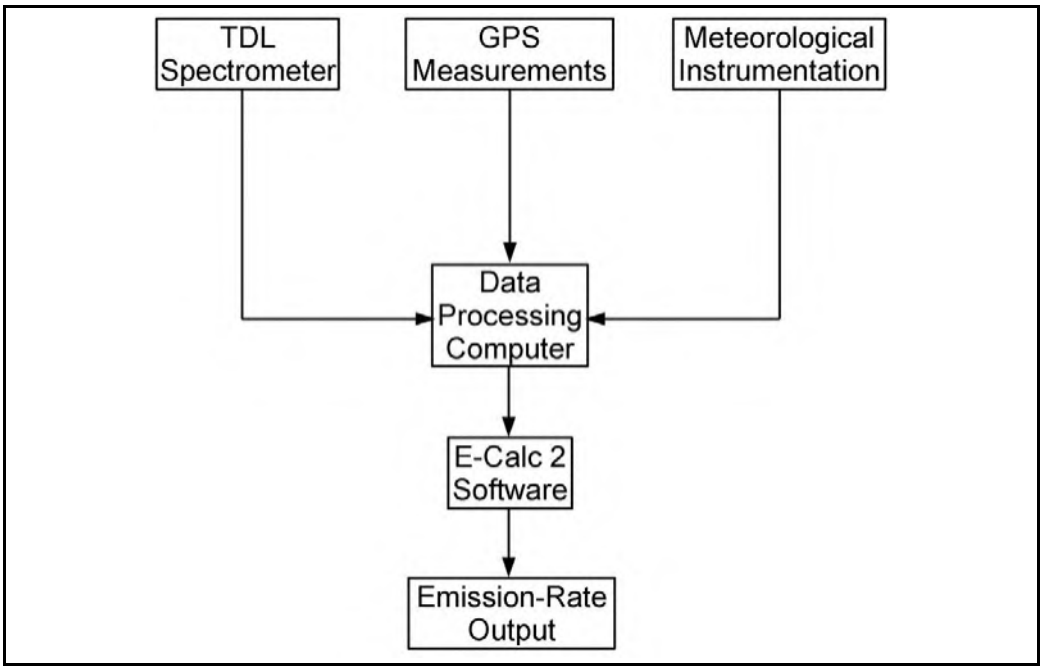

The System is comprised of the following components:

- e-Calc 2
- Boreal Laser GasFinder3-OP TDL system
- Met One Instruments meteorological system
- global positioning system
- data acquisition and processing

E-Calc 2

The e-Calc 2 software is supported by a PC with a Windows 10, 7, or XP operating system, on which Microsoft Visual Basic, Microsoft Access Database, and Seagate Crystal Report Professional are installed. The PC has a 64-bit operating system (at a minimum), 1.50 GHz processor, and 4.0 GB of RAM.

Boreal Laser GasFinder3-OP TDL System

Components for the TDL system include a spectrometer, a retroreflector, and a PC containing the manufacturer's DAS and reporting software.

Met One Instruments Meteorological System

The Met One meteorological system is a specially designed collection of components, some of which are from other manufacturers. These components include: an RM Young ultrasonic 3D anemometer; Met One's sensors to measure temperature, relative humidity, barometric pressure; and a Climatronics Corporation data logger. (It should be noted that Climatronics Corporation is wholly owned and operated by Met One Instruments, Inc.)

Global Positioning System

A Trimble GPS (or equivalent) is required.

Data Acquisition and Processing

Figure 6-2 depicts a data-acquisition and processing diagram for the System.

FIGURE 6-2. SYSTEM DATA ACQUISITION AND PROCESSING

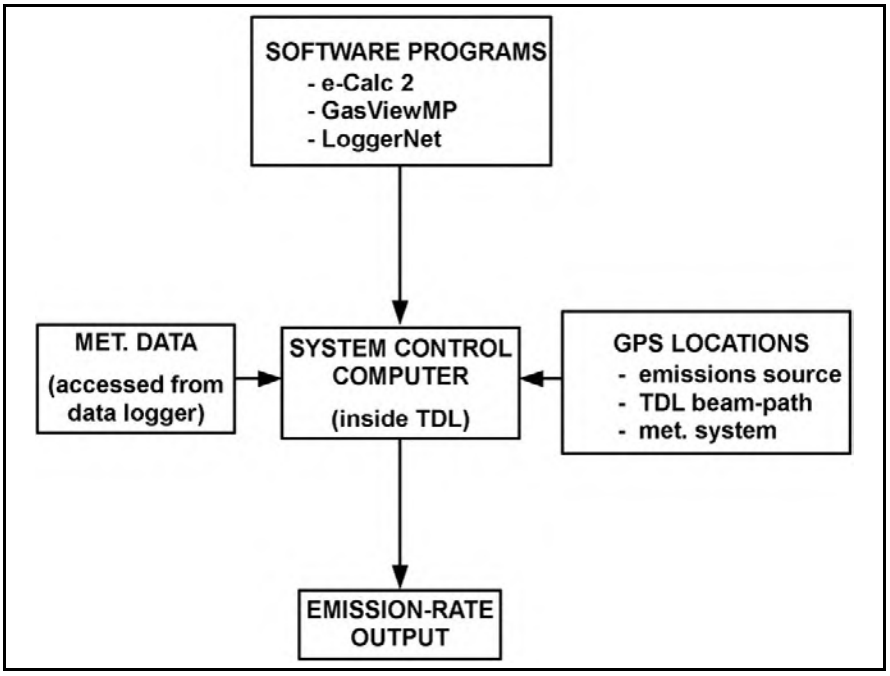

All data-acquisition activities and e-Calc 2 applications are controlled by the System Control Computer located inside the Boreal TDL. This PC contains the e-Calc 2 software, the LoggerNet 4.5 (or equivalent) software for meteorological system operation, and the existing GasViewMP software for TDL system operation. Manual GPS entry of all location coordinates is required for the emissions source, the TDL beam-path end-points, and the meteorological system.

The GasViewMP program is used to control and operate the TDL, and to generate the methane attribution measurement in a form suitable for input to e-Calc 2. This program also facilitates data storage (including supporting QC information) and data-generation results (in this case, text or CSV), suitable for automated polling by the e-Calc 2 software.

A dedicated data logger for the Met One system (separate from the System Control PC) is employed for assembly of all measured data, and for calculation and assembly of all other data, in forms suitable for input to e-Calc 2 (text or CSV). Automated communication between the data logger and the System Control PC is accomplished via direct cable connection (RS232/USB) or via wireless communication technology. Set-up, control, and management of all data-logger operations is accomplished via specialized LoggerNet software, including uploading of programs, data polling, and data storage.

From the System Control PC, e-Calc 2 generates real-time, event-specific results, once automated access to the TDL and meteorological data is established. Results can be presented on-screen, as well as in hard-copy reports.

6.3 System Recommendations and Limitations

Based on the results of the requisite analyses described in Section 6.1, the following recommendations and limitations were included in the initial System specification.

Recommendations

In general, the results of the preceding analyses enabled us to successfully remove enough P/A emission-rate inconsistency so that the initial System specification could be confidently developed. In addition to recommending that the average of four successive monitoring events be used to generate a methane emission rate (refer to Section 6.1.2), these specifications contained recommendations concerning two other issues:

- Optimal wind-speed range
- Treatment of background methane

Optimal Wind-Speed Range

Based on the limited results presented in Table 6-2, we concluded that a mean wind speed range between about 2.0 and 5.0 m/s will yield the best results. This is not to say that wind speeds greater than 5 m/s will necessarily yield erroneous results; however, we believe that more testing is needed during these greater wind speeds.

On the other hand, wind speeds less than 2 m/s should be avoided due to documented issues with AERMOD performance during low wind speeds (e.g., plume meander).

Treatment of Background Methane

We recommended that six or more consecutive background measurements (i.e., upwind of the source) be made prior to initiating 15-minute monitoring events. If these readings are sufficiently constant, a final background measurement should be made immediately after the last of the successive monitoring events.

If there is too much variability in the initial background readings, the use of two comparably performing TDL systems was recommended (one upwind and one downwind of the source).

Limitations

There were two areas which these analyses were unable to address in the initial System specification:

- Nighttime operations
- Applicability to booster stations

Nighttime Operations

From the Milestone F Report, the only simulated nighttime field testing occurred on Day 9. No monitoring events survived the background acceptance criterion on that day. Therefore, nighttime operations were not addressed in the initial (or final) System specification.

Applicability to Booster Stations

Field testing of the simulated booster station was limited to Days 1 and 2, and no monitoring events survived the background acceptance criterion on either of these days. Additionally, the methane release height for this source was 3 meters, while the release height from the other three simulated sources was 1 meter or less.

Because all TDL measurements were made at a height of 1 meter, and since all three of these other simulated sources (gas-gathering pipeline, gas-transmission line, and production pad) comprised the initial universe of acceptable monitoring events (see Table 6-1), we are unable to justify application of these results to the booster-station simulation.

The supplemental booster-station analysis is presented next.

SECTION 7 – SUPPLEMENTAL BOOSTER-STATION ANALYSIS

This section summarizes the supplemental analysis for the booster station. **Section 7.1** presents the analysis objective and the method employed. **Section 7.2** discusses a new scheme developed for the treatment of background methane. **Section 7.3** presents the results of this supplemental analysis. **Section 7.4** presents final System recommendations and caveats.

As a recap, significant temporal variability in the measured background methane concentrations led to a lack of consistency in the P/A ratios derived from the controlled-release results (Section 5). This prevented us from developing the System specifications based on the full complement of measured data. We therefore committed to perform, in the Milestone H Report (Section 6), the additional critical examination and analysis of the background data necessary to remove most of this P/A inconsistency, and to move forward with this effort. In the end, we were able to sufficiently evidence that the accuracy of certain background measurements was compromised, largely by initiating these measurements before all of the methane had completely cleared the TDL beam-path.

When the affected monitoring events were removed from further consideration, confidence in the remaining P/A results was deemed sufficient for (initial) specification development, but the situations where System applicability still could not be demonstrated were: (a) during nighttime conditions; and (b) when assessing emissions from the booster-station simulation. Nighttime data were collected only during Day 9 (gas-gathering pipeline), and booster-station data were collected only during Days 1 and 2. None of monitoring events during these three days passed the methane background criterion developed in the Milestone H Report.

However, in the ERA Progress Report #8, we committed to reassess System applicability for the booster station in this Final Project Report. As shown below, we were able to distill some meaningful results from this supplemental analysis, and extend the System specification to include the booster station. Unfortunately, we were unable to salvage any of the nighttime data collected during Day 9.

7.1 Objective and Method

The objective of this supplemental analysis was to reassess P/A emission-rate results for the booster station, based on an alternative source treatment method for simulating the methane release from atop the building enclosure.

The first such option examined involved modeling the booster station as a point release, using AERMOD's building-downwash pre-processing program. It was hypothesized that this method would more realistically simulate plume dispersion downwind of this somewhat elevated source (3-meter height). However, because the extent of the downwind cavity region is a function of wind

speed, the results under the particular conditions observed were actually worse than originally obtained.

The next option examined involved modeling the booster station as a volume source in AERMOD, with the controlled release assumed to be non-buoyant (i.e., the methane temperature the same as, or colder than, the ambient air). Assuming no plume rise, the entire plume mass will descend from the building's downwind roof-top edge into the building-wake or cavity-recirculation region (volume source), immediately adjacent to, and to the lee of, the building. This simulation, judged the most realistic for this elevated source, necessitated the modification of e-Calc 2 (hereafter referred to as the "modified e-Calc 2 version") for use with the booster station, and other similarly elevated sources.

7.2 New Scheme for Background Methane Treatment

Because the refined Milestone H background analysis failed to yield acceptable background data for any of the booster-station monitoring events, we needed to develop and apply a new background scheme to retain some of the results from these days (Days 1 and 2).

7.2.1 Day 1

Upon further consideration, we concluded there was no reason to reject the initial measured background concentration of 1.976 ppm during Day 1, despite concerns about the final concentration (1.861 ppm; refer to Table 5-2). Therefore, we chose to accept the first four monitoring events from this day's block of data. However, because of uncertainty in the final measured concentration, we elected to hold the background concentration constant at 1.976 ppm for all four events.

7.2.2 Day 2

While the same logic as above might be applied to the first block of data for this day (Table 5-2), we chose not to accept any of these monitoring events. Because the final measured methane concentration for this block was greater than any interpolated value, the argument that the methane had not cleared the TDL beam-path could not be supported and, therefore, there was evidence that the actual background was changing over this data block.

As for the second block of data for Day 2, we concluded the first group four monitoring events was acceptable, based on the same logic applied to the Day 1 analysis. The background concentration was held constant at 2.077 ppm for these four events.

7.3 Results

Table 7-1 presents, for the booster station, a comparison between the results from e-Calc 2 (area-source) and the modified e-Calc 2 version (volume source), based on assignment of a constant methane background concentration for each block of data as discussed above. Predicted, event-specific emission rates are shown for both source-type simulations, with the P/A biases calculated for each. The measured wind speeds are also shown. A single volume source is assumed, and plume parameters are estimated using U.S. EPA's suggested procedure as described in the AERMOD User's Guide (EPA-454/B-16-011):

- The lateral dimension was estimated by dividing the structure width (10 feet, or 3.05 meters) by 4.3, which yields 0.71 meters.
- The vertical dimension was estimated by dividing the structure height (also 10 feet, or 3.05 meters) by 2.15, which yields 1.42 meters.
- The volume source height above grade was assumed equal to one-half the structure height, height of the adjacent building, 1.52 meters.

TABLE 7-1. BOOSTER-STATION ANALYSIS: AREA-SOURCE VS. VOLUME-SOURCE SIMULATIONS

Event No.	Event End-Time (MDT) (hh:mm)	TDL Methane Attribution (ppm-m)	TDL Methane Attribution (mg/m2)	Area-Source Prediction Emission Rate (P) (mg/s)	Area-Source Prediction Plume Capture (%)	Volume-Source Prediction Emission Rate (P) (mg/s)	Volume-Source Prediction Plume Capture (%)	Actual Emission Rate (A) (mg/s)	P/A Bias Area Source (%)	P/A Bias Volume Source (%)	Wind Speed (m/s)
Day 1 (August 14, 2018)											
1	10:15	55.46	34.15	734.3	100.0	438.8	98.8	403.2	82.1	8.8	3.549
2	10:30	51.55	31.72	739.4	100.0	407.8	98.8	403.2	83.4	1.1	3.709
3	10:45	51.08	31.40	695.3	100.0	416.8	99.1	403.2	72.5	3.4	3.909
4	11:00	46.31	28.41	677.8	100.0	386.6	99.1	403.2	68.1	-4.1	4.005
			Mean	**711.7**		**412.5**			**76.5**	**2.3**	**3.793**
Day 2 (August 15, 2018)											
5	12:30	70.60	43.58	329.2	90.8	312.0	86.9	322.7	2.0	-3.3	2.099
6	12:45	50.59	31.19	238.0	87.3	239.0	83.4	322.7	-26.3	-25.9	2.080
7	13:00	69.09	42.57	328.2	97.3	289.6	95.5	322.7	1.7	-10.3	2.337
8	13:15	43.96	27.06	234.6	93.2	213.5	90.8	322.7	-27.3	-33.9	2.458
			Mean	**282.5**		**262.5**			**-12.5**	**-18.3**	**2.244**

The modified e-Calc 2 version (volume-source simulation) shows a marked improvement over the area-source simulation for the first block of data (Day 1, Events 1-4), as determined by the calculated P/A biases. For the second block of data (Day 2, Events 5-8), the area-source simulation actually yields better results, although the difference is judged not significant.

7.4 Final System Recommendations and Caveats

In addition to the System recommendations and limitations discussed in Section 6.3, the following recommendations and caveats apply to booster stations (and any other somewhat elevated sources), based on results from Table 7-1.

When the wind speed is 3 m/s or greater, we strongly recommend the modified e-Calc 2 version be employed for measuring booster-station emission rates.

When the wind speed is between 2 and 3 m/s, either e-Calc 2 version is acceptable; in such cases, however, both versions should be used, and the more conservative measurement (i.e., higher emission rate) should be accepted. Wind speeds below 2 m/s should be avoided.

SECTION 8 – FINAL SYSTEM SPECIFICATION

Section 8.1 presents the final System overview and components. **Section 8.2** presents the final System recommendations and limitations.

8.1 System Overview and Components

Overview

The supplemental booster-station analysis (Section 7) resulted in no change to the overall System design; therefore, the reader is directed to Section 6.2 for a description of the final System overview.

Components

Table 8-1 depicts the final System component specifications. This itemization incorporates results from the Major Deliverables for Milestone B (Field-Work Planning), Milestone F (Controlled-Release Program), Milestone H (Initial System Specification), and Milestone I (Supplemental Booster Station Analysis).

TABLE 8-1. FINAL SYSTEM COMPONENT SPECIFICATIONS

Component	Manufacturer	Model No.	Purpose
Tunable diode laser	Boreal Laser	GasFinder3-OP	Methane measurement
3D ultrasonic anemometer	R.M. Young	8100	WS, WD, σ_ϕ, u*, z_0, H, L
Ambient temperature sensor	Met One	064	H, L, wind profile
Relative humidity sensor	Met One	083	L
Barometric pressure sensor	Met One	092	Concentration correction, L
Portable 3m tripod	Met One	905	Sensor mounting
Crossarm assembly	Met One	191-1	Sensor mounting
Meteorological DAS	Met One (Climatronics)	IMP-865	Meteorological data processing
LoggerNet software	Met One (Climatronics)	Version 4.5	Meteorological data processing
Tablet computer	Dell Inspiron (or equiv.)	P24T	QC, internet access for forecasting
Global positioning system	Trimble (or equivalent)	GEO 5T	UTM coordinate measurements
Emission-calculation software	Minnich and Scotto	e-Calc 2	Ground-level emissions
Emission-calculation software	Minnich and Scotto	modified e-Calc 2	Elevated emissions (booster station)

8.2 System Recommendations and Limitations

The supplemental booster-station analysis resulted in some recommendations and caveats, specifically for this source, as discussed in Section 7.4.

Table 8-2 presents a summary compilation of the final System recommendations and limitations.

TABLE 8-2. FINAL SYSTEM RECOMMENDATIONS AND LIMITATIONS

Issue	Methane Emissions Source	Recommendation	Limitation
Monitoring events	(all)	Four successive 15-minute events to form an hourly-average emission rate	Plume meander and other short-term effects may adversely impact 15-minute averages
Wind speed	- Booster stations	Use e-Calc 2 or modified version for WS between 2.0 and 3.0 m/s	- Avoid WS less than 2.0 m/s - Use caution with WS greater than 5.0 m/s
		Use modified version for WS greater than 3.0 m/s	
	- Gas-gathering pipelines - Gas-transmission lines - Production pads	Use e-Calc 2 for WS between 2.0 and 5.0 m/s	
Background	(all)	Minimum of six consecutive measurements	If measurements are not consistent, use dual TDL units (simultaneous upwind / downwind measurements)
Nighttime application	(all)	(none)	Nighttime application is not supported